The Role of PKCalpha-Mediated p120-Catenin

Phosphorylation on Endothelial Permeability

BY

EMILY ELIZABETH VANDENBROUCKE ST AMANT
B.A., Miami University, 2005

THESIS

Submitted as partial fulfillment of the requirements
for the degree of Doctor of Philosophy in Pharmacology
in the Graduate College of the
University of Illinois at Chicago, 2012

Chicago, Illinois

Defense Committee:

Dr. Asrar Malik, Chair and Advisor
Dr. Dolly Mehta
Dr. Richard Minshall
Dr. Yulia Komarova
Dr. Lester Lau, Biochemistry and Molecular Genetics

This thesis is dedicated to my Mom and Dad, and to my wonderful husband Joe.

ACKNOWLEDGEMENTS

I would like to thank my thesis committee—Dr. Malik, Dr. Mehta, Dr. Minshall, Dr. Komarova and Dr. Lau—for their time and support. Their guidance and thoughtful suggestions helped me to look from all possible angles while interpreting data, and to ask insightful questions. I would like to thank Dr. Malik for all his help and guidance as my advisor. He set a high level of expectations, and attempting to go above and beyond them forced me to become better scientist. I am particularly grateful for the multitude of opportunities he provided me. Whether it was having me write a review early in my career or sending me to different conferences, he helped me to seize every possible opportunity to gain experience publishing and presenting, all while making a name for myself.

A number of individuals were essential in gathering data. I would like to thank both Dr. Tauseef and Dr. Vogel for their help in gathering permeability measurements. I am thankful for the all the help that Dr. Uzma Saqib gave, and for her expertise and research in designing the PKCα blocking peptide. I would also like to thank Dr. Jeffery Molkentin for *prkca*$^{-/-}$ mice, and Dr. Al Reynolds for providing the p120 cDNA constructs. I would further like to thank all of the Malik lab members, post and present, that have helped with protocols, sharing reagents and offering helpful advice whenever I needed it. I am also incredibly indebited to Dr. Gao and Lan for all the time and patience they spent teaching me and answering all of my questions, especially in the beginning of my time at UIC. I am sure I would not have made it far without them.

I would be remiss if I did not give a special thanks to Dr. Komarova for all of her help and guidance. She went above and beyond to help me troubleshoot when things weren't going as planned, was kind enough to pass along her wealth of knowledge on microscopy and, perhaps most importantly,

spent an incredible amount of time helping me to become more proficient scientific writer. I cannot thank her enough for her time and effort helping to shape me into a better scientist.

Also, I have to thank my friends, family, parents and sisters. Their love and support over the years gave me the confidence to go to graduate school to begin with, and their support during the last few years motivated me to keep going. Their happiness at all my achievements, big or small, was the highlight of this whole experience for me, and I hope I made them all proud.

And finally, to my parents and Joe- I cannot say thank you enough. The example all of them have set for me has been an inspiration. My mother received an advanced degree in math, and had both a fulfilling career and a family life. My husband's ambition and motivation in everything he does in life, not to mention his unconditional support, has been invaluable. But without the advice, opportunities, support, education and patience I've received over the years from my father, I would have never achieved this. I could not have asked for better role models in my life.

EEVSA

TABLE OF CONTENTS

TABLE OF CONTENTS (continued)

LIST OF FIGURES

LIST OF FIGURES (continued)

LIST OF ABBREVIATIONS

ALI	Acute Lung Injury
AJs	Adherens Junctions
AP-2	Adaptor Protein-2
ARDS	Adult Respiratory Distress Syndrome
ARM	Armadillo Repeat Motif
ARVCF	Armadillo Repeat gene deleted in Velo-Cranial-Facial syndrome
BSA	Bovine Serum Albumin
CTD	C-Terminal Domain
DAG	Diacylglycerol
DDAB	Dimethyldioctadecyl-Ammonium Bromide
DIPA	Delta Interacting Protein A
DOC	Deoxycholate
DTT	Dithiothreitol
EBA	Evans Blue Albumin
E-cadherin	Epithelial Cadherin
EDTA	Ethylenediaminetetraacetic acid
FAK	Focal Adhesion Kinase
FBS	Fetal Bovine Serum
GDI	Guanine Nucleotide Dissociation Inhibitor
GFP	Green Fluorescent Protein
GPCR	G-Protein Coupled Receptor
HLMVEC	Human Lung Microvascular Endothelial Cell
HPAEC	Human Pulmonary Aortic Endothelial Cells
ICAM	Intercellular Adhesion Molecule
IP_3	Inositol Trisphosphate
JMD	Juxtamembrane Domain
$K_{f,c}$	Microvessel Filtration Coefficient
LPS	Lipopolysaccharide
MLC	Myosin Light Chain
MLCK	Myosin Light Chain Kinase
MM control	Mismatch control
MyD88	Myeloid Differentiation 88
N-cadherin	Neuronal cadherin
NTD	N-Terminal Domain
p120	p120-Catenin
PAF	Platelet Activating Factor
PAK	p21 Activating Kinase
PAR-1	Protease Activated Receptor-1
PCR	Polymerase Chain Reaction
PIP_2	Phosphatidylinositol 4,5-biPhosphate
PLC-β	Phospholipase C β
PMA	Phorbol 12-Myristate 13-Acetate
PMSF	Phenylmethylsulfonyl Fluoride
PKCα	Protein Kinase C-α
prcka$^{-/-}$	PKCα knockout

LIST OF ABBREVIATIONS (continued)

PVDF	polyvinylidene difluoride
RACKS	Receptor to Activated C Kinase
ROCK	Rho Kinase
RTK	Receptor Tyrosine Kinase
S1P	Sphingosine-1-Phosphate
S879	Serine 879
S879A	Serine 879 mutated to Alanine
S879D	Serine 879 mutated to Aspartic Acid
SFK	Src Family Kinase
SHP2	Src Homology 2 domain containing tyrosine Phosphatase
SPR	Surface Plasmon Resonance
TAMP	Tight Junction Associated MARVEL Proteins
TER	Transendothelial Electrical Resistance
Thr	Thrombin
TJs	Tight Junctions
TLR	Toll-Like Receptor
TRPC	Transient Receptor Potential Cation Channel
VE-Cadherin	Vascular Endothelial Cadherin
WT	Wild-Type

SUMMARY

Endothelial cells form a semi-permeable barrier that lines all blood and lymphatic vessels in the body, and regulates exchange of fluid and nutrients between the blood and surrounding tissues. Changes in vascular permeability can be initiated by inflammatory mediators or growth factors that bind receptors on endothelial cells and trigger internal signaling cascades. Increased endothelial permeability in the lungs can result in unchecked leakage of liquid and proteins into tissues, edema formation and impaired gas exchange. Understanding the molecular mechanisms regulating permeability is imperative in order to identify therapeutic targets to treat inflammatory disorders, reduce edema and prevent diseases such as Acute Respiratory Distress Syndrome (ARDS).

Interendothelial junctions are important in regulating endothelial permeability. The majority of interendothelial junctions in the lung vasculature are adherens junctions (AJs), which are formed through vascular endothelial (VE)-cadherin adhesions. p120-catenin (p120) binds and stabilizes VE-cadherin at the junction, and inhibits VE-cadherin internalization, but the mechanism regulating p120 association with VE-cadherin is not well understood. Pro-inflammatory mediators, such as thrombin and LPS, bind endothelial cells and induce disassembly of interendothelial junctions to increase permeability.

This thesis is divided into two parts. The first part focuses on the role of protein kinase C (PKC)-α on VE-cadherin stability, barrier function and lung vascular permeability. PKCα is activated downstream of inflammatory mediators and causes increased permeability. PKCα has been shown to induce changes in phosphorylation of several AJ proteins, but the effect of these modifications is not clear. In Chapter 3, we investigate the role of PKCα in regulation of AJ stability. We used an *in vivo*

knockout mouse model, and observed that deletion of PKCα diminished the increase in lung vascular permeability in response to protease activated receptor (PAR)-1 peptide stimulation by almost 50%. Using PKCα siRNA, we observed that cells depleted of PKCα maintained intact junctions and retained VE-cadherin at the junction after thrombin stimulation. We found that PKCα induces p120 dissociation from VE-cadherin, and PKCα-regulated disassembly of the p120/VE-cadherin complex increased binding of VE-cadherin to a clathrin adaptor protein, causing VE-cadherin internalization. We also found that PKCα phosphorylates serine 879 (S879) on p120 in response to thrombin, which occurs in conjunction with p120 dissociation from VE-cadherin. Finally, we verified that PKCα causes both an increase in permeability, and phosphorylation of S879 on p120, in response to LPS as well as thrombin.

The second part investigates the role of PKCα-mediated phosphorylation of S879 on p120, and the resulting effect on p120/VE-cadherin association and endothelial permeability. Chapter 4 examines the effect of S879 phosphorylation on p120 binding affinity for VE-cadherin, VE-cadherin stability and endothelial barrier function. We expressed phosphodefective p120, as well as a phosphomimic p120, in endothelial cells and found that phosphorylation of S879 caused p120 to dissociate from AJs, and disrupted monolayer integrity. Inhibition of S879 phosphorylation of p120 in mouse lung vessels significantly reduced the permeability increase seen in response to the pro-inflammatory mediators thrombin and LPS.

In both sections we exploited a variety of methodologies and approaches, including expression of p120 phospho-mutants in primary endothelial cells and mouse lungs, quantitative fluorescence microscopy and biochemistry, functional assessments of barrier function and measurement of vascular

permeability *in vivo*, to understand how PKCα-mediated phosphorylation of S879 on p120 affects VE-cadherin stability and vascular permeability. We found that inhibition of PKCα-mediated S879 phosphorylation on p120 is sufficient to decrease edema formation, and identified a novel potential anti-inflammatory target.

1. LITERATURE REVIEW

1.1 Endothelial Permeability

The endothelium is a semi-permeable barrier which lines all blood and lymphatic vessels, and regulates exchange of fluids and solutes between the blood and the surrounding tissue (1). Regulation of endothelial permeability is imperative for transfer of nutrients and oxygen, as well as transmigration of white blood cells and angiogenesis. Dysfunction of the endothelial barrier results in protein-rich tissue edema (2), adult respiratory distress syndrome (ARDS) (3) and increased metastasis (4). Circulating inflammatory mediators, such as thrombin (5), lipopolysaccharide (LPS)(6) and histamine (7), bind to receptors on the surface of endothelial cells and activate signaling cascades that result in increased permeability across the vasculature (1).

The endothelium is permeable via two routes. The transcellular pathway allows passage across the endothelial barrier via vesicular transport, carrier proteins or ion channels. The paracellular route goes between endothelial cells, through interendothelial junctions. Unlike transcytosis, transport through the paracellular route is passive and driven by gradients (8), and therefore has lower selectivity. Paracellular passage is controlled by the integrity of cell-cell junctions. The junctions function to control movement across the endothelial barrier and maintain gradients. Decreased barrier integrity, which occurs during an inflammatory response, is a result of disassembly of interendothelial junctions and leads to unchecked transport of protein-rich fluid through the endothelium. The aim of this thesis is to understand regulation of paracellular permeability by interendothelial junctions, so henceforth all references to endothelial permeability refer only to paracellular permeability.

Influx of protein-rich fluid into cells through the paracellular pathway is a passive process that relies on gradients and differences in oncotic pressure (9). The Starling equation describes the

hydrodynamic forces that regulate fluid movement across the endothelium (Figure 1) (10). The equation was recently revised to account for the effect the glycocalyx has on restricting permeability (11,12). The new equation states:

$$J_v/A=L_p[(P_c-P_i)-\sigma(\pi_p-\pi_g)]$$

where J_v is the fluid volume filtration rate (mL/s), A is the endothelial surface area (cm^2), P_c is the hydrostatic pressure inside the capillary (mm Hg), P_i is the hydrostatic pressure in the interstitium outside the capillary (mm Hg), π_p is the oncotic pressure of the plasma (mm Hg), L_p is the hydraulic conductivity (cm/s/mm Hg), and σ is the reflection coefficient, which describes the permeability of the capillary wall (σ = 0 means completely permeable; σ = 1 means completely impermeable) (9,12). The revision comes with π_g, which is interstitial oncotic pressure of the intercellular cleft (mm Hg), but was previously π_i, the oncotic pressure of the interstitum (Figure 1) (11). This change was implemented to account for the previously unknown effects of the glycocalyx. The glycocalyx is a network of glycoproteins and polysaccharides, primarily proteogylcans and glycoaminoglycans, which sit on the luminal side of the endothelium and form an additional semi-permeable barrier due to the extensive branching and negative charge (11,13). A healthy influx of protein-rich fluid can be cleared away by lymphatics, but if the rate of fluid entering exceeds a critical amount, or offsetting the increase in fluid by changing the interstitial pressure or increasing lymphatic flow in the area fails to reduce accumulating fluid, edema occurs (2). This can occur during inflammation, when endothelial cells are signaled to disassemble AJs to create interendothelial gaps, allowing protein-rich fluid to flow unchecked between

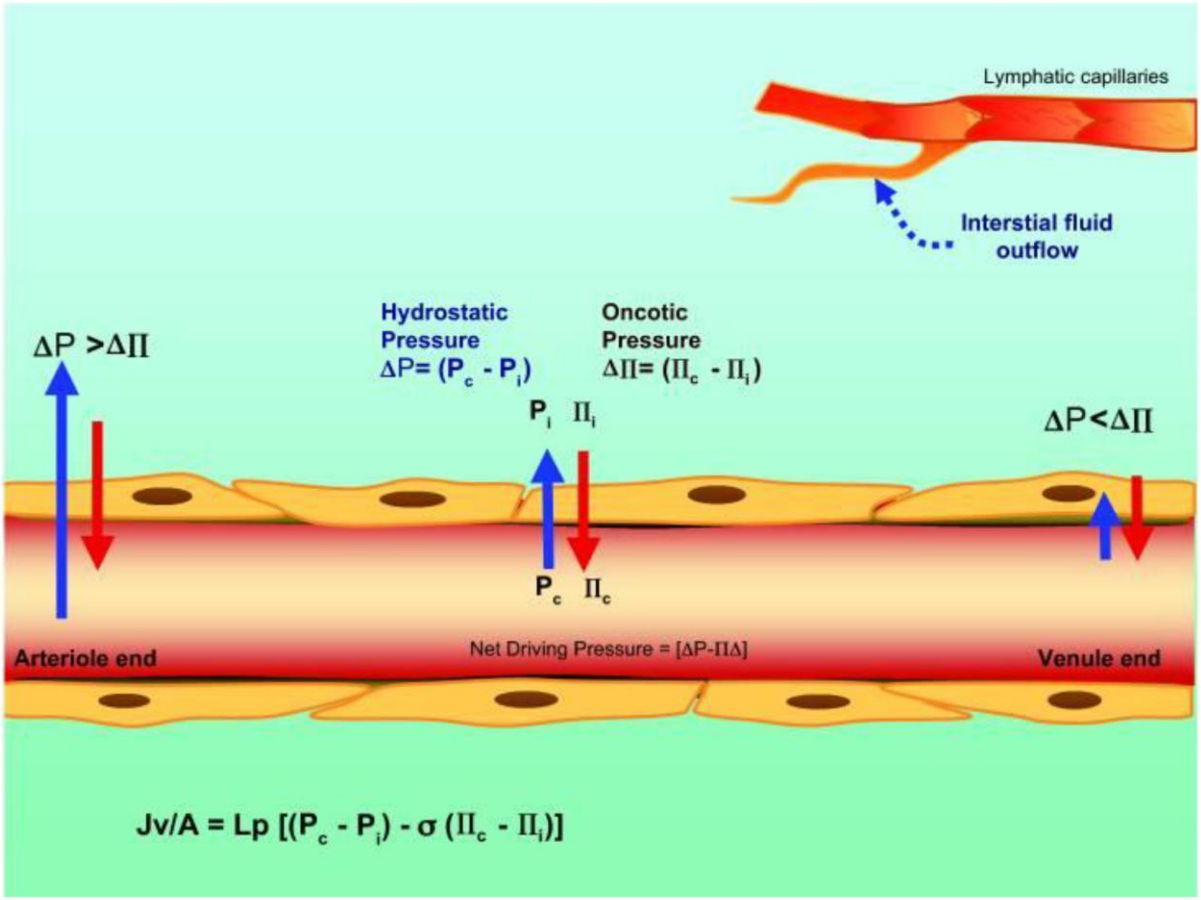

Figure 1: Effect of Starling forces on endothelial barrier function. The Starling equation describes the hydrodynamic forces that regulate fluid movement in the endothelium. Starling forces describe the difference in hydrostatic pressure and oncotic pressure between the lumen and the interstitum, factoring in hydraulic conductivity and the permeability of the vessel wall to fluid. Lymphatic vessels clear away excess interstitial fluid. Reproduced with permission from Yuan and Rigor "Regulation of Endothelial Barrier Function", 2011 (11).

cells (2). Interendothelial gaps are morphological changes between cells due to disruption of interendothelial junctions, and a gap can form as a result of a single pore or multiple pores combined (14,15). Gap formation and reassembly of junctions are transient processes than can occur without disrupting cell behavior (16), and reassembly can reinstate fluid homeostasis across the endothelium.

1.2 Structure and Function of Interendothelial Junctions

Cell adhesion is controlled by the strength of cell-cell junctions and the intracellular binding partners (17). Endothelial cells form tight junctions (TJs) and adherens junctions (AJs) to create a semi-permeable barrier, as well as a signaling interface between cells. TJ-associated MARVEL proteins (TAMPs), claudins and occludin, are the structural core of TJs (18). Claudins are the main adhesive component of TJs, forming both homo- and heterotypic interactions. Expression of claudins is tissue-specific, and claudin-5 the only endothelial-specific isoform (19,20), but endothelial cells also express claudin-3, 12 (21) and 15 (22). Occludin was previously thought to also be a structural protein but evidence now suggests its major role is signal transduction (23,24). Generally, TJs reside on the apical border of endothelial cells and are more restrictive than AJs, which form on the basolateral side. There is crosstalk between the junctions, and there is mounting evidence that TJ structure and function is regulated by AJs (20,25,26).

AJs are the primary intercellular junction in the lung microvasculature. AJs are formed through cadherins clustering and binding cadherins on adjacent cells in a Ca^{2+}-dependent manner (Figure 2)(27). Cadherins are comprised of five ectodomains, which are characterized by 110 repeating amino acids (27,28). The ectodomains control cis and trans cadherin binding and require Ca^{2+} to link the domains together (29,30). Cadherins also contain a transmembrane domain and an intracellular domain, which

contains the highly conserved juxtamembrane domain (JMD) and the C-terminal domain (CTD). Intracellularly, cadherins bind catenins, which regulate AJ stability and signaling. p120-catenin (p120) binds cadherins at the JMD (31) and regulates cadherin stability at AJs (32,33). The CTD of cadherins anchors AJs to the actin cytoskeleton through binding of β-catenin or plakoglobin, both of which bind α-catenin, and connect the junction to the actin filaments protruding from the cortical actin band (1). α-catenin is the only catenin that contains a defined actin-binding domain (34), that allows it to bind and actively regulate the association between the actin cytoskeleton and junction (35). It shifts between a monomer and dimer to regulate interaction with actin and β-catenin, thereby contributing to the dynamic nature of AJs (36,37). A connection between AJs and the actin cytoskeleton allows intracellular signaling and coordination between the cytoskeleton and the junction. It has recently been suggested that α-catenin interacts directly with p120, and reinforces the p120/cadherin interaction, however the importance of this interaction is still unclear (38).

Endothelial cells express both Vascular Endothelial (VE)- and Neuronal (N)-cadherins (39). Cadherins have similar protein expression in endothelial cells, but they differ in their localization within the cell (40). N-cadherin is distributed over the entire plasma membrane and is vital for organization of the junctions during development, as well as cell proliferation and motility (40,41). Functionally, N-cadherin stabilizes mature blood vessels through homotypic binding of cadherins on smooth muscle cells and pericytes (42,43). VE-cadherin resides at interendothelial junctions, regulating barrier function by binding surrounding endothelial cells (44-46). Both cadherin knockouts are embryonic lethal (26,47), stressing the independent yet necessary functions of both cadherins despite some functional overlap.

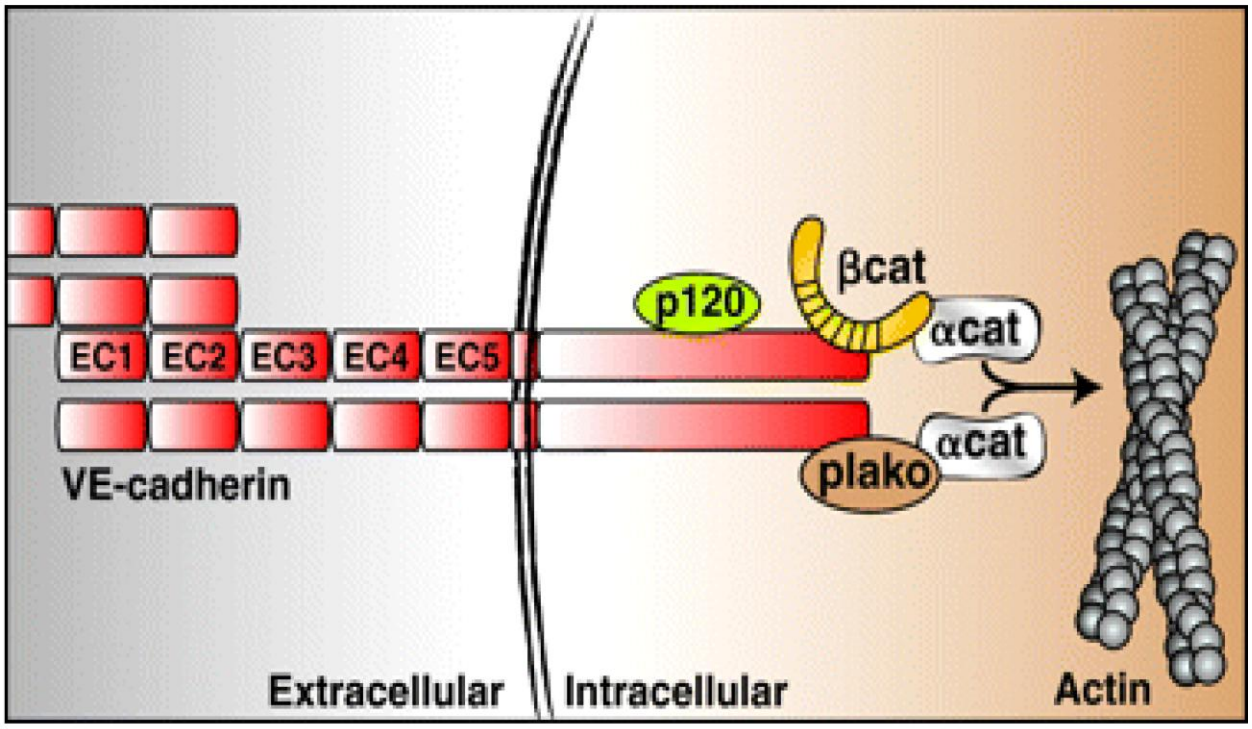

Figure 2: Adherens junction structure. VE-cadherin clusters bind cadherins on adjacent cells in a Ca^{2+}-dependent manner, primarily through interaction of EC1 and EC2 domains. Intracellularly, AJs are stabilized by the CTD of VE-cadherin binding to β-catenin, or plakoglobin, which binds α-catenin, connecting the junction to the actin cytoskeleton. VE-cadherin is stabilized at the junction p120 binding to the JMD, and preventing internalization. Reproduced with permission from Dejana, E. et al. J Cell Sci 2008;121:2115-2122 (17).

Increased expression of N-cadherin has been shown to compensate for depleted VE-cadherin in cell culture, and vice-versa, however this is dependent on maturity of the endothelial monolayer (48). Both VE-cadherin and N-cadherin bind p120, and it has been suggested that the surface expression of VE- and N-cadherin are inversely related due to competition for p120 binding in mature vessels (48,49).

1.3 Regulation of Vascular Permeability During Inflammation

Regulation of endothelial permeability is critical during an immune response (1). Increased permeability allows invasion of neutrophils into tissue, as well as protein-rich fluid containing nutrients and other support for the affected tissue. Circulating inflammatory agents, such as thrombin (50), increase vascular permeability via activation of their respective G protein-coupled receptors (GPCR) expressed on endothelial cells (51). Inflammatory mediators act on the endothelium to form interendothelial gaps through AJ disassembly (16), as well as induce rearrangement of the actin cytoskeleton into stress fibers (52). Specifically, thrombin binds and activates protease activated receptor (PAR)-1 on endothelial cells (50), and induces a transient intracellular signaling cascade that results in increased intracellular Ca^{2+}, activation of protein kinase C (PKC)-α and a reversible increase in permeability through AJ disassembly and increased RhoA GTPase activation (51). PKCα signaling increases endothelial permeability through several diverging pathways, including RhoA activation and phosphorylation of AJ proteins (Figure 2) (5). RhoA is a small GTPase that regulates actin dynamics by reorganizing cortical actin into stress fibers in response to inflammation (53). The stress fibers, with phosphorylated myosin light chain (MLC) (54), cause myosin-actin crossbridge cycling. This results in cell rounding and contraction, and increases permeability (55). MLC is phosphorylated by myosin light chain

kinase (MLCK) in a Ca^{2+}-calmodulin-dependent manner. RhoA also increases MLC phosphorylation by inhibiting the MLC phosphatase PP-1 and activation of Rho Kinase (ROCK). Cell contraction alone is not sufficient to create interendothelial gaps (56), so to elicit the maximum increase in permeability both cell contraction and AJ disassembly must occur (2,57). This signaling pathway is outlined in Figure 3.

LPS is an endotoxin that resides on gram negative bacteria and causes inflammation. It binds toll-like receptors (TLR) to initiate an innate immune response (58). TLR activation causes the release of pro-inflammatory mediators into the blood, which bind and cause increased permeability of the endothelium (59). TLR activation can lead to sepsis, which has a mortality rate approaching 25% and is the leading cause of death in critically ill patients (60). LPS specifically increases vascular permeability in endothelial cells by activating TLR-4 and CD14 (61), leading to activation of Src-family kinases (SFK) (62) and myeloid differentiation factor (MyD)-88 (6), among other things. LPS-induced activation of TLR-4 increases Ca^{2+} through activation of transient receptor potential cation channel (TRPC)6, and expression of TRPC6 is required to increase permeability following LPS stimulation (63). AJ protein p120 was recently implicated in LPS signaling by suppressing TLR-4 association with MyD88 (64), thus reducing the inflammatory response to LPS. TLR-4 has been shown to activate PKCα in neutrophils (65), and more recently in brain endothelial cells where it disrupts interendothelial junctions (66), however the effect of PKCα activation downstream of LPS in the lung vasculature is unknown.

Endothelial cells have intrinsic feedback mechanisms to combat increased permeability and reform junctions during inflammation (37,67). Thrombin increases sphingosine-1-phosphate (S1P) signaling to increase AJ reannealing (37,68), possibly in a PKC-dependent manner (69). Activation of monomeric GTPases Cdc42 and Rac1 rearrange the actin cytoskeleton to promote reassembly of AJs and

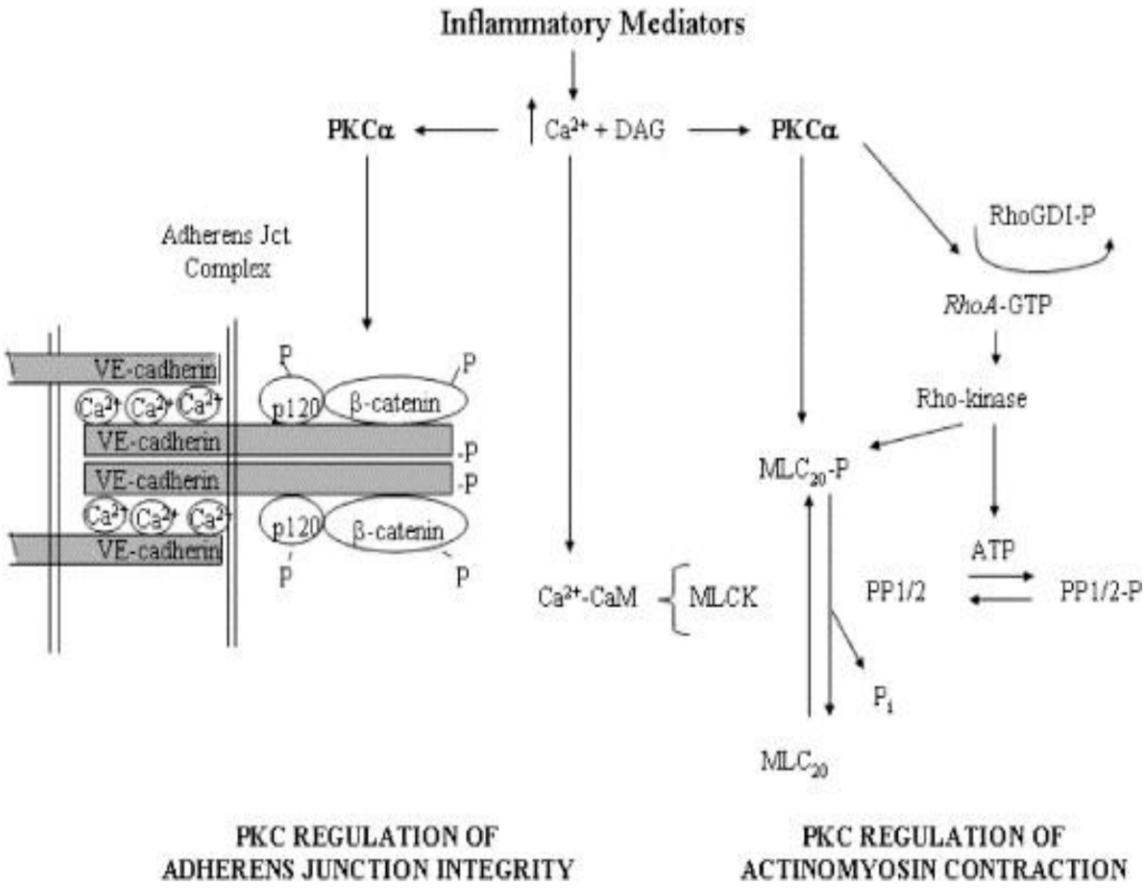

Figure 3: PKCα signaling during inflammation. Inflammatory mediators bind endothelial cells, cleaving PIP_2, and producing DAG and increased intracellular Ca^{2+} to activate PKCα. Activation of PKCα increases actinomyosin contraction through activation of RhoA and dephosphorylation of MLC. PKCα also causes changes in phosphorylation of AJ proteins to destabilize AJ integrity. Both cell contraction and decreased AJ integrity result in increased endothelial permeability. Reprinted from Vascular Pharmacology, 39(4-5), Tiruppathi C, Minshall RD, Paria BC, Vogel SM, Malik AB. "Role of Ca^{2+} Signaling in the regulation of endothelial permeability", 2002, 173-185, with permission from Elsevier (70).

reestablish endothelial barrier integrity (71). Activation of small GTPase Cdc42 contributes to AJ reformation of AJs by increasing binding of α-catenin with β-catenin (72). VE-cadherin outside-in signaling, as well as S1P receptor 1 signaling, activate Rac1, which induces remodeling of actin into cortical bundles to stabilize AJs (73-75). Changes in phosphorylation of AJ proteins have also been implicated in junctional reannealing. Src homology 2 domain containing tyrosine phosphatase (SHP2) decreases tyrosine phosphorylation of β-catenin to allow reassembly of AJs (76), and activated focal adhesion kinase (FAK) associates with p120 to promote reannealing of AJs (77).

1.4 AJ Regulation and Signaling

Maintaining endothelial permeability in the lung microvasculature relies on VE-cadherin expression at AJs. Cadherins are continuously reorganizing, laterally and through endocytosis, and recycle back to the membrane (78), which is essential for proper tissue organization (30). Stimulation of endothelial cells by inflammatory mediators increases disassembly of AJs and internalization of VE-cadherin (79). Internalization of VE-cadherin occurs primarily through clathrin-dependent endocytosis, although caveolae-mediated endocytosis has also been shown (80,81). During clathrin-mediated internalization, VE-cadherin binds adaptor protein (AP)-2, which recruits VE-cadherin into clathrin-coated pits, resulting in endocytosis (81). AP-2 functions as a cargo adaptor for clathrin, and nonspecifically binds to tyrosine-based sorting signals on the cytoplasmic regions of transmembrane proteins to induce endocytosis (82). Because permeability increases can be reversible, VE-cadherin is often recycled back to the plasma membrane, allowing AJs to reassemble and permeability to return to prior levels.

p120 is known to regulate cadherin stability and turnover (32,33,83). Decreased protein expression of p120 leads to a decrease in the surface expression of cadherins (32). Loss of p120 binding at the JMD causes cadherin internalization (32,80,81,84,85), and subsequent disassembly of AJs (33,85). As shown in Figure 4, binding of p120 to the cadherin JMD physically blocks binding of AP-2 by masking the AP-2 binding site on cadherins (81,86), inhibiting VE-cadherin recruitment into clathrin-coated pits and subsequent internalization (80,81). The JMD is the most conserved region on cadherins, and therefore p120 is hypothesized to bind all cadherins in the same manner (87). The crystal structure of the p120/E-cadherin binding interaction was recently published, and it exposed two different binding motifs between p120 and cadherins (86). The stronger, static interaction encompasses a greater portion of p120 bound to the JMD, whereas the dynamic interaction masks the AP-2 binding site on E-cadherin and forms a weaker interaction that is subject to regulation (86). It confirms that p120 binding sterically hinders binding of endocytotic machinery to prevent internalization of VE-cadherin, and the dynamic interaction is weak enough that single residue mutation of p120 could be sufficient to uncouple p120 from the JMD (86).

Regulation of VE-cadherin membrane stability has long been speculated to be the result of post-translational modifications, mainly phosphorylation. It was commonly thought that Src-mediated tyrosine phosphorylation of VE-cadherin on tyrosine 658 and 731 induced formation of interendothelial gaps via AJ disassembly by inhibiting p120 and β-catenin binding to VE-cadherin (7,17,88,89), but recently this view has been challenged. Adam *et al.* published that Src-induced phosphorylation was not sufficient to decrease barrier function of the endothelium alone (90). Interestingly enough, phosphorylation of tyrosine residues do regulate leukocyte extravasation in endothelial cells (91), but

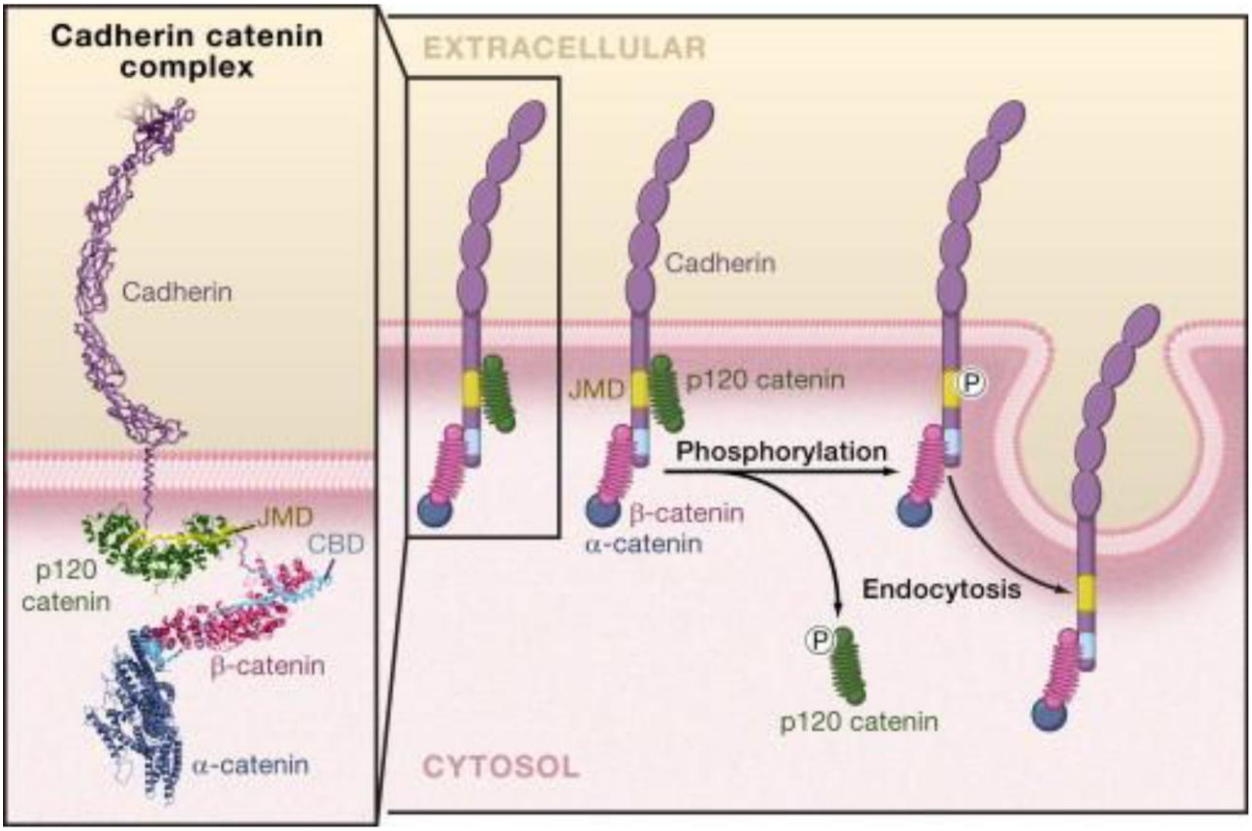

Figure 4: Proposed model of p120 regulation of cadherin internalization. Left panel: The structure of AJs shows p120 binding to the JMD of cadherins. Right panel: A hypothesized model of p120 dissociation from VE-cadherin involves either p120 phosphorylation or cadherin phosphorylation. Once p120 dissociates from the cadherin, it can be recruited into clathrin-coated pits by AP-2, and internalized. Reprinted from Cell, 141 (1), Reynolds AB, "Exposing p120 Catenin's most intimate affair", 2010, 20-22, with permission from Elsevier (92).

not overall vascular permeability. Phosphorylation of p120 has also been hypothesized to regulate cadherin binding and stability, which we discuss in depth in Section 1.6, but again, the results are inconclusive. S-nitrosation of both p120 and β-catenin, caused by an increased in nitric oxide in response to platelet activating factor (PAF), is yet another post-translational modification that was recently shown to reduce binding to VE-cadherin, and induce hyperpermeability (93). Overall, there have been many post-translational modifications of cadherins and catenins identified, but most are still poorly understood.

Not only do cadherins regulate AJ integrity, they also function as signaling hotspots to communicate with surrounding cells. Signal transduction occurs bi-directionally through the cadherin (30); both outside-in and inside-out signaling is transduced through AJs. Inside-out signals are transduced from the cell through changes in intracellular binding of catenins, and through changes in the actin cytoskeleton (94). Extracellular signals are exchanged through alterations of cell-cell adhesion and the resulting conformational changes in cadherin ectodomains are relayed into the cell (95). These signals are vital to coordinate tissue architecture and remodeling, and both VE-cadherin and N-cadherin can be involved in endothelial signaling based on the requirement of the cell (27,96), . This type of signaling, orchestrated through cadherins to communicate and coordinate movement, is vital to the integrity of the vasculature.

Regulation of AJ integrity also affects transcription. Increased VE-cadherin expression at junctions decreases β-catenin transcriptional activity by sequestering β-catenin at the junction (97). β-catenin is a co-activator of the canonical Wnt signaling pathway, which regulates vascular development,

proliferation and cell survival (97,98). Transcriptional activity of the β-catenin/Wnt pathway upregulates claudin-5 (20) and N-cadherin expression (96), as well as genes linked to angiogenesis and cancer (99,100). VE-cadherin similarly regulates p120 transcriptional activity through binding cytoplasmic p120, preventing translocation into the nucleus and transcriptional regulation (101). In the nucleus, p120 binds transcription suppresor Kaiso, and removes the suppression from target genes (102). p120 also increases β-catenin nuclear activity by inhibiting Kaiso suppression of β-catenin transcriptional activity (103,104). Release of both p120 and β-catenin from AJs following thrombin stimulation can result in translocation of both to the nucleus, resulting in an angiogenic response to increased permeability (104).

1.5 Protein Kinase C

PKC is a serine/threonine kinase that is known to be involved in the formation of pulmonary edema (105). PKC has 10 different isoforms, and they are separated into three different groups based on structure and method of activation (Figure 5). Classical isoforms (PKCα, β_I, β_{II} and γ) require binding of Ca^{2+} and diacylglycerol (DAG), while the novel isoforms (δ, ε, η and θ) require only binding to DAG (106). The atypical isoforms (ζ and ι/λ) lack the Ca^{2+} binding domain altogether and the mechanism of activation is unknown, although they still bind phospholipids, such as phosphatidylserine, at the membrane (107). PKC Figure 5 illustrates the "classical" signaling pathway to induce PKC activation downstream of GPCRs or Receptor Tyrosine Kinases (RTKs), both of which activate phospholipase C-β (PLC-β) to cleave phosphatidylinositol 4,5-bisphosphate (PIP_2) into DAG and inositol trisphosphate (IP_3) (106). IP_3 binds the endoplasmic reticulum and releases intracellular stores of Ca^{2+}, which binds the C2

domain on classical PKC isoforms (108). DAG binds the C1 domain on both the classical and novel isoforms, and removes the pseudosubstrate inhibition on the catalytic domain (108). DAG also increases the affinity of PKC for phospholipids (109). Receptor to Activated C Kinase (RACKs) proteins also bind the C1 domain during activation of PKC and different RACKS proteins are thought to bind specific isoforms of PKC to influence PKC subcellular localization (110). Furthermore, PKCs undergo autophosphorylation on 3 different residues after removal of the pseudosubtrate inhibition, which are important for prolonged activation (108). Activation of PKC occurs within 90 seconds of GPCR activation, and can last upwards of an hour (111). Termination of PKC activity occurs with reverse translocation of PKC away from the membrane (108).

Despite the structural differences in isoforms, there are still overlapping substrates and functions of PKCs. PKC signaling has been implicated in changes in endothelial permeability (5). Back in the 1980s, it was observed that phorbol 12-myristate 13-acetate (PMA), a potent PKC activator, induced a pathophysiology that was similar to ARDS in terms of increased endothelial permeability followed by edema (105,112). Since then, PKC has been studied for its role in regulating vascular permeability. PKC has been shown to phosphorylate AJ proteins, as well as increase RhoA activity, to increase endothelial permeability (113-116). Nephropathy and vascular abnormalities in renal, retinal and cardiovascular tissues in diabetic patients have all been linked to activation of PKC, as has transitioning to a malignant cancer phenotype due to loss of integrity of cell-cell junctions (117,118).

PKCα is a ubiquitously expressed isoform that has been shown to be the primary isoform responsible for increasing endothelial permeability in the lung vasculature in response to inflammatory

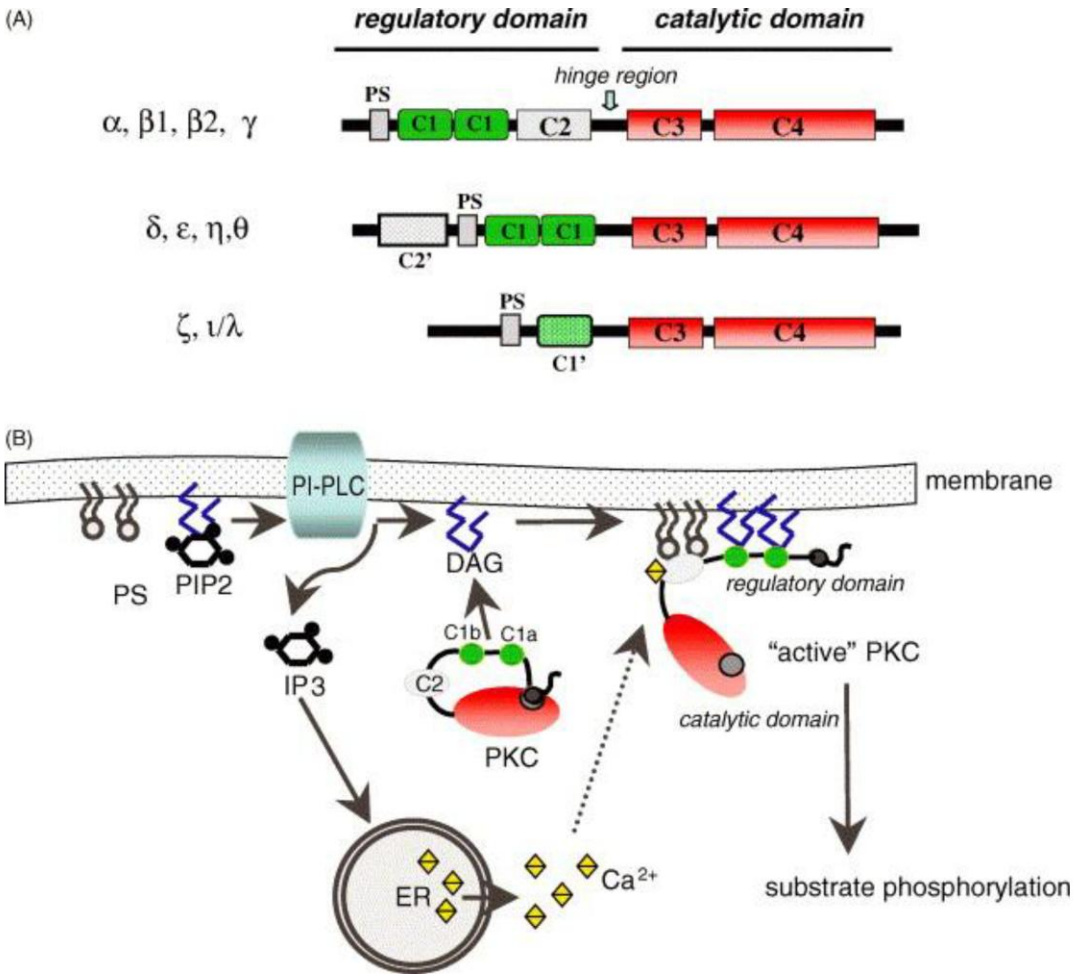

Figure 5: Structure and activation of PKC isoforms. (A) PKCs contain a regulatory domain, which varies between different isoforms, and a catalytic domain. The regulatory domain is conserved among PKC isoforms, and contains a C3, ATP-binding domain and a C4, substrate-binding domain. The catalytic domain may contain a C1, DAG/phorbal ester-binding domain and a C2, Ca^{2+}-binding domain. The catalytic domain also contains a pseudosubstrate (PS) domain, which binds the catalytic domain in the inactive state, and is released upon activation. (B) GPCR or RTK activate PLC-β (PI-PLC) to cleave PIP_2 into DAG and IP_3. IP_3 binds the endoplasmic reticulum (ER), causing it to release intracellular Ca^{2+}, which binds the C2 domain on classical PKC isoforms. PKCs translocate to the membrane to bind DAG, which removes the pseudosubstrate inhibition on the catalytic domain, allowing PKC to bind and phosphorylate substrates. Reprinted from Drug Resistance Updates: Reviews and Commentaries on Antimicrobial and Anticancer Chemotherapy, 6 (6), Lorenzo PS and PA Dennis. "Modulating Protein Kinase C (PKC) to increase the efficacy of chemotherapy: Stepping into the darkness", 2003, 329-339, with permission from Elsevier (119).

mediators (114,120). Activation of PKCα increases RhoA activity and stress fiber formation through phosphorylation of p115RhoGEF (116) and RhoGDI-1 (115). PKCα activation has also been shown to alter the phosphorylation state of VE-cadherin, β-catenin and p120, resulting in disruption of VE-cadherin adhesion (114), however the mechanism in which PKCα disrupts junctions has not been fully elucidated.

1.5.1 Statement of Aim 1

PKCα has been shown to regulate endothelial permeability and AJs, however the mechanism is unclear. This is in part due to the lack of a relevant physiologic model to determine the effect of PKCα activation on increased permeability and resulting edema. In Section 3, we address PKCα regulation of endothelial permeability, specifically regulation of AJ integrity. We utilize a PKCα knockout mouse model, among other methods, to show the impact PKCα has on lung permeability and to determine a therapeutic target to reduce edema caused by PKCα activity.

1.6 p120-catenin

p120 was originally discovered as a Src substrate and classified as an oncoprotein (121). Later, it was found to bind cadherins and was placed as a member of the catenins family due to the repeated, highly conserved amino acid sequence it contains to bind cadherins, known as armadillo repeat motifs (ARM). p120 contains 10 ARMs, and uses ARM 1-5 to bind cadherins (86) (Figure 6). The ARM repeats are flanked by a short CTD, with an unknown function, and a regulatory N-terminal domain (NTD), which contains a phosphorylation domain. There are 4 ATG start sites, resulting in 4 p120 isoforms (122), with

p120-1 and p120-3 the most widely expressed in humans (123). p120-1 is the only isoform that contains the coiled-coil domain, which recently has been suggested to also bind cadherins (124). It also is able to bind other coiled-coil-containing proteins, such as delta interacting protein A (DIPA) (125), highlighting the functional diversity of p120 isoforms. p120 also contains 3 alternatively spliced exons (A, B and C), giving rise to different splice variants (122), however the functional consequence of different splice variants is under investigation.

p120 stabilizes cadherins by binding to the JMD, preventing internalization of the cadherin (126). It is a ubiquitously expressed member of a subset of the ARM family of proteins that include δ-catenin (127), ARVCF (Armadillo Repeat gene deleted in Velo-Cranial-Facial syndrome) (128), p0071 (129), and plakophilins (130) . There are functional redundancies between proteins within the family, however p120 expression is essential in vertebrates while the loss of other family members are tolerated (131). p120 has a homolog in Drosophila, which is non-essential, and two splice variants in mice, M1 and M3, which correspond to human p120-1 and p120-3 (123,131). p120 isoforms exhibit tissue-specific localization, with the long isoform (p120-1) expressed in vascular endothelial junctions, and p120-3 in epithelial cells and fibroblasts (123). Isoform p120-4 lacks the NTD phosphorylation domain altogether, and is rarely expressed in tissue (131).

In the last 20 years, p120 downregulation has been attributed to disease states such as ARDS, diabetes-associated vascular disease, Crohn's Disease and several different cancers (132-134). Mouse models using p120 deletion and cell depletion of p120 have provided interesting insights to the diverse function of p120. Global knockout of p120 in mice is early embryonic lethal due to impaired

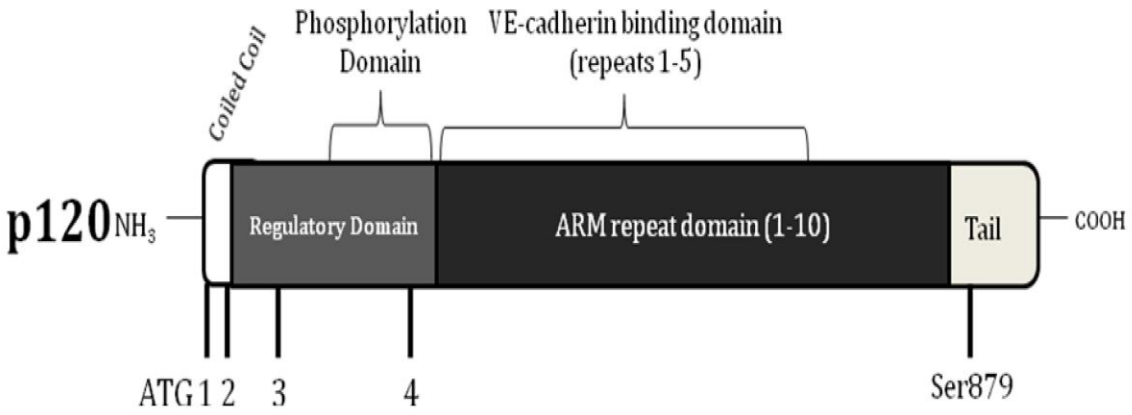

Figure 6: p120 structure. p120 is subdivided into 4 domains. The NTD regulatory domain contains the majority of the phosphorylation sites, which is termed the phosphorylation domain, and contains 9 tyrosine residues and 6 serine/threonine residues that have been shown to be phosphorylated. The armadillo repeat domain contains 10 ARM repeats, which bind cadherins at repeats 1-5. The CTD tail contains 2 phosphorylation sites, S879 and threonine 910, with an unknown function. There are 4 different ATG start sites, which gives rise to 4 different isoforms. While they all contain the ARM domain and the CTD, p120-1 is the only isoform to contain the coiled-coil domain and p120-4 lacks the phosphorylation domain.

microvessel formation (135). Conditional p120 knockout mouse models have shown that p120 is essential for regulating cadherin expression during vascular development (135), as well as assembly of AJs (136,137). Loss of p120 in the neonatal intestinal barrier leads to catastrophic inflammation (136), and loss of p120 in other tissues has been shown to lead to development of a tumor microenvironment by increasing immature myeloid cells (137). Decreased p120 in tumor cells lines predicts a more invasive phenotype, presumably due to the resulting decrease in surface expression of cadherins (133). Similarly, a decrease in p120 results in more severe inflammation and increased mortality (64). Conditional knockout of p120 increases inflammation by increased cytokine production (136) and increased NF-κB activity (134). It also reduces the response to LPS by interfering with TLR-4 signaling (64).

The mechanisms behind these phenotypes are not completely understood, but it is clear that different cellular pools of p120 have different functions. As previously mentioned, nuclear p120 regulates expression of pro-inflammatory genes through binding transcription suppressor Kaiso (102). p120 suppresses transcription of pro-inflammatory mediators, including Intercellular Adhesion Molecule (ICAM)-1, NF-κB, AP-1 and E and P-selectins (138,139), which may be part of a feedback mechanism to reduce inflammation once p120 is lost from AJs. Cytoplasmic p120 is involved in cadherin trafficking to the cell surface during junction reassembly, as well as regulation of RhoA activity (126,140). p120 regulates cadherin trafficking by acting as a scaffold and recruiting the microtubule motor protein kinesin, then moving in a unidirectional manner on microtubules to relocate cadherins to AJs (141). p120 inhibits RhoA activity by directly functioning as a Rho Guanine nucleotide Dissociation Inhibitor

(GDI), which p120 is only able to do if not bound to cadherins (140). p120 can also indirectly inhibit RhoA activity while incorporated in AJs through binding and suppressing p190RhoGAP (142). Finally, p120 was recently shown to affect cell cycle progression in cancer cells by causing up-regulation of cyclin D1 and cyclin E, possibly in conjunction with Kaiso or β-catenin (143).

Studies examining p120 regulation of cadherin stability have focused on post-translational modifications of its NTD that contains multiple phosphorylation sites (144). Tyrosine phosphorylation of p120 NTD controls p120 binding to RhoA (145), allowing p120 to function as a Rho GDI, yet it is insufficient to increase endothelial permeability (90). Furthermore, p120 maintains VE-cadherin surface expression and endothelial permeability independent of the presence of NTD (146). We focused on the CTD of p120, the domain containing two phosphorylation sites: threonine 916 and serine 879 (S879) (147). Threonine 916 phosphorylation does not appear to affect VE-cadherin interaction with p120 (148). However, S879 is of particular interest since it in is a PKC consensus motif. Phosphorylation of S879 is PKCα-dependent, and S879 is phosphorylated in response to inflammatory mediators and growth factors in endothelial cells, epithelial cells, and fibroblasts (147,149,150), but no functional significance of S879 phosphorylation has even been shown. The majority of serine or threonine phosphorylation on p120 is constitutive (148), and S879 is a rare site that is unphosphorylated under resting conditions and phosphorylated during inflammation. Likewise, while PKC activation causes de-phosphorylation of several residues, S879 is the only site that is phosphorylated in response to PKC activation (147).

1.6.1 Statement of Aim 2

S879 on p120 is phosphorylated in response to many different pro-inflammatory mediators, however no downstream mechanisms have even been elucidated. p120 is vital to regulation of VE-cadherin stability at AJs, and for the integrity of interendothelial junctions and vascular permeability. We know that S879 is phosphorylated by PKCα, which has previously been suggested to cause disassembly of AJs during inflammation. In Section 4, we address the role of S879 phosphorylation of p120 by PKCα in regulation of endothelial permeability, specifically regulation of p120 binding affinity toward VE-cadherin. We utilize primary cell culture, as well as expression of p120 mutants in mice, to dissect the effect S879 phosphorylation has on the p120/VE-cadherin complex, and the resulting effect it has on AJ integrity.

2. MATERIALS AND METHODS

2.1 Materials

Primary endothelial cells and media were obtained from Lonza (Basel, Switzerland). Human α-thrombin was obtained from Enzyme Research (South Bend, IN) and LPS from Sigma (St. Louis, MO). PAR-1 agonist peptide (TFLLRNPNDK-NH_2) was synthesized (151). PKCα siRNA (UAAGGAACCACAAGCAGUAUU) and mismatch (MM) control (UAAGGAGCCACGAGCGGUAUU) siRNA were purchased from Dharmacon (Lafayette, CO). Anti-p120, anti-VE-cadherin, and anti-GAPDH were purchased from Santa Cruz Biotechnologies (Santa Cruz, CA) and anti-PKCα, anti-p-PKCα, and anti-Na-K ATPase from Cell Signaling (Beverly, MA). pS879-p120 was purchased from BD Biosciences (San Jose, CA) and anti-GFP from GeneTex (San Antonio, TX). EZ-Link Sulfo-NHS-SS-Biotin and high capacity Streptavidin Agarose Resin were from Thermo Fisher (Rockford, IL). AlexaFluor 488 and 594 secondary antibodies and ProLong were from InVitrogen (Grand Island, NY). S879A-p120-1A and WT-p120-1A cDNA were gifts from Dr. Al Reynolds (Vanderbilt University) and S879D-p120-1A was generated using the QuikChange site-directed mutagenesis kit from Stratagene (Santa Clara, CA). Primers used to create p120-S879D mutation were 5' CCCCTCATTGACCGGAATCAAAAAGATGATAAGAAACCTGACCGG 3'(sense) and 5' CCGGTCAGGTTTCTTATCATCTTTTTGATTCCGGTCAATGAGGGG 3' (antisense).

2.2 Mice

prkca$^{-/-}$ mice were a gift from Dr. Jeffrey Molkentin (University of Cincinnati) (152). Genetic background of *prkca*$^{-/-}$ mice is C57/Bl6. *prkca*$^{-/-}$ mice had no overt phenotype through 16 weeks of age (152), and appeared normal in terms of viability and fertility. Control mice were of C57/Bl6 genetic background (obtained from Jackson Laboratory, Bar Harbor, ME). Experiments were made using 8-10

week old males. All mice were bred and maintained in the Association for Assessment and Accreditation of Laboratory Animal Care-accredited facilities at the University of Illinois at Chicago in accordance with NIH guidelines. Approval for animal care and for all experiments was granted by the IUCAC of University of Illinois at Chicago.

2.2.1 Genomic Analysis of Mice

Genotype of *prkca*$^{-/-}$ mice was confirmed using DNA extracted from a tail snip from 10-14 day old pups. DNA was extracted and amplified using the REDExtract-N-Amp tissue PCR kit from Sigma (St Louis, MO) and primers 5'-GCGCATCGCCTTCTATCGC-3', 5'-AGCTAGGTCCTGTTGGTAAC-3', 5'-CCAAGTGTGAAGTGTGTGAG-3', as according to the protocol.

2.3 Mouse Lung Preparation and Permeability Measurement

2.3.1 Microvessel Filtration Coefficient

Wild-type control (WT) and *prkca*$^{-/-}$ mice were placed in chamber and anesthetized with 3% halothane with an air flow rate of 2 ml/min. The microvessel filtration coefficient ($K_{f,c}$) is a measure of pulmonary microvascular permeability to fluid and is defined as the rate of weight gain over the imposed change in capillary pressure (50). Mouse lungs were perfused *in situ* using a peristaltic pump, excised and placed on a force-displacement transducer. The lung weight was electronically nulled and the outflow pressure was then elevated by 10 cm H_2O for 30 minutes. The weight gain was recorded, $K_{f,c}$ (ml x min^{-1} x cm H_2O) was calculated from the slope of the weight gain and normalized to the dry lung weight (lungs were dried overnight at 60°C).

2.3.2 Evans Blue Albumin Extravasation

Evans Blue Albumin (EBA; 20 mg/kg) was injected using a retro-orbital i.v. injection together with PAR-1 peptide (TFLLRNPNDK-NH_2, 1 mg/kg) 30 minutes before euthanasia (68). Blood was collected from the right ventricle into heparinized syringes and plasma was separated by centrifugation at 1,300 *x g* for 10 minutes. The lungs were perfused with PBS containing 5nM EDTA via thoracotomy, excised *en bloc*, blotted dry, weighed and snap frozen. The right lung was homogenized in PBS (1 ml/100 ug tissue), incubated with 2 volumes formamide for 18 hours at 60°C, centrifuged at 5,000 *x g* for 30 minutes, and the optical density of the supernatant was measured with a spectrophotometer at 620 nm. The extravasated EBA concentration was calculated against a standard curve (µg Evans blue dye/lung). Finally, the left lung from the same mouse were excised and dried at 60°C overnight for calculation of wet-dry ratio.

2.4 Liposome Preparation and Delivery of cDNA

Cationic liposomes (100 µl) were prepared using a 1:1 molar ratio of dimethyldioctadecyl-ammonium bromide (DDAB; Sigma) and cholesterol (Calbiochem, La Jolla, CA) in chloroform (77). The solution was dried with a Rotavaporator (Brinkmann, Westbury, NY), dissolved in 5% glucose and sonicated for 20 minutes. 50 µg cDNA was mixed with 100 µl of liposomes, and injected via a retro-orbital i.v.

2.5 Cell culture and transfection

Human lung microvascular endothelial cells (HLMVECs) and human pulmonary artery endothelial cells (HPAECs) were cultured in T-75 flasks on 0.1% gelatin in EBM-2 or EGM-2 (Lonza), respectively, supplemented with 10% FBS. Cells were kept at 37°F in humid air with 5% CO_2, and all cells were used between passages 4-7. HLMVECs were transfected with siRNA at 80% confluence by nucleofection, using the AMAXA kit (Lonza), and used 72 hours post-transfection. HPAECs were transfected at 70% confluence using Turbofect (Fermentas, Glen Burnie, MD) as according to the instructions, and used 48 hours post-transfection.

2.6 Transendothelial Electrical Resistance

Transfected cells were seeded on a gelatin-coated gold electrode ($5.0\times10^4/cm^2$) and grown to confluence. The small electrode and the larger counter-electrode were connected to a phase-sensitive lock-in amplifier. A constant current of 1 μA was supplied by a 1-V, 4000-Hz AC signal connected serially to a 1 MΩ resistor between the electrodes. The voltage was monitored by a lock-in amplifier, stored and processed by a computer. The same computer controlled the amplifier output and switched the measurement to different electrodes during an experiment. Before each experiment, endothelial monolayers were washed with serum-free medium and used for measuring changes in transendothelial electrical resistrance (TER). TER was measured in real-time using ECIS software (Applied Biophysics, Troy, NJ) and expressed as specific electrical resistance ($\Omega\ cm^2$). Data are presented as the change in resistance, normalized to its value at time 0.

2.7 Fluorescent Imaging

Cells were grown to confluence on glass coverslips, serum-starved, and treated with thrombin (4 U/ml). Cells were fixed in 4% paraformaldehyde and permeabilized with 0.05% Triton-X. Cells were incubated in primary antibodies, then secondary, fluorescently labeled secondary antibody and finally mounted on slides with ProLong anti-fade reagent (Invitrogen). Cells were visualized using a 63x 1.2 NA objective on a LSM 510 Meta confocal microscope (Carl Zeiss, Inc.) with Ar ion and dual HeNe lasers, driven by LSM software.

2.7.1 Time-Lapse Imaging

Cells were serum starved in phenol-free EBM media (Lonza) and maintained at 37°C with a stage heater (Tempcontrol-37, Zeiss, Thornwood, NJ). Images were acquired every 10 seconds using the Nikon Eclipse TE-2000S microscope equipped with UltraView confocal head (PerkinElmer Life Sciences), ORCA-ER-1394 camera (Hamamatsu, Bridgewater, NJ), AR/KR 3-line laser (λ=488, 568 and 647 nm) Plan Apo 100x 1.4NA objective and Volocity 5 software (Improvision, Waltham, MA). Thrombin (4 U/ml) or PBS was applied to cells after the second exposure. As we observed no significant photobleaching, no correction for photobleaching was required.

2.7.2 Image Analysis

Interendothelial gap area and average fluorescence intensity of p120 and VE-cadherin at AJs was quantified using MetaMorph software (Molecular Devices, Sunnyville, CA). Projection images were generated by collecting the maximum pixel intensity from each image of the z-stack and projecting

pixel intensity onto the single (projection) image. The relative accumulation of VE-cadherin or p120 (mean fluorescence intensity) at AJs and the area of gaps were measured on projected images. The 12-bit images were thresholded by subtracting the intracellular background, and the mean fluorescence intensity at AJs was measured. The area of intercellular gaps was quantified using MetaMorph 7.1.0 by manually outlining cells and selecting for gaps. The values are expressed as a percentage of the total surface area. The dissociation of p120-GFP and mutants from AJs was quantified by kymograph analysis and expressed as fluorescence decay.

2.8 Biochemical Analysis

Cells were lysed with a modified ODG buffer (50 mM Tris-HCl, pH 8, 150 mM NaCl, 1% Triton X-100, 5% glycerol, 10 µg/ml leupeptin, 10 µg/ml aprotinin, and 0.1 mM PMSF) (153), centrifuged at 14,000 rpm for 20 minutes at 4°C, and pellets were removed and discarded. Equal protein concentration of the resulting lysate was determined using a BCA protein assay kit (Pierce) following the manufacturer's instructions. Samples were run on 4-12% gradient NuPAGE gels (Invitrogen) as according to the protocol. Proteins were transferred to a PVDF membrane, blocked with 3% BSA and incubated in primary antibody. For immunoprecipitation experiments, 350 µg of total protein was incubated with a primary antibody at 4°C, and precipitates were collected with protein A/G agarose beads (Santa Cruz) and analyzed by Western Blot. Densitometry of scanned protein bands was perfomed using ImageJ software (NIH, Bethesda, MD), and changes in protein expression were normalized to loading controls.

2.8.1 Cell Fractionation

Cells were washed with cold PBS, manually scraped off plates using PBS, and centrifuged at 7,000 rpm for 10 minutes at 4°C. Cells were resuspended in Lysis Buffer A (50 mM HEPES-NaOH pH 7.4, 1 mM DTT, 10 µg/ml leupeptin, 10 µg/ml aprotinin, and 0.1 mM PMSF) and lysates were sonicated briefly, then centrifuged at 40,000 rpm for 20 minutes at 4°C. The supernatant was collected and set aside as the cytosolic portion. The remaining pellet was resuspended in Lysis Buffer B (50 mM HEPES-NaOH pH 7.4, 10 mM DTT, 1% Triton-X, 1% DOC, 0.1% SDS, 10 µg/ml leupeptin, 10 µg/ml aprotinin, and 0.1 mM PMSF), then centrifuged at 55,000 rpm for 40 minutes at 4°C. The supernatant contained the membrane-bound fraction. Both lysates were assayed for total protein, and were analyzed by Western Blot as previously described.

2.8.2 Biotinylation

Cells were placed on ice and rinsed with PBS containing Ca^{2+} and Mg^{2+}. Cells were then labeled with 0.2 mg/ml sulfo-NHS-SS biotin in Ca^{2+} and Mg^{2+}-containing PBS for 45 minutes on ice. Cells were rinsed with Ca^{2+} and Mg^{2+}-containing PBS on ice, then incubated in for 10 minutes in 50 mM Tris (pH 8) with 100 mM NaCl to quench unbound biotin. Cells were rinsed again with PBS, then lysed as described for immunoprecipitation. Biotinylated proteins were precipitated overnight with streptavidin agarose resin at 4°C, and precipitated proteins were analyzed by Western Blot as previously described.

2.9 Surface Plasmon Resonance

Proteins were generated from cDNA using *in vitro* protein expression kit (Pierce, Rockford, IL) as according to the instructions. Surface plasmon resonance (SPR) biosensor binding experiments were

done at 25°C on a CM-5 sensor chip (GE Healthcare, Burr Ridge, IL) using a 150 mM NaCl (pH 7.4), 10mM HEPES, 3 mM EDTA and 0.005% Surfactant P20 running buffer. VE-cadherin was immobilized directly on the chip, and was achieved at pH 5.0. p120 was programmed to flow over VE-cadherin at rate of 10 μg/min for 180 seconds for binding analysis. Between samples, chips were washed with running buffer to remove bound p120, and regeneration was done at pH 2.5. Non-specific binding was calculated by subtracting the response of p120 binding to an empty cell from p120 binding to VE-cadherin. At least 7 different concentrations of each analyte were used to assess binding affinity, and the ligand was not allowed to be saturated to avoid binding to non-functional or dead ligands. Measurements were made using Biacore T100 (GE Healthcare), and calculations of binding affinity were made using the Biacore T100 Evaluation Software.

2.10 Peptide Generation and Application

PKCα blocking peptide (Myr-LIPDPKNESKQKTKTIRS) is the sequence of PKCα from amino acid 200-217, and was generated based on the peptide used by Martelli *et. al* (2002) (154). Varying concentrations of the peptide were directly applied to HPAECs in serum-free medium, prior to thrombin stimulation, for 30 minutes. Antennapedia (RQIKIWFQNRRMKWKK), a cell permeable peptide, was used as a control.

2.11 Statistical Analysis

Student's *t* test and ANOVA with Bonferroni post-hoc tests were used to determine significance. $P < 0.05$ denoted a significant difference.

3. PKCα REGULATES ADHERENS JUNCTION INTEGRITY

*Portions of the text and figures 8, 9, 11-14 and 16-21 were reprinted with permission from Vandenbroucke St Amant, E., Tauseef, M., Vogel, S.M., Gao, X., Mehta, D., Komarova, Y. and Malik, A.B. (2012) PKCalpha activation of p120-catenin serine 879 phospho-switch disassembles VE-cadherin junctions and disrupts vascular integrity. *Circulation Research*, 111, 739-749.

3.1 PKCα Activation Increases Endothelial Permeability

To determine the role of PKCα in increasing vascular permeability *in vivo*, we obtained PKCα knockout mice (*prkca*$^{-/-}$). The knockout mice were created to investigate the role of PKCα in cardiac contractility (152), and showed that PKCα deletion increased contractility in response to pressure-induced overload in murine hearts due to changes in Ca^{2+} signaling, and protected against cardiomyopathy and heart failure (152). Before we assessed the effects of PKCα deletion on lung permeability, genotypes of *prkca*$^{-/-}$ mice were verified with PCR (Figure 7). The *prkca*$^{-/-}$ cassette is 100 bp longer than the *prkca*$^{+/+}$ (WT), and we confirmed that all transgenic mice were *prkca*$^{-/-}$. Using WT and *prkca*$^{-/-}$ mouse lungs, we measured the change in total PKC activity and found deletion of PKCα caused a 50% reduction in total activity (Figure 8A). We also looked for possible compensation in expression of PKC isoforms β, δ, ε and ζ, which are also expressed in mouse lungs. However, western blot analysis showed no change in protein expression of other PKC isoforms in the lung (Figure 8B).

To assess the effect of PKCα deletion on endothelial barrier function, we measured the $K_{f,c}$ in WT and *prkca*$^{-/-}$ mice. $K_{f,c}$ is a measure of vessel wall permeability to fluid, based on the hydraulic conductivity and the surface area available for exchange (50). We used PAR-1 agonist peptide, which activates PKCα downstream of PAR-1 in endothelial cells, to stimulate increased permeability (5,113).

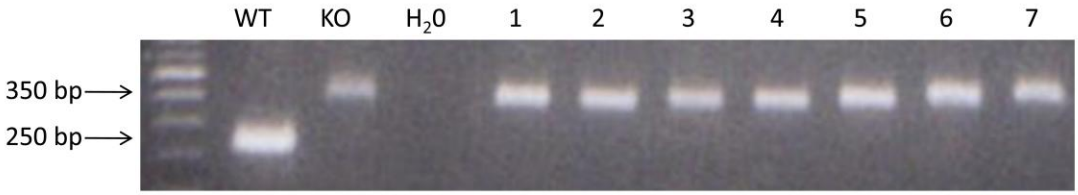

Figure 7. Genomic analysis of *prkca*$^{-/-}$ mice. PCR of *prkca*$^{-/-}$ mouse tail snips, used to extract DNA and confirm expression of the targeting vector and deletion of PKCα. Samples 1-7 were transgenic mice, and WT, plasmid (KO) and H_20 were used as controls.

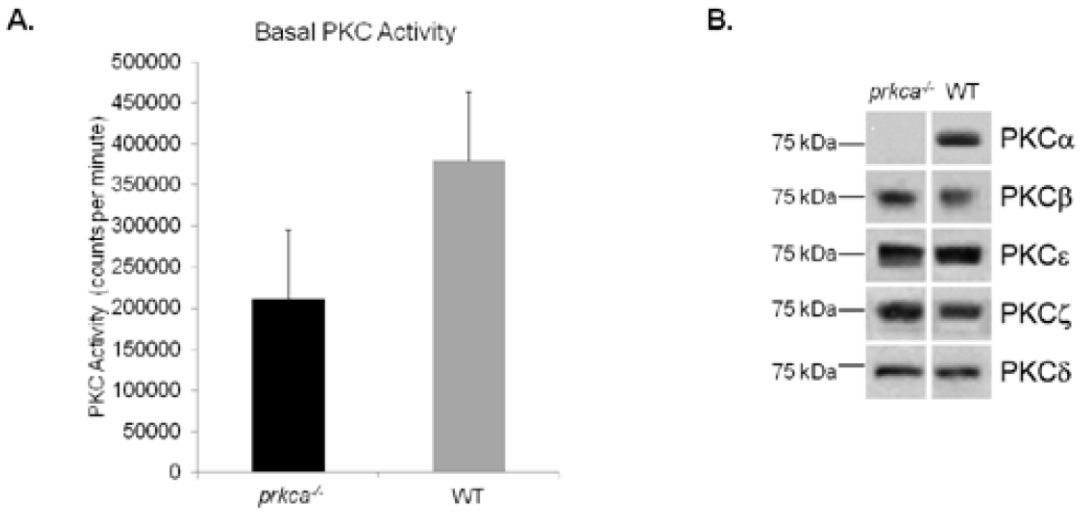

Figure 8: PKCα deletion decreases total PKC activity without altering expression of other PKC isoforms. (A) WT or PKCα null lungs were homogenized and total PKC activity was determined using myelin basic proteins. WT lung homogenates show 50% more PKC enzyme activity as compared to *prkca*$^{-/-}$ mice. (B) Immunoblots of lung homogenates show no alteration in protein expression of any other PKC isoforms known to be expressed in the lung. Reproduced with permission from Vandenbroucke St Amant, E. et al. *Circ Res* 2012;111:737-749(155).

There was no statistical difference in baseline $K_{f,c}$ between *prkca*$^{-/-}$ and WT lungs (Figure 9). Activation of PAR-1 increased the $K_{f,c}$ of WT lungs to 1.90 $\pm$ 0.06 ml/m/cm H_2O/g dry lung weight, whereas the $K_{f,c}$ of *prkca*$^{-/-}$ lungs increased to only 0.69 $\pm$ 0.04. The significantly higher change in permeability of WT lungs, as compared to *prkca*$^{-/-}$ lungs, confirms that PKCα is required to elicit a full increase in permeability downstream of PAR-1 activation.

To dissect the mechanism in which PKCα is increasing vascular permeability, we created a model of PKCα depletion in HLMVECs using PKCα siRNA. Cells were treated with four different PKCα siRNAs (1-4), lysed and immunoblotted with anti-PKCα after 72 or 96 hours to determine the siRNA that was most effective in reducing PKCα protein expression (Figure 10). A scramble siRNA and transfection reagent alone (untreated) were used as controls. PKCα siRNA-1 at 72 hours was the most effective at depleting PKCα, achieving over 90% depletion. We used PKCα siRNA-1 on HLMVECs for 72 hours to decrease PKCα expression in the following studies. We mutated three residues on the PKCα siRNA-1 sequence to create a mismatch (MM) control siRNA.

Using PKCα-depleted HLMVECs, we questioned the role of PKCα in mediating the stability of interendothelial cell junctions. We transfected HLMVECs with PKCα or MM control siRNA, stimulated with thrombin to activate PAR-1, and measured TER changes to assess the change in monolayer permeability (Figure 11). Baseline TER values were similar between PKCα siRNA and MM control-treated monolayers, however, thrombin stimulation produced only a 35% decrease in TER in PKCα-depleted monolayers while TER decreased 70% from baseline in MM control monolayers (Figure 11B).

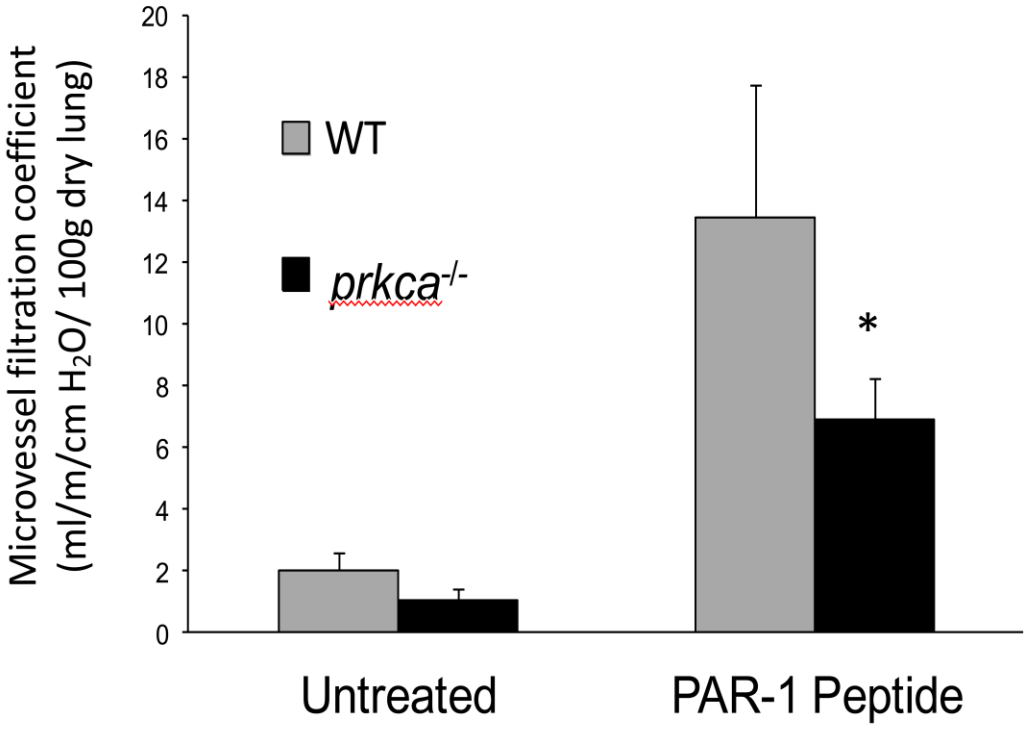

Figure 9: PKCα knockout mice exhibit a decreased permeability response to PAR-1 activation. Lungs from PKCα knockout (*prkca*$^{-/-}$) and wild-type (WT) mice were perfused with PAR-1 agonist peptide (1 mg/kg) or untreated (control). Graph shows $K_{f,c}$ as mean ± SEM (n=4). * $p<0.05$ denotes significance from WT after PAR-1 peptide stimulation. Reproduced with permission from Vandenbroucke St Amant, E. et al. *Circ Res* 2012;111:737-749(155).

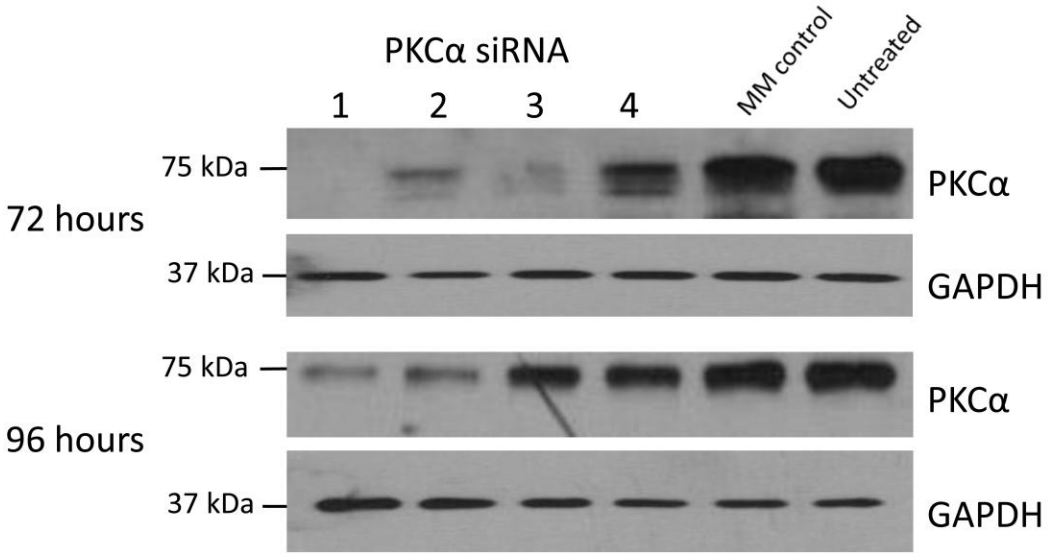

Figure 10: siRNA-induced depletion of PKCα. Immunoblots show PKCα expression in HLMVECs at 72 hours (top) or 96 hours (bottom) after treatment with PKCα siRNA (1-4), MM control siRNA or untreated cells. GAPDH is shown as loading control.

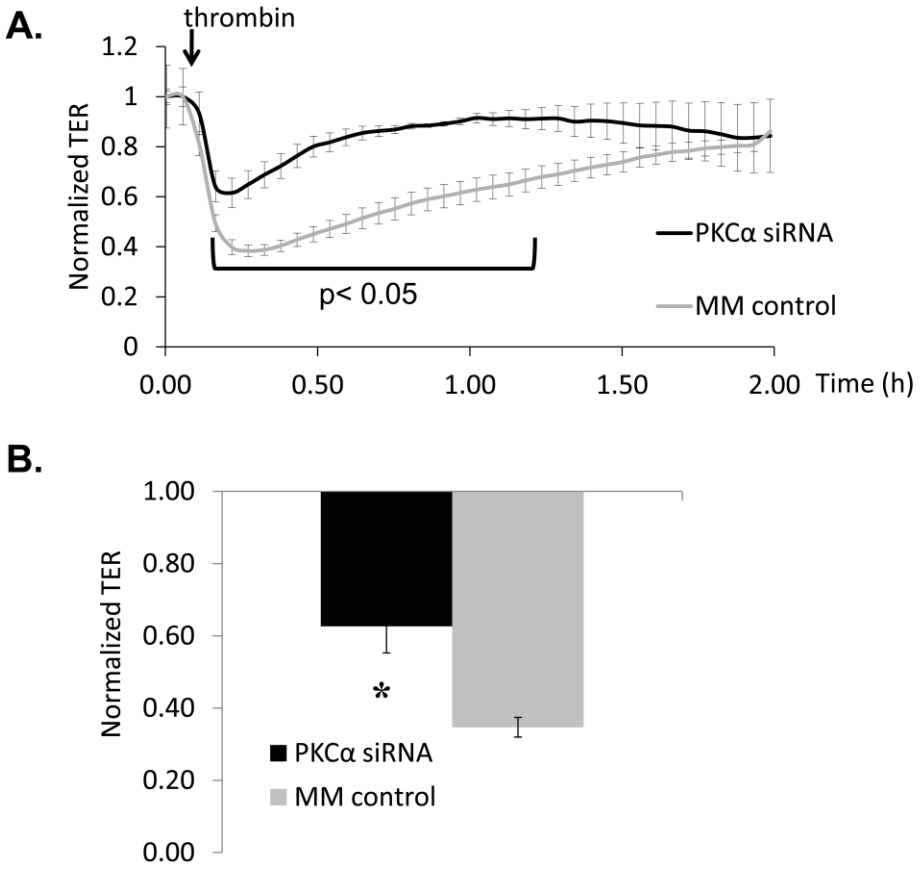

Figure 11: Deletion of PKCα reduces the thrombin-induced decrease in TER. (A) Traces show the change in TER in HLMVECs transfected with PKCα siRNA or MM control siRNA. Arrow shows addition of thrombin (4 U/ml). Results are expressed as mean ± SEM (n=3). (B) Mean ± SEM of the maximum decrease in TER after thrombin stimulation (n=3). * denotes significance ($p<0.05$). Reproduced with permission from Vandenbroucke St Amant, E. et al. *Circ Res* 2012;111:737-749 (155).

Cells depleted of PKCα maintained a more intact endothelial monolayer, confirming that PKCα expression decreases monolayer integrity in response to thrombin.

3.2 PKCα Induces Formation of Interendothelial Gaps

PKCα has been shown to disrupt endothelial permeability via regulation of RhoA (66,115). PKCα has also been shown to alter phosphorylation of AJ proteins (114), but the effects of PKCα-induced changes in phosphorylation and the role of PKCα in AJ regulation and interendothelial gap formation is not well understood. To determine if PKCα-induced alteration in phosphorylation of AJs causes disassembly of AJs, we first questioned whether PKCα activity is required to disrupt AJs. PKCα-depleted cells were stimulated with thrombin and immunostained for VE-cadherin and PKCα (Figure 12). Interendothelial gap formation was apparent within 15 minutes of thrombin stimulation in control cells, while gaps were barely visible in the PKCα-depleted monolayer. After 30 minutes of stimulation, gaps covered 11% of the monolayer in control cells but only 3% of monolayer in PKCα-siRNA treated cells (Figure 12B), confirming that PKCα causes interendothelial gap formation. We also quantified VE-cadherin retention at AJs after thrombin stimulation to determine if PKCα contributed to gap formation through regulation of VE-cadherin stability at AJs. MM control-treated cells lost 66% of VE-cadherin from AJs by 30 minutes after thrombin, whereas only 22% of VE-cadherin was lost in PKCα-depleted cells (Figure 12C). The significant change in VE-cadherin retention at AJs suggests that PKCα reduces VE-cadherin stability at AJs after thrombin stimulation, causing disassembly of AJs and interendothelial gap formation.

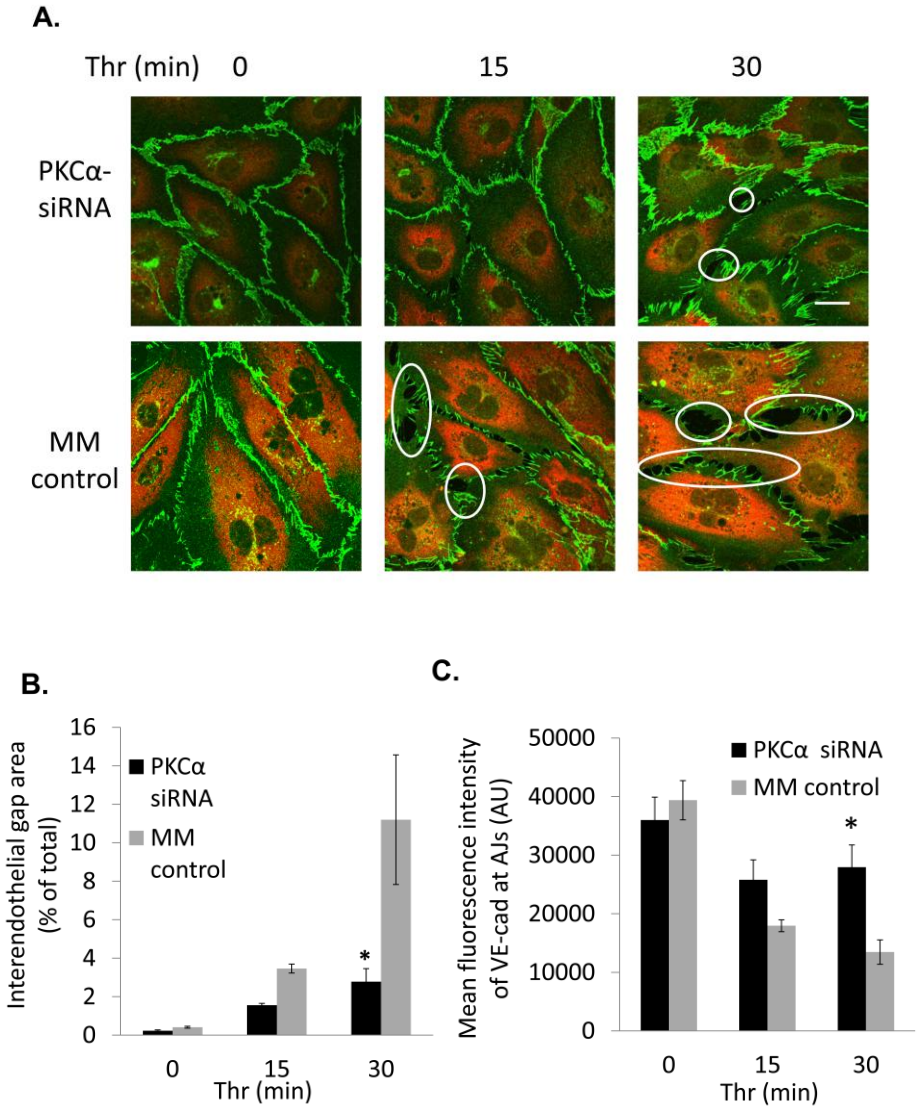

Figure 12: PKCα decreases VE-cadherin at AJs in response to thrombin stimulation. (A) Immunofluorescent staining of HLMVECs transfected with PKCα or MM control siRNA for VE-cadherin (green) and PKCα (red) post-thrombin stimulation (Thr; 4 U/ml). Circles indicate interendothelial gaps. Scale bar, 10 μm. (B) Bar graph shows mean ± SEM of interendothelial gap area expressed as percent of total area in cells expressing PKCα siRNA or MM control siRNA. (n=5). (C) Bar graph shows mean ± SEM of fluorescence intensity of VE-cadherin at AJs in cells expressing PKCα siRNA or MM control siRNA (n=5). * denotes diffeence ($p<0.05$) between MM control and PKCα. Reproduced with permission from Vandenbroucke St Amant, E. et al. *Circ Res* 2012;111:737-749(155).

3.3 p120 Localization is Regulated by Activation of PKCα

VE-cadherin plasma membrane stability is regulated by binding to p120 (32,33), so we hypothesized that PKCα decreases VE-cadherin at AJs by signaling dissociation of p120 from VE-cadherin. We immunoprecipitated p120 from HLMVEC lysates and immunoblotted with activated PKCα (p-PKCα) or VE-cadherin to determine if active PKCα alters the interaction of p120 with VE-cadherin (Figure 13). p120 association with p-PKCα was evident within 5 minutes after thrombin stimulation, with maximum association occurring at 15 minutes (Figure 13B). p120 basally interacted with VE-cadherin but the interaction decreased by 73% after 15 minutes of thrombin stimulation. The inverse relationship between p120 association with VE-cadherin and p120 association with PKCα suggests once p120 binds PKCα, it decreases its association with VE-cadherin.

p120 is localized at the plasma membrane through its association with VE-cadherin. We addressed whether thrombin stimulation alters p120 localization at AJs, as it does VE-cadherin localization. Western blotting of cytosolic and membrane fractions showed that p120 is translocated to the cytosol after thrombin stimulation (Figure 14). Quantification of immunoblots revealed that 90% of p120 localizes at AJs in unstimulated cells, but within 15 minutes of thrombin stimulation 73% of p120 is relocated away from the junction, in the cytosol (Figure 14B). This indicates that thrombin induces p120 to localize away from AJs.

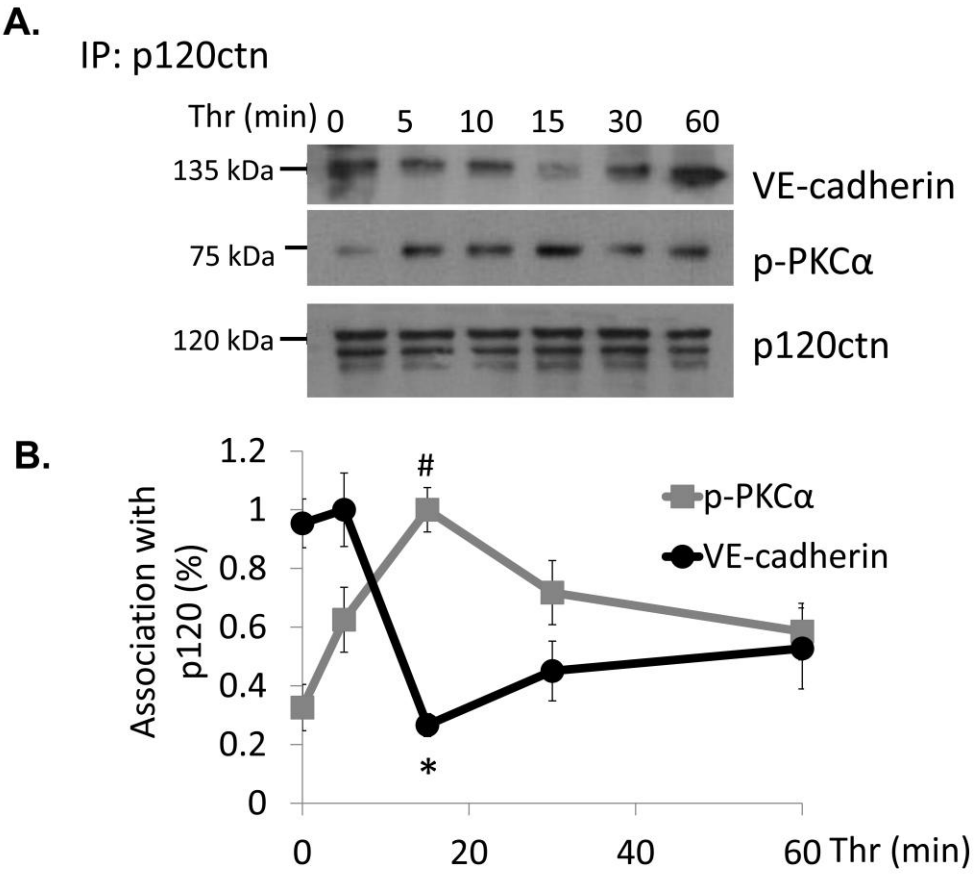

Figure 13: Thrombin alters p120 association with VE-cadherin and PKCα. (A) p120 was immunoprecipitated from HLMVEC lysates at indicated time points after thrombin stimulation (4 U/ml), and precipitates were immunoblotted for phospho-PKCα (p-PKCα; p-Ser657), VE-cadherin and p120. (B) Densitometric analysis of interactions of VE-cadherin and PKCα with p120. Data represent mean ± SEM (n=3). * and # denote difference from baseline ($p<0.05$). Reproduced with permission from Vandenbroucke St Amant, E. et al. *Circ Res* 2012;111:737-749(155).

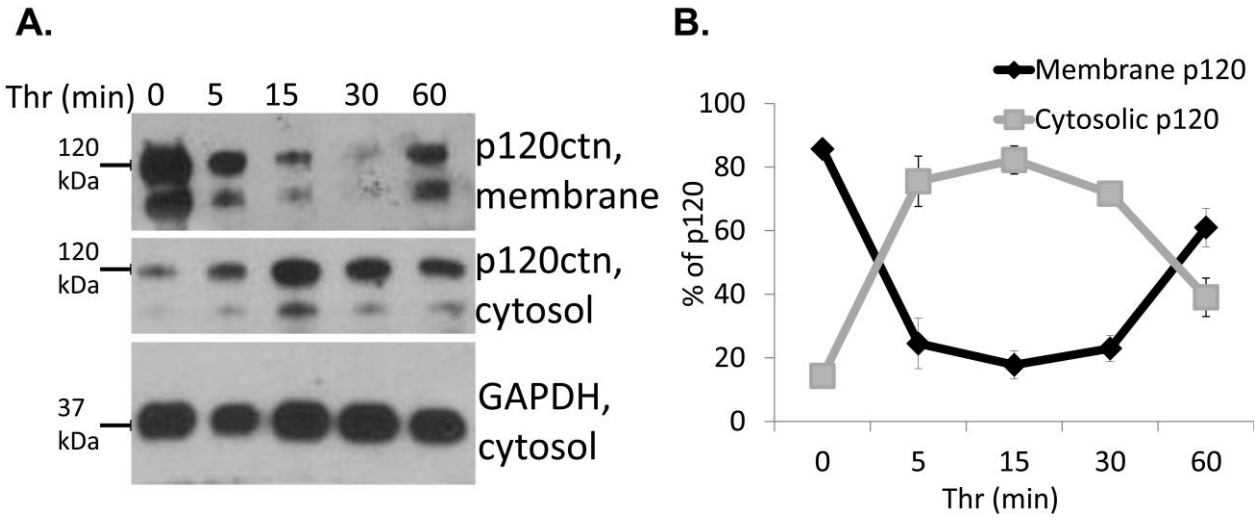

Figure 14: Thrombin induces redistribution of p120 in endothelial cells. (A) Lysates from thrombin-stimulated HLMVECs were separated into cytosolic and membrane-bound fractions and analyzed by Western Blot using anti-p120 antibody. Immunoblots with anti-Na-K ATPase and anti-GAPDH antibodies were used as loading controls. (B) Graph of changes in p120 distribution after thrombin stimulation. Densitometry of western blots is expressed as a percent of total p120; mean $\pm$ SEM (n=3). Reproduced with permission from Vandenbroucke St Amant, E. et al. *Circ Res* 2012;111:737-749(155).

We measured VE-cadherin retention at AJs to determine the time course of VE-cadherin internalization after thrombin stimulation (Figure 15). HLMVECs were stimulated with thrombin at indicated time points, and VE-cadherin that remained at AJs was labeled with biotin, then immunoprecipitated with streptavidin and analyzed by Western blot. Immunoblots of biotin-labeled VE-cadherin showed 73% of VE-cadherin was internalized within 30 minutes of thrombin stimulation. p120 achieves maximum localization away from AJs after 15 minutes of thrombin stimulation (Figure 14), suggesting that p120 dissociates and translocates away from AJs prior to VE-cadherin internalization.

To determine if the change in p120 localization induced by thrombin is regulated by PKCα, we used PKCα-depleted cells and quantified the change in p120 localization. HLMVECs treated with PKCα siRNA or MM control were treated with thrombin at indicated times, then immunostained for PKCα and p120 (Figure 16). Quantification of p120 fluorescence intensity revealed MM control cells had a 67% reduction in p120 staining at AJs after 30 minutes of thrombin stimulation but PKCα-depleted cells lost only 38% of the p120 from AJs (Figure 16B). PKCα depletion increased retention of p120 at AJs, confirming that PKCα causes p120 translocation away from the junction, possibly through regulation of the VE-cadherin/p120 complex.

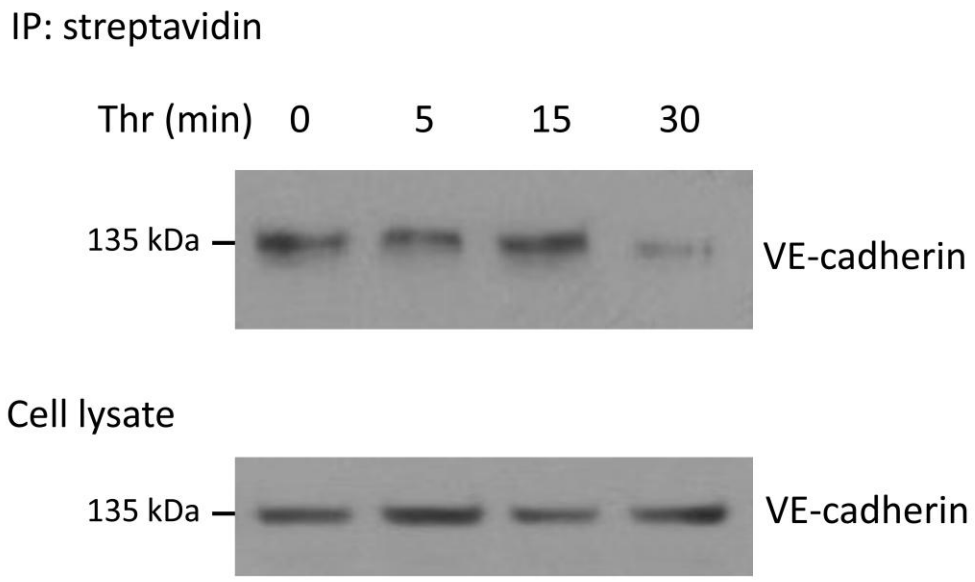

Figure 15: VE-cadherin is internalized following thrombin stimulation. HLMVECs were treated with thrombin then incubated with biotin. Cells were lysed and immunoprecipitated with streptavadin, followed by Western Blotting with anti-VE-cadherin antibody. Immunoblot shows VE-cadherin at the plasma membrane. Total VE-cadherin from cell lysate is shown as a loading control.

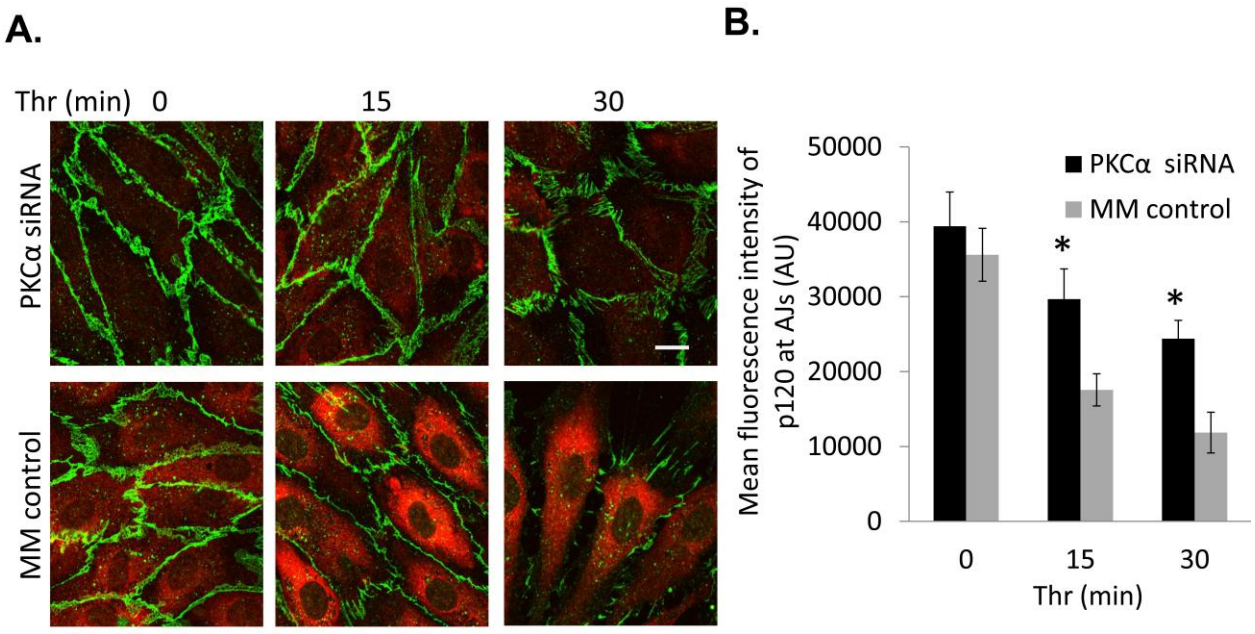

Figure 16: p120 is retained at AJs in PKCα-depleted cells. (A) siRNA-treated HLMVECs were immunostained for p120 (green) and PKCα (red). Representative images are shown at indicated times after thrombin stimulation. Scale bar, 10 µm. (B) Bar graph; mean ± SEM of fluorescence intensity of p120 at junctions (n=5). * denotes significance from MM control ($p<0.05$). Reproduced with permission from Vandenbroucke St Amant, E. et al. *Circ Res* 2012;111:737-749(155).

3.4 PKCα Regulates VE-Cadherin Stability and Association with p120

We next addressed whether p120 dissociates from VE-cadherin as a result of PKCα (Figure 17). We treated PKCα-depleted cells with thrombin, immunoprecipitated VE-cadherin and analyzed p120 association by Western Blot. Immunoblots showed only 7% of p120 dissociated from VE-cadherin in PKCα-depleted cells whereas 47% of p120 dissociated in MM control cells (Figure 17B). Cells depleted of PKCα maintained p120 binding to VE-cadherin after thrombin stimulation, indicating that PKCα is required to cause dissociation of p120 from VE-cadherin.

PKCα causes dephosphorylation of several residues on p120 (148), but causes phosphorylation of only one, at S879 (149). As previously mentioned, S879 is of particular interest because it is phosphorylated in response to several pro-inflammatory mediators, and because of its unique location on the CTD of p120 (149). To show S879 phosphorylation occurs in response to thrombin in HLMVECs, we performed Western blot analysis on HLMVEC lysates using an anti-pS879-p120 (Figure 18). The immunoblots confirmed that S879 was phosphorylated in response to thrombin stimulation, with maximum phosphorylation occurring between 5 and 15 minutes after thrombin. The lack of any detectable pS879-p120 in PKCα-depleted cells also confirmed that S879 phosphorylation is PKCα-dependent. The time course of S879-p120 phosphorylation correlates with p120 dissociation from VE-cadherin (Figure 13), suggesting that phosphorylation of S879 on p120 may induce p120 dissociation from VE-cadherin.

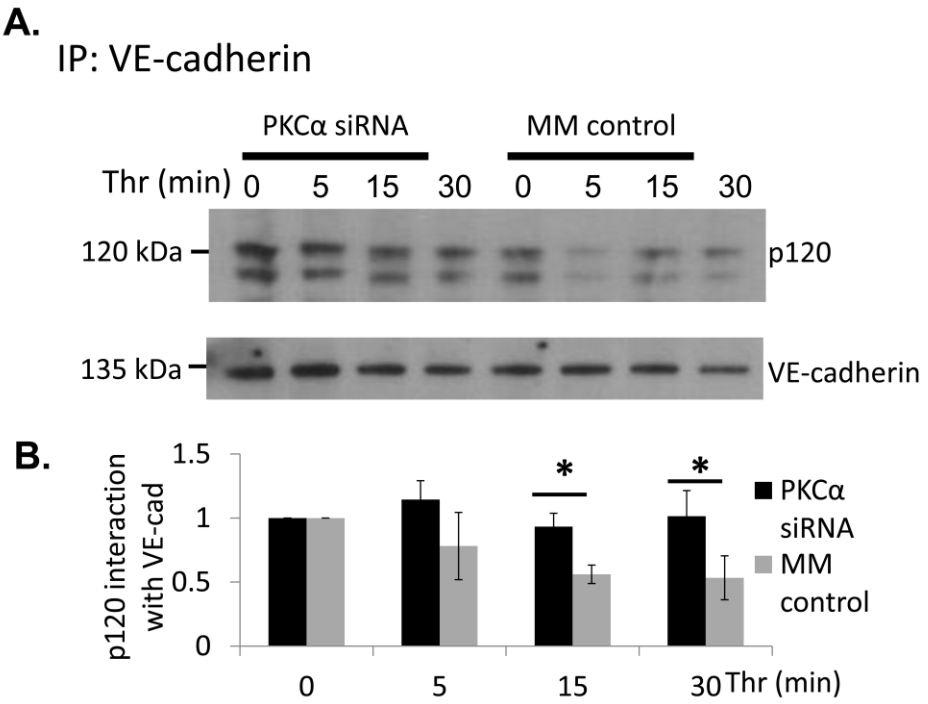

Figure 17: PKCα depletion prevents p120 dissociation from VE-cadherin. (A) VE-cadherin was immunoprecipitated from PKCα siRNA or MM control-transfected HLMVEC lysates at indicated times after thrombin stimulation. Precipitates were immunoblotted with anti- p120 and anti-VE-cadherin antibodies. (B) Bar graph shows densitometic analysis (n=3); * denotes difference from MM control ($p<0.05$). Reproduced with permission from Vandenbroucke St Amant, E. et al. *Circ Res* 2012;111:737-749 (155).

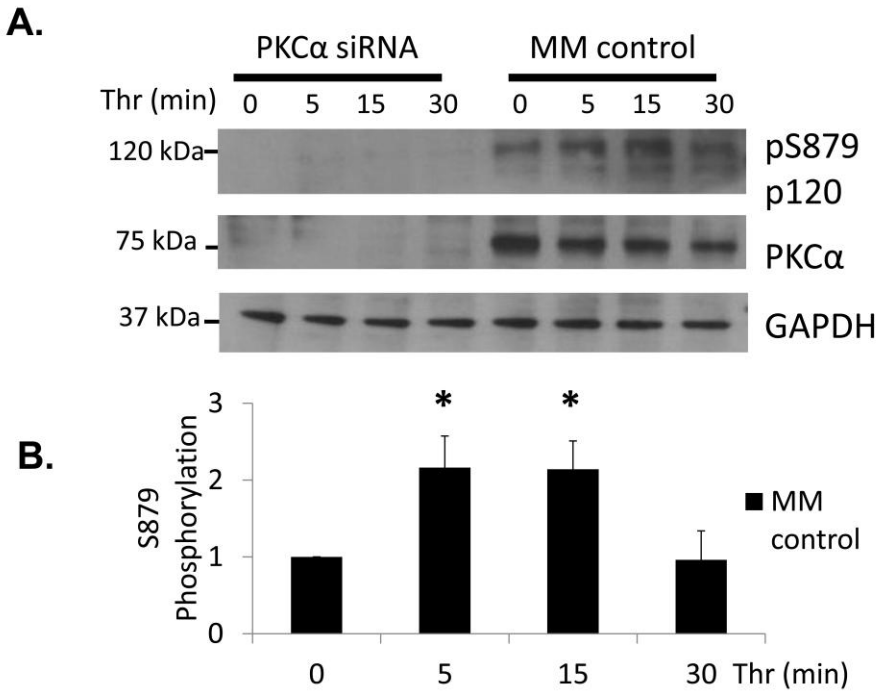

Figure 18: Thrombin-induced S879 phosphorylation of p120 is PKCα-dependent. (A) Western blot analysis was performed using lysates from HLMVECs transfected with PKCα-siRNA or MM control siRNA were treated with thrombin. Immunoblots show phosphorylation of S879 on p120 (pS879-p120). Immunoblot with anti-PKCα was used as control for PKCα depletion, and anti-GAPDH as a loading control. (B) Bar graph shows densitometric analysis of pS879-p120 (n=3), * denotes difference from MM control 0 timepoint. Reproduced with permission from Vandenbroucke St Amant, E. et al. *Circ Res* 2012;111:737-749 (155).

p120 binds the same residues on cadherins as the clathrin adaptor AP-2 (81,86), and functions as a cap to prevent AP-2 binding (81). p120 dissociation from VE-cadherin enables AP-2 binding, which results in VE-cadherin recruitment into clathrin-coated pits and internalization (81). To ascertain if PKCα activity affects AP-2 binding to VE-cadherin, we treated endothelial cells with thrombin, immunoprecipitated VE-cadherin and analyzed AP-2 association by Western Blot (Figure 19). Quantification of immunoblots showed that MM control cells had almost a 4-fold increase in AP-2 association with VE-cadherin within 15 minutes of thrombin stimulation, while PKCα-depleted cells had no significant increase in association, indicating that PKCα-depletion prevents AP-2 association with VE-cadherin.

3.5 LPS-Induced Increase in Endothelial Permeability Requires PKCα

To prove that PKCα increases endothelial permeability in a physiologically significant model, we challenged *prkca*$^{-/-}$ and WT mice with LPS (40 mg/kg) and measured the change in vascular permeability using $K_{f,c}$. At 6 hours post-LPS, the $K_{f,c}$ of WT mouse lungs increased to 0.120 $\pm$ 0.01 ml/m/cm H_2O/g dry lung weight whereas the $K_{f,c}$ of *prkca*$^{-/-}$ mouse lungs was markedly reduced, and increased only to 0.067 $\pm$ 0.02 (Figure 20). This agrees with our previous data using PAR-1 peptide that demonstrated that deletion of PKCα reduces the increase in lung vascular permeability by almost 50%, and proves that PKCα is required to elicit a full increase in permeability during sepsis.

To verify that the mechanism of PKCα-induced increase in permeability is the same in response to PAR-1 activation and LPS stimulation, we homogenized lungs from *prkca*$^{-/-}$ and WT mice after LPS treatment. Immunoblots of lysates from WT mouse lungs showed p120 was phosphorylated on S879

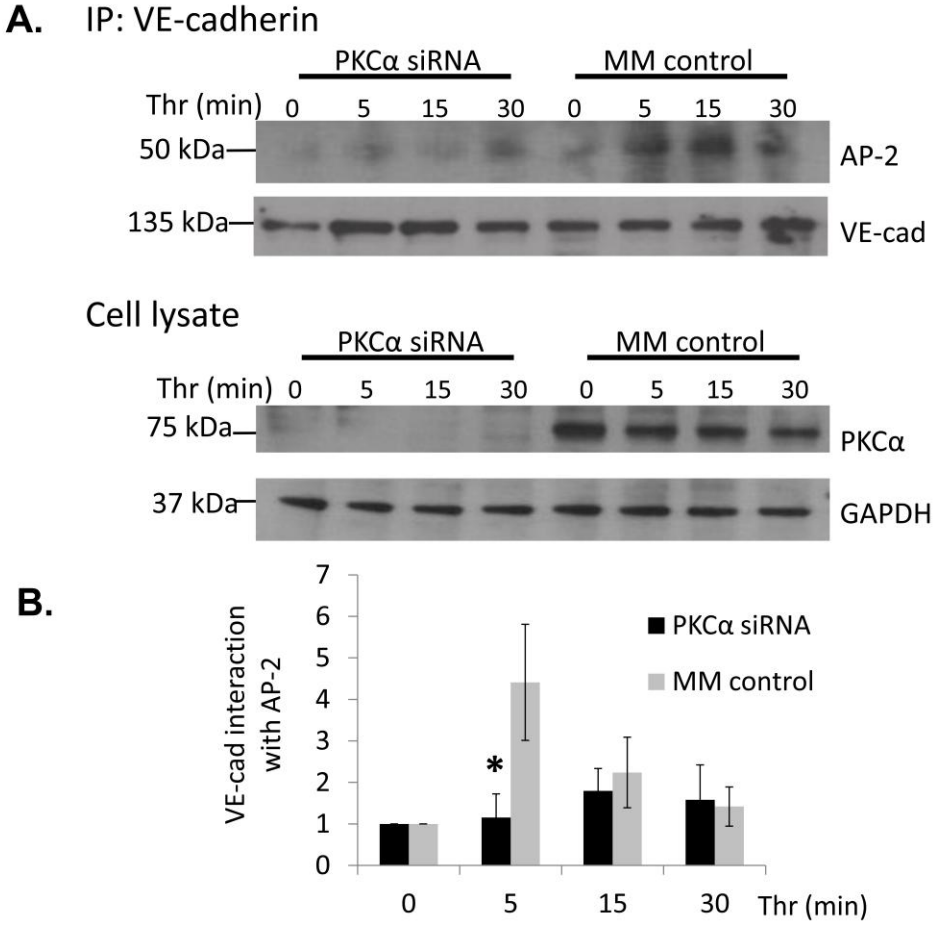

Figure 19: PKCα depletion decreases VE-cadherin interaction with AP-2. (A) VE-cadherin was immunoprecipitated in HLMVECs treated with PKCα or MM control siRNA. Immunoblots show AP-2 interaction with VE-cadherin. Immunoblots from cell lysates show equal knockdown of PKCα. (B) Bar graph shows densitometric analysis (n=3); * denotes significance from MM control ($p<0.05$). Reproduced with permission from Vandenbroucke St Amant, E. et al. *Circ Res* 2012;111:737-749(155).

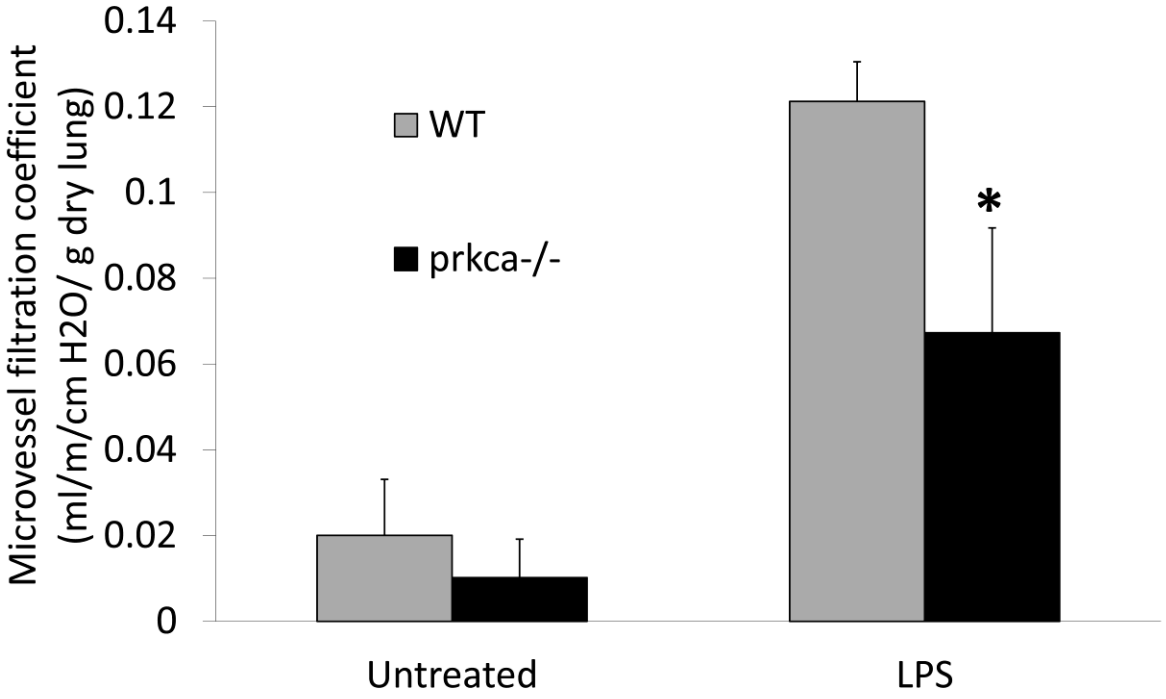

Figure 20: PKCα knockout mice display a decreased permeability response to LPS treatment. Lungs from *prkca*$^{-/-}$ and WT mice were perfused with LPS (40 mg/kg) and compared to untreated control group (from previous data; Figure 6). Bar graph shows $K_{f,c}$ as mean ± SEM (n=3). * $p<0.05$ denotes significance from WT after 6 hours LPS treatment. Reproduced with permission from Vandenbroucke St Amant, E. et al. *Circ Res* 2012;111:737-749(155).

within 1 h of LPS treatment, and phosphorylation increased through 3 hours (Figure 21). The lack of S879 phosphorylation in *prkca*$^{-/-}$ mice after LPS treatment again proved that S879 phosphorylation is PKCα-dependent.

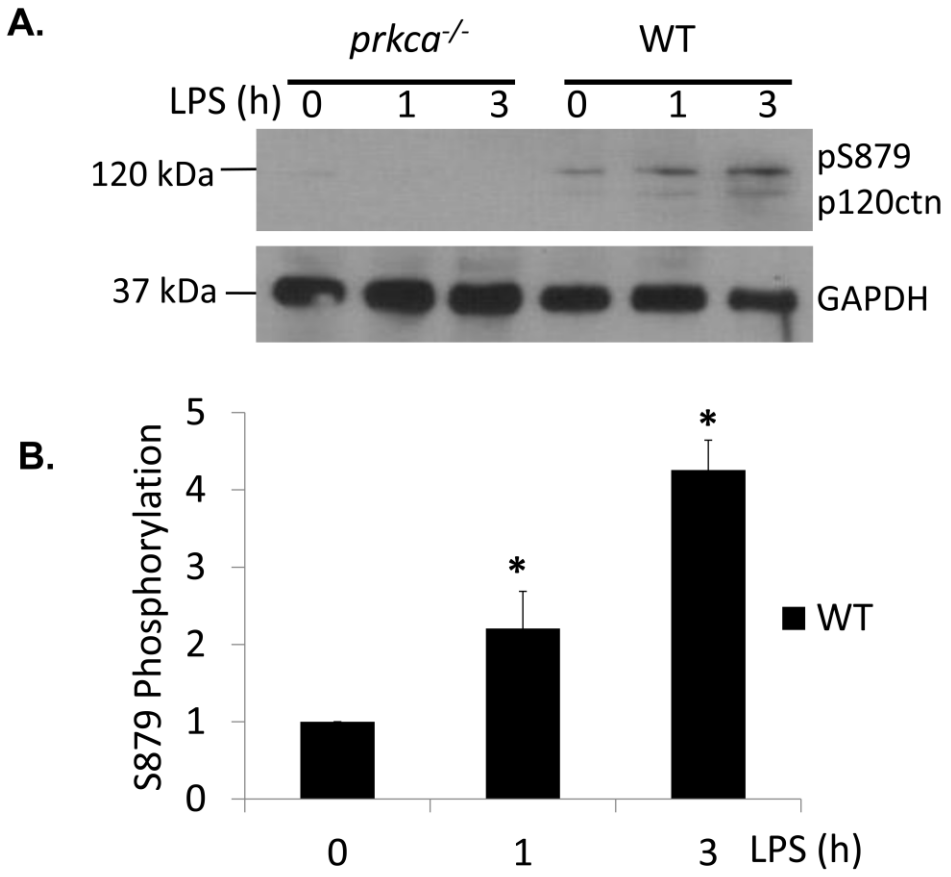

Figure 21: LPS induces PKCα-dependent phosphorylation of S879 on p120. (A) Western blot analysis was performed on mouse lung homogenates after mice were challenged with LPS (40 mg/kg) at indicated times. Immunoblots show phosphorylation of S879 on p120 after LPS treatment and deletion of PKCα. (B) Bar graph shows densitometric analysis (n=3); * denotes significance from WT 0 timepoint ($p<0.05$). Reproduced with permission from Vandenbroucke St Amant, E. et al. *Circ Res* 2012;111:737-749(155).

4. SERINE 879 PHOSPHORYLATION REGULATES ENDOTHELIAL PERMEABILITY

*Portions of the text and figures 22 and 24-30 were reprinted with permission from Vandenbroucke St Amant, E., Tauseef, M., Vogel, S.M., Gao, X., Mehta, D., Komarova, Y. and Malik, A.B. (2012) PKCalpha activation of p120-catenin serine 879 phospho-switch disassembles VE-cadherin junctions and disrupts vascular integrity. *Circulation Research*, 111, 739-749.

4.1 S879 Phosphorylation of p120 Alters p120 Localization

We previously showed that PKCα reduces VE-cadherin at AJs and increases vascular permeability during inflammation. We found this was due to dissociation of the p120/VE-cadherin complex and the resulting increase in VE-cadherin internalization. We also found that PKCα-dependent S879 phosphorylation occurs as p120 is uncoupling from VE-cadherin. To determine how S879 phosphorylation effects endothelial permeability, we first looked at the consequence of S879 phosphorylation on p120 localization. We immunostained cells with anti-VE-cadherin antibody along with anti-p120 antibody (Figure 22A, top panel) or anti-pS879 p120 antibody (pS879-p120, bottom panel), and quantified the localization of total p120 and phosphorylated p120 (Figure 22B-C) using fluorescence intensity. We found that phosphorylation of S879 on p120 modified p120 localization within cells. pS879-p120 was primarily localized to the cytosol, with an increase of pS879-p120 at both AJs and the cytosol at 15 minutes after thrombin stimulation, which correlated with the increase in S879 phosphorylation shown previously. Total p120 was localized at AJs in unstimulated cells, but only 27% of total p120 remained at AJs after 30 minutes of thrombin stimulation. This evidence suggests that p120 phosphorylated on S879 does not localize to AJs.

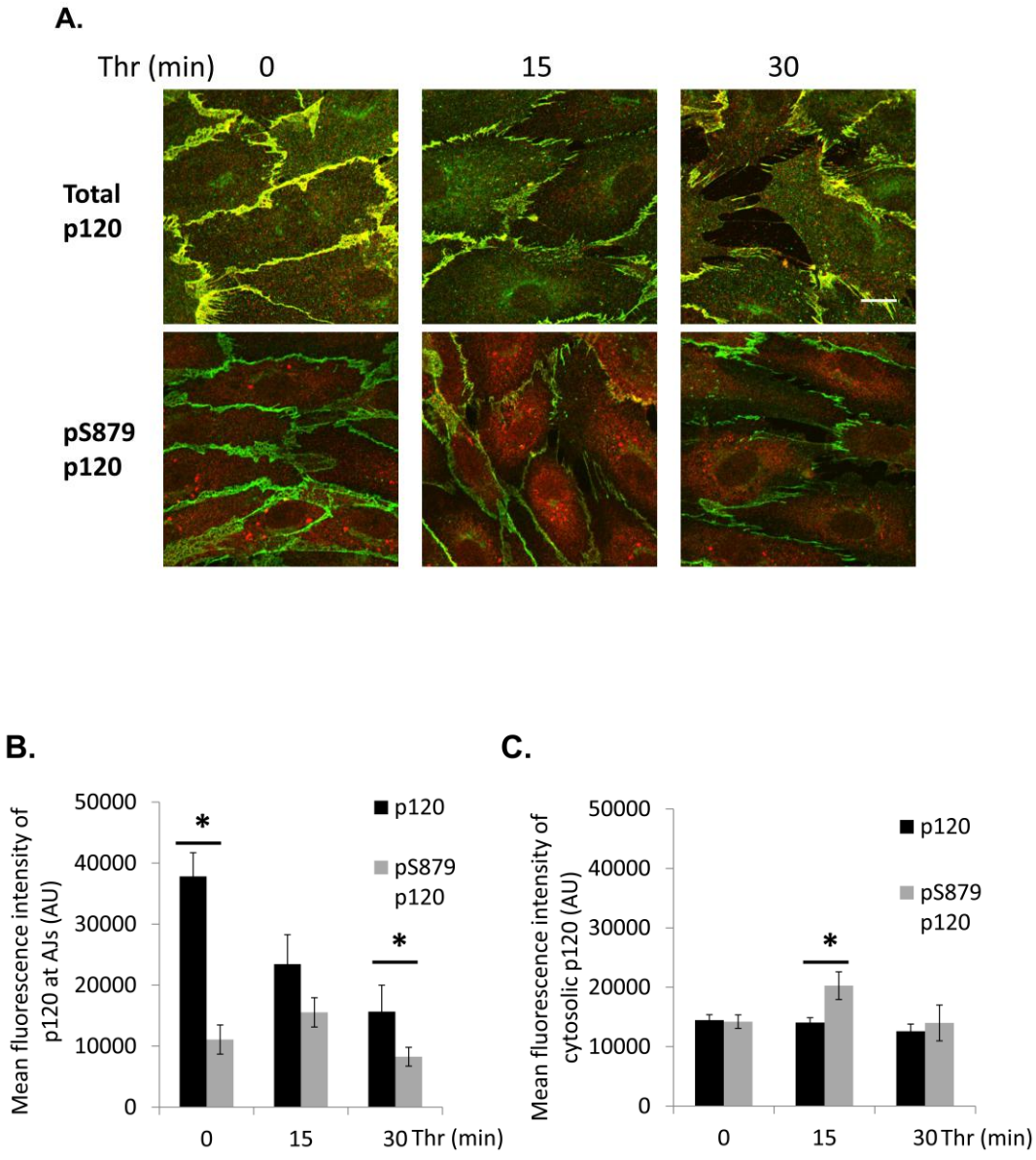

Figure 22: Phosphorylation of S879 on p120 alters p120 localization. (A) HLMVECs were co-immunostained for VE-cadherin (green) and p120 (top panel; red) or pS879 p120 (bottom panel; red). Representative images show total p120 or pS879-p120 localization at indicated times after thrombin stimulation (4 U/ml). Scale bar, 10 μm. (B-C) Graph of p120 accumulation at AJs (B) or in cytosol (C) shown as mean fluorescence intensity ± SEM (n=5). * denotes difference from total p120 ($p<0.05$). Reproduced with permission from Vandenbroucke St Amant, E. et al. *Circ Res* 2012;111:737-749(155).

4.2 S879 Phosphorylation Reduces p120 Affinity for VE-Cadherin

To further investigate the effects of S879 phosphorylation on vascular permeability, we mutated S879 to alanine to create a phosphodefective p120 mutant (S879A-p120), and to aspartic acid to create a phosphomimetic mutant (S879D-p120). The p120 phospho-mutants, along with wild-type (WT) p120 cDNA, were cloned into vectors containing a green fluorescent protein (GFP) tag and expressed in HPAECs. We used cDNA to generate WT-p120, phosphomimetic p120 mutant and VE-cadherin protein using a cell-free protein expression kit. Immunoblots of p120 and VE-cadherin verified protein expression, and GFP-p120-transfected cell lysate was used as a control (Figure 23).

To determine if S879 phosphorylation of p120 induces dissociation from VE-cadherin, we used SPR to determine alterations in binding affinity of p120 for VE-cadherin (Figure 24). We immobilized VE-cadherin on a CM-5 sensor chip, which was then exposed to increasing concentrations of WT-p120 or S879D-p120 to determine the binding affinity of p120 for VE-cadherin. Both WT-p120 and S879D-p120 increased binding to VE-cadherin in a dose-dependent manner, however, phosphomimetic p120 displayed an order of magnitude less affinity to VE-cadherin ($K_d = 3.3 \times 10^{-9}$) as compared to the WT p120 ($K_d = 4.2 \times 10^{-10}$), indicating that phosphorylation of S879 alone causes a significant decrease in p120 binding affinity to VE-cadherin.

To confirm S879 phosphorylation alters p120/VE-cadherin binding in endothelial cells, we transfected HPAECs with phosphodefective p120, phosphomimic p120 or WT p120. Expression of the p120 constructs was achieved over endogenous p120, and the GFP tag was utilized to differentiate exogenously expressed p120 from endogenous. We compensated for any effects of overexpression of

p120 by using WT p120, instead of an empty vector, as a control. 48 hours post-transfection, we immunoprecipitated VE-cadherin and probed resulting precipitates with anti-GFP antibody (Figure 25). The phosphodefective p120, S879A-p120, showed basal association with VE-cadherin and significantly increased association with VE-cadherin after thrombin stimulation (Figure 25B). The phosphomimic mutant, S879D-p120, exhibited weak interaction with VE-cadherin under basal conditions and decreased further after thrombin stimulation. Immunoblots of GFP-p120 from cell lysates show equal expression of exogenous p120, and GAPDH is shown as a loading control. Phosphodefective p120 remained bound to VE-cadherin after thrombin stimulation, suggesting S879 phosphorylation may function as an essential phospho-switch, disrupting p120 interaction with VE-cadherin.

4.3 Phosphorylation of p120 Induces VE-Cadherin Dissociation from AJs

We next addressed whether S879 phosphorylation of p120 causes decreased VE-cadherin stability at AJs, and formation of interendothelial gaps. HPAECs transfected with GFP-tagged p120 phospho-mutants were treated with thrombin and immunostained for VE-cadherin (Figure 26). VE-cadherin accumulation at AJs and interendothelial gap formation were quantified (Figure 26B-C). Monolayers expressing S879A-p120 had interendothelial gaps covering 7% of total area, and lost only 21% of VE-cadherin from junctions after 30 minutes of thrombin stimulation. S879D-p120-expressing monolayers had gaps covering 15% of total area and lost 73% of VE-cadherin from AJs, indicating that S879 phosphorylation promotes disassociation of VE-cadherin from AJs and causes formation of interendothelial gaps.

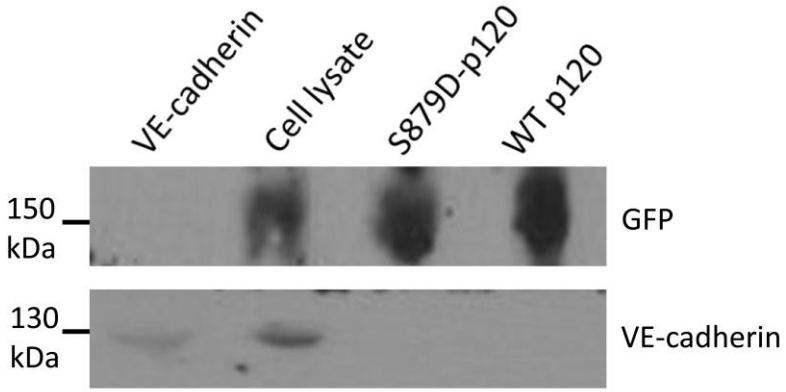

Figure 23: Generation of p120 mutants. Proteins were generated from cDNA with a cell-free protein expression kit, as according to the protocol. To verify the protein products, the generated proteins (S879D-p120, WT p120 and VE-cadherin) and a control cell lysate were analyzed by Western Blot and immunoblotted first with anti-GFP, then anti-VE-cadherin antibody.

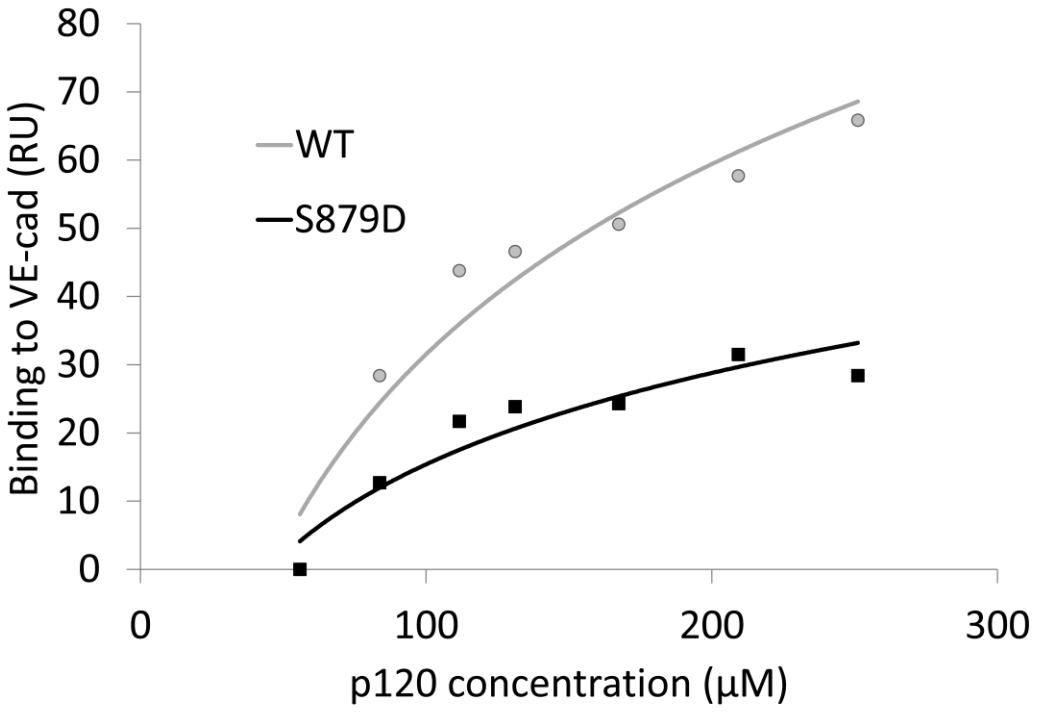

Figure 24: Phosphomimicking p120 exhibits decreased affinity to VE-cadherin. Increasing concentrations of WT-p120 or S879D-p120 protein were exposed to immobilized VE-cadherin, and bound p120 was measured using SPR. Results are expressed as a best-fit concentration-response curve. Reproduced with permission from Vandenbroucke St Amant, E. et al. *Circ Res* 2012;111:737-749 (155).

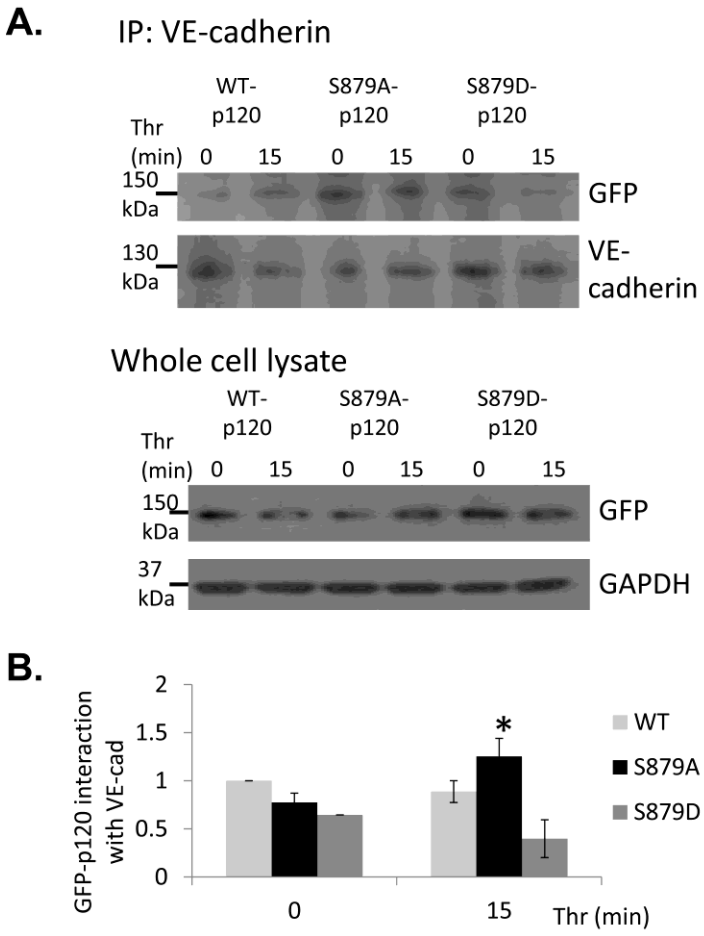

Figure 25: VE-cadherin remains bound to phosphodefective p120 after thrombin stimulation. (A) VE-cadherin was immunoprecipitated from HPAE lysates expressing WT p120, S879A-p120, or S879D-p120. Immunoblots show association of VE-cadherin with GFP-tagged p120 (GFP) mutants following thrombin stimulation (4 U/ml). (B) Bar graph shows densitometric analysis (n=3); * denotes difference from WT-p120 ($p<0.05$). Reproduced with permission from Vandenbroucke St Amant, E. et al. *Circ Res* 2012;111:737-749 (155).

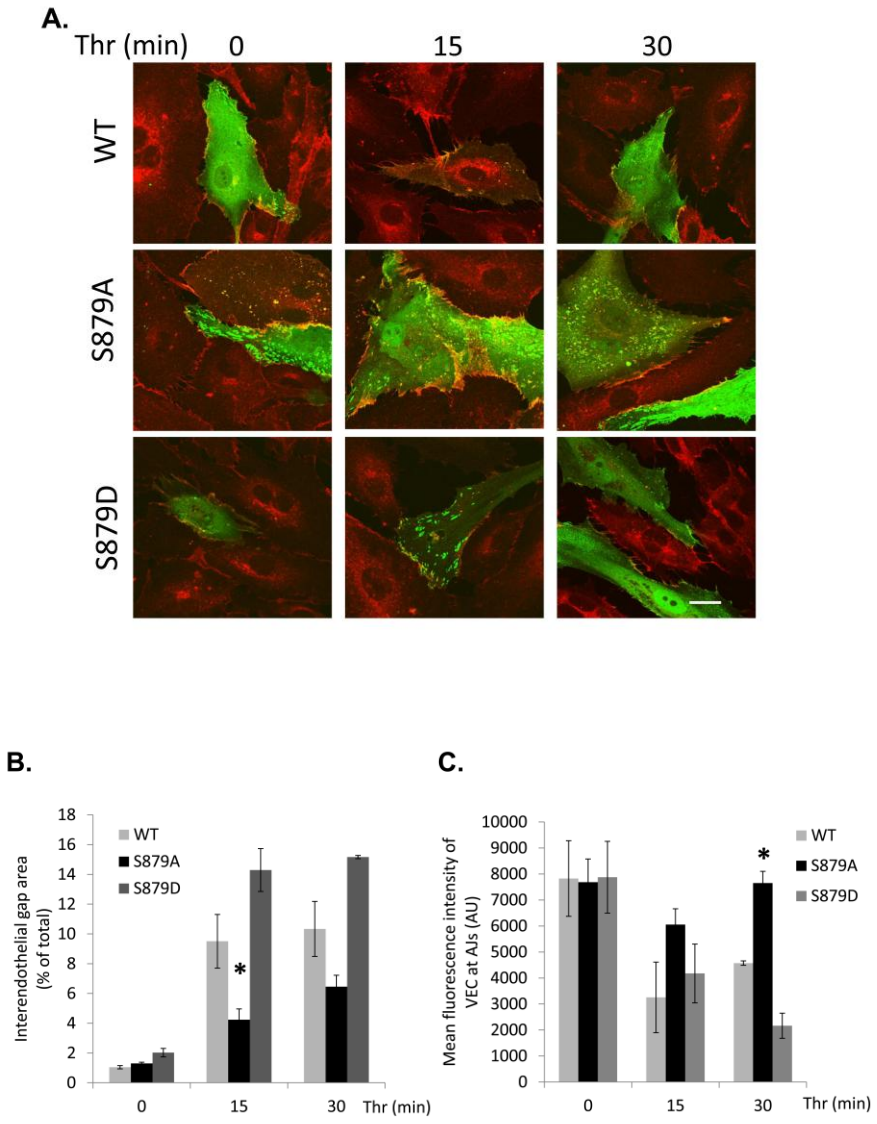

Figure 26: Monolayers expressing phosphodefective p120 form fewer interendothelial gaps after thrombin stimulation. (A) HPAECs transfected with GFP-p120 phospho-mutants were imaged before and after thrombin stimulation (4 U/ml). Representative (B) Graph of mean ± SEM of interendothelial gap area expressed as percent of total area (n=5). (C) Graph of average fluorescence intensity of VE-cadherin at AJs. Results are expressed as mean ± SEM (n=5). * denotes difference from WT ($p<0.05$). Reproduced with permission from Vandenbroucke St Amant, E. et al. *Circ Res* 2012;111:737-749 (155).

We next determined the effect of S879 phosphorylation of p120 on VE-cadherin association with AP-2. 48-hours post-transfection with p120 phospho-mutants, VE-cadherin was immunoprecipitated and resulting precipitates were immunoblotted with anti-AP-2 antibody (Figure 27). Cells expressing S879A-p120 showed no significant increase in VE-cadherin binding to AP-2. Expression of S879D-p120 increased the interaction between VE-cadherin and AP-2 before and after thrombin stimulation, indicating phosphorylation of S879-p120 increases VE-cadherin internalization by increasing interaction of VE-cadherin with AP-2.

4.4 Phosphodeficient p120 Remains at AJs after Thrombin Stimulation

To determine effects of S879 phosphorylation on p120 localization at AJs, we performed time-lapse imaging of GFP-tagged p120 mutants expressed in HPAECs after stimulation with thrombin (Figure 28). Average fluorescence intensity of GFP at AJs over time was quantified by kymograph analysis (Figure 28B). The p120 phospho-mutants localized similarly at AJs in unstimulated monolayers, and the amount of S879A-p120 at AJs remained unchanged after 12 minutes of thrombin stimulation. Dissociation of WT-p120 was evident after 5 minutes of thrombin stimulation, which corresponds to when PKCα-dependent S879 phosphorylation of p120 occurs, and continued to decrease to 40% of the initial value by 12 minutes. S879D-p120 dissociated from AJs immediately following thrombin stimulation and continued to decrease to 25% of the initial value at AJs. The slope of the dissociation of WT p120 from AJs after 5 minutes of thrombin stimulation and the overall slope of S879D-p120 dissociation was the same (-.04 and -.05 pixels/min, respectively), suggesting that dissociation occurred

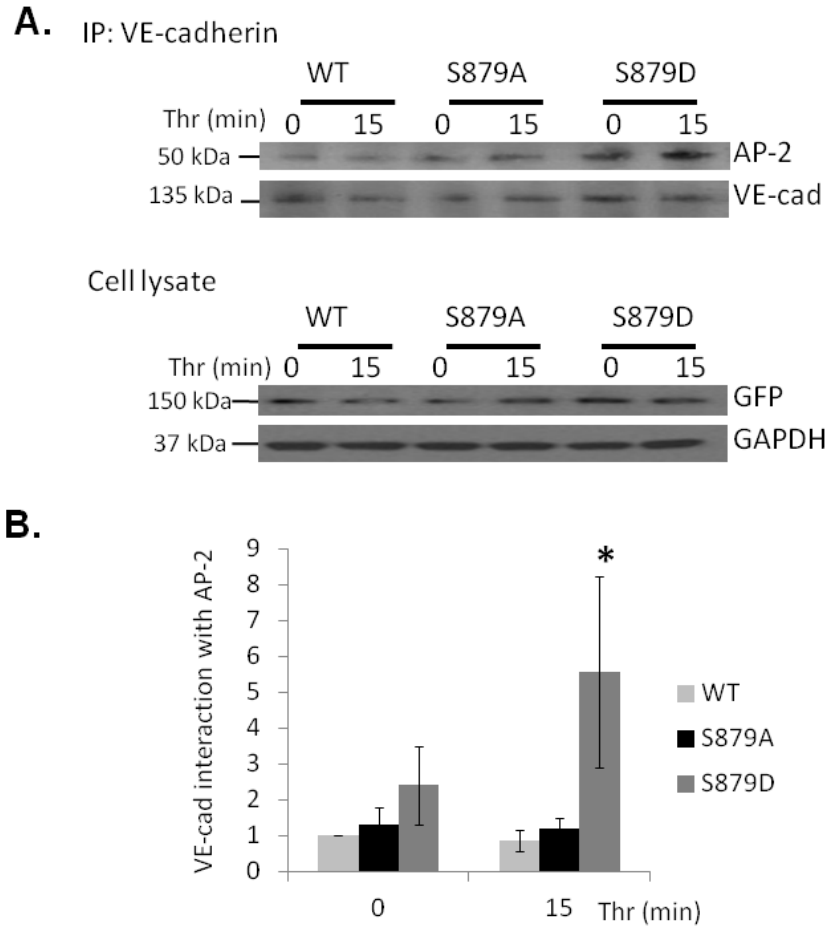

Figure 27: S879 phosphorylation of p120 increases VE-cadherin binding to AP-2. (A) VE-cadherin was immunoprecipitated in HPAECs transfected with indicated p120 phospho-mutants; precipitates were immunoblotted for AP-2 and VE-cadherin (n=3). Immunoblots from whole cell lysates show equal expression of p120 phospho-mutants. (B) Bar graph shows densitometric analysis; * denotes significance from WT-p120 ($p<0.05$). Reproduced with permission from Vandenbroucke St Amant, E. et al. *Circ Res* 2012;111:737-749 (155).

Figure 28: Phosphorylation of S879 on p120 regulates p120 localization at AJs. (A) Cells transfected with GFP-tagged p120 mutants were imaged before and after thrombin stimulation (4 U/ml). Representative time-lapse images show p120 localization at AJs at indicated time points after thrombin. Scale bar, 2 µm. (B) Fluorescence intensity of GFP at AJs was quantified and expressed as percent change in average fluorescence intensity over time (n=25 cells). Reproduced with permission from Vandenbroucke St Amant, E. et al. *Circ Res* 2012;111:737-749 (155).

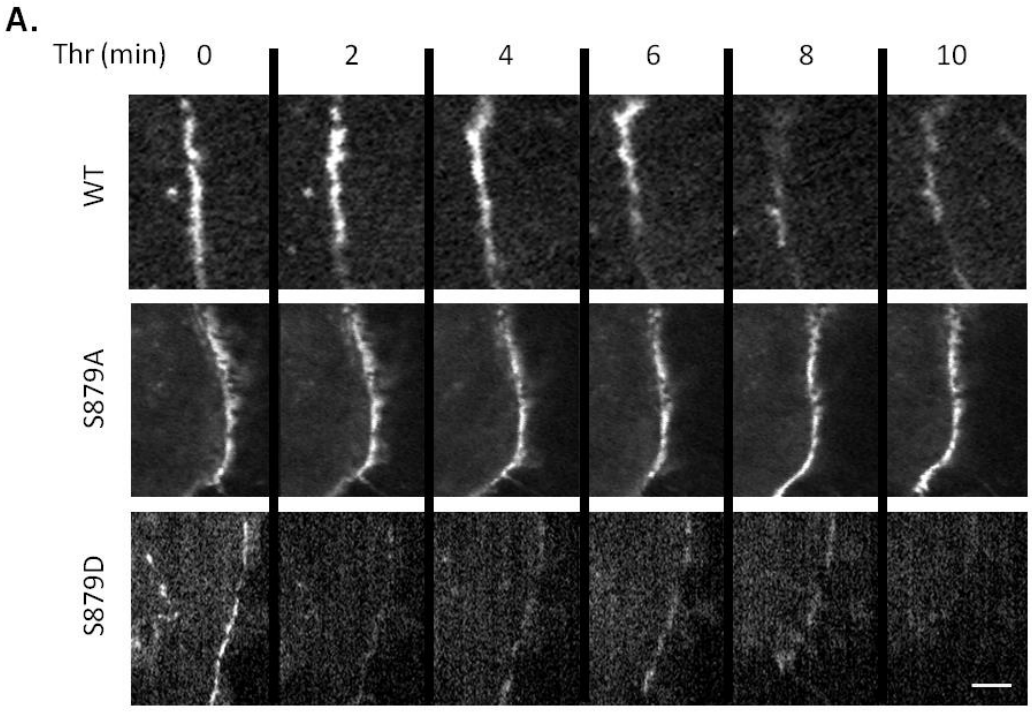
A.
Thr (min)
0
2
4
6
8
10
WT
S879A
S879D

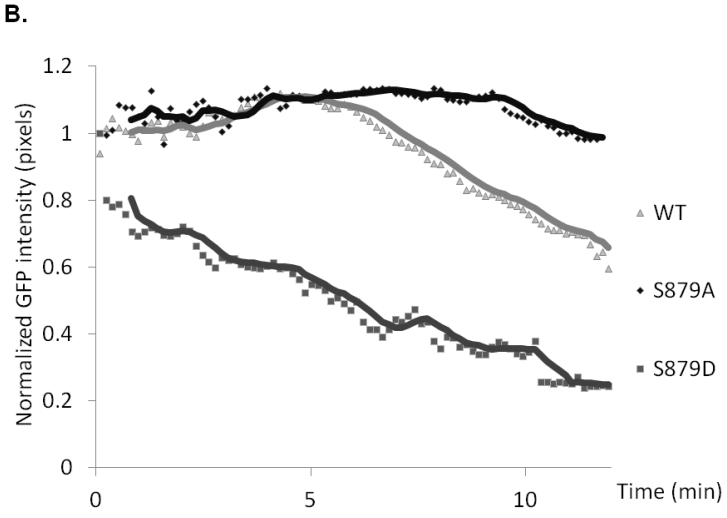
B.
Normalized GFP intensity (pixels)
1.2
1
0.8
0.6
0.4
0.2
0
0
5
10
Time (min)
WT
S879A
S879D

at the same rate once p120 was phosphorylated on S879. These findings further support the key role of S879 phosphorylation as a phospho-switch regulating p120 association with VE-cadherin at AJs.

4.5 S879 Phosphorylation Increases Vascular Permeability

To determine whether p120 S879 phosphorylation contributes to increased endothelial monolayer permeability, we quantified changes in TER of monolayers transfected with WT, S879A-p120, and S879D-p120 cDNA (Figure 29). Cells expressing S879A-p120 showed a modest (16%) decrease in TER in response to thrombin, whereas TER decreased 30% and 44% from baseline in cells expressing WT-p120 and S879D-p120, respectively. These data reveal the protective effect of the S879A-p120 mutant in decreasing the permeability response.

To address the barrier-protective effect of the S879A-p120 mutant *in vivo*, we expressed S879A-p120, WT p120 or GFP alone in the mouse lung vasculature using liposomes (68) and assessed the change in vascular permeability after stimulation with PAR-1 agonist peptide (Figure 30). Western blotting confirmed equal expression of WT-p120 and S879A-p120 in mouse lungs (Figure 30A). Lung vascular permeability in mice expressing GFP, WT-p120 and S879A-p120 was measured 30 minutes after infusion of PAR-1 agonist peptide. Extravasation of EBA, a measure of albumin transvascular permeability, increased to 30.1 mg/m dry lung in mice expressing S879A-p120, whereas mice expressing WT-p120 increased significantly higher, to 46.7 mg/m dry lung (Figure 30B). Measurements of lung wet:dry ratio (a measure of tissue edema) also showed that expression of S879A-p120 significantly reduced lung edema formation in mice receiving PAR-1 agonist peptide compared to expression of both

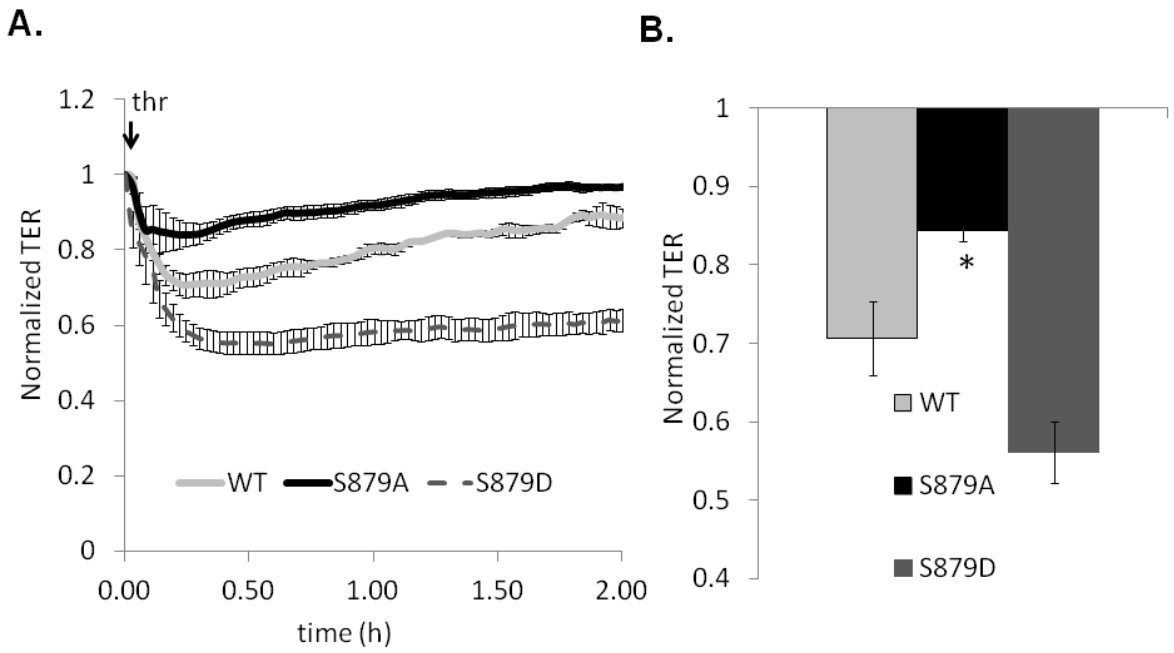

Figure 29: Phosphodefective p120 maintains endothelial monolayer integrity after thrombin stimulation. (A) Representative traces of the change in TER in HPAECs transfected with p120 mutants. Arrow shows addition of α-thrombin (Thr; 4 U/ml). Results are expressed as mean ± SEM (n=3). (B) Mean ± SEM of the maximum decrease in TER after thrombin stimulation (n=3). * denotes significance ($p<0.05$) from WT p120. Reproduced with permission from Vandenbroucke St Amant, E. et al. *Circ Res* 2012;111:737-749 (155).

Figure 30: Expression of phosphodefective p120 abrogates increased permeability *in vivo.* WT-p120, S879A-p120, or empty vector (GFP) were transduced in WT mouse lung endothelia using liposomes. (A) Immunoblots show expression of GFP (28 kDa), GFP-tagged WT-p120 and S879A-p120 (150 kDa) in whole lungs. Actin is shown as a loading control. (B-C) Evans blue was simultaneously injected i.v. with PAR-1 agonist peptide (1 mg/kg). After 30 minutes we determined (B) EBA extravasation and (C) lung wet:dry ratio. Data represent mean $\pm$ SEM (n=4). * denotes difference from GFP and ** denotes difference from WT-p120 ($p<0.05$). Reproduced with permission from Vandenbroucke St Amant, E. et al. *Circ Res* 2012;111:737-749 (155).

A.

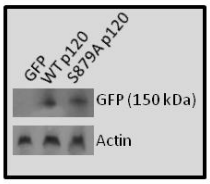
GFP
WT p120
S879A p120
GFP (150 kDa)
Actin

B.

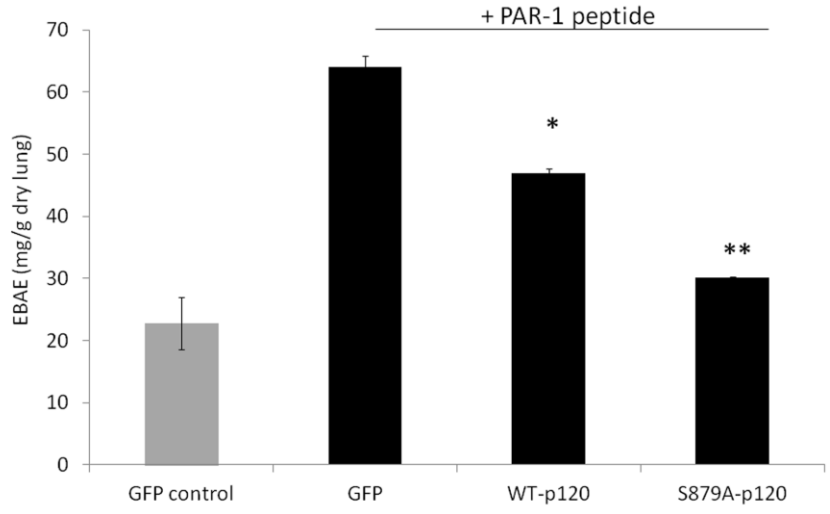
+ PAR-1 peptide
EBAE (mg/g dry lung)
70
60
50
40
30
20
10
0
*
**
GFP control
GFP
WT-p120
S879A-p120

C.

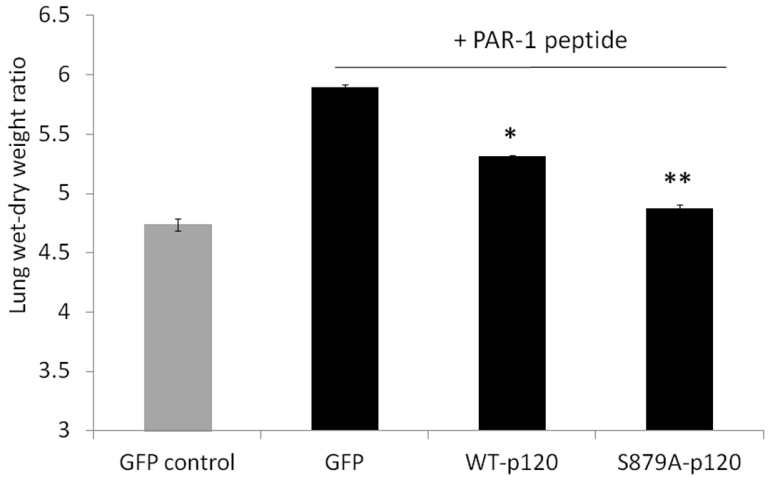
+ PAR-1 peptide
Lung wet-dry weight ratio
6.5
6
5.5
5
4.5
4
3.5
3
*
**
GFP control
GFP
WT-p120
S879A-p120

WT-p120 and GFP control (Figure 30C). The results indicate that inhibition of S879 phosphorylation may be a possible therapeutic target used to prevent edema during inflammation.

4.6 The Thrombin-Induced Decrease in TER is Diminished by the PKCα Blocking Peptide

To determine if inhibition of S879 phosphorylation is a plausible therapeutic option, we created a peptide that binds p120, and acts as a competitive inhibitor to PKCα in order to reducing phosphorylation of S879. Our peptide was based on a previously published peptide that blocked PKCα binding to lamin A (152). It mimics the PKCα sequence in the C2 domain, but does not require Ca^{2+} or DAG to bind (154). To test the efficacy of the peptide in inhibiting S879 phosphorylation of p120, HPAECs were incubated with increasing concentrations of the PKCα blocking or control peptide (antennapedia). Immunoblots detected S879 phosphorylation within 15 minutes of thrombin stimulation (Figure 31). Cell incubated with the control peptide showed no change in phosphorylation with increasing peptide concentration, while the cells treated with the PKCα blocking peptide showed a dose-dependent decrease in S879 phosphorylation. These results show that the peptide can functionally block S879 phosphorylation on p120 in endothelial cells in response to thrombin stimulation.

To reveal whether the PKCα-blocking peptide is able to combat an increase in permeability, we measured TER of HPAECs treated with the PKCα blocking peptide or a control peptide. After 30 minutes,

cells were treated with thrombin (Figure 32). Cells incubated with the PKCα blocking peptide showed 21% less of a decrease in TER than control cells (Figure 32B), suggesting that the blocking peptide does have a functional effect on endothelial barrier function and may be a useful therapeutic option to combat increasing endothelial permeability during inflammation.

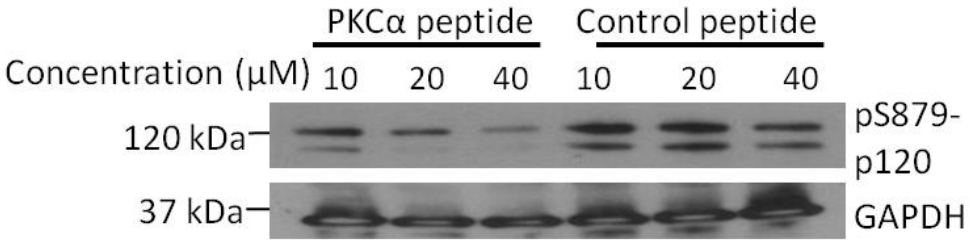

Figure 31: PKCα blocking peptide decreases p120 phosphorylation on S879. HPAECs treated with indicated concentrations of PKCα blocking peptide or control peptide were stimulated with thrombin (4 U/ml) for 15 minutes. Immunoblots show S879 phosphorylation of p120, and GAPDH as a loading control.

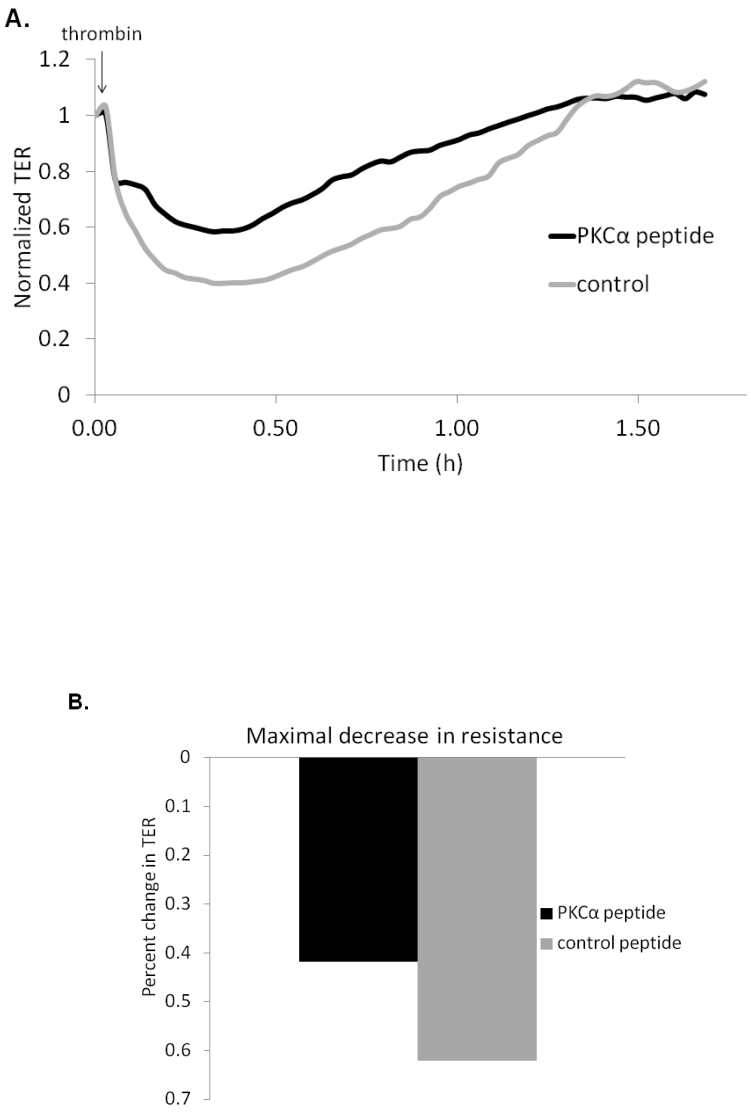

Figure 32: Thrombin-induced increase in monolayer permeability is reduced with the PKCα blocking peptide. (A) Representative traces of the change in TER in HPAECs treated with PKCα blocking peptide or control peptide. Arrow shows addition of α-thrombin (Thr; 4 U/ml). Results are expressed as mean ± SEM (n=3). (B) Mean ± SEM of the maximum decrease in TER after thrombin stimulation (n=3). * denotes significance ($p<0.05$).

5. CONCLUSIONS AND DISCUSSION

PKC was identified as a mediator of pulmonary edema after it was observed that PMA, a potent PKC activator, induced a phenotype similar to acute lung injury (ALI) and ARDS, in which increased permeability results in protein-rich edema in the lungs (112). Studies utilizing isoform-specific activators and inhibitors were able to show that PKCα is the primary isoform responsible for the pathophysiological hyperpermeability in the lungs during inflammation (66,113,120). Mechanistically, PKCα has been shown to increase permeability in response to histamine and thrombin, among others, by inducing rearrangement of the actin cytoskeleton and causing disassembly of AJs (9,105,116,156). Our lab has previously shown that PKCα induces endothelial barrier dysfunction through changes in phosphorylation of AJ proteins VE-cadherin, β-catenin and p120 (114). Research of the effects of PKCα on vascular permeability was limited to cell culture systems until creation of a PKCα global knockout mouse (152). Using these mice, we were able to study the role of PKCα on lung permeability *in vivo*. We found that PKCα deletion partially blocked the increase in lung permeability upon activation of the PAR-1 receptor, which we confirmed using primary endothelial cells depleted of PKCα. We assessed VE-cadherin localization and found that cells depleted of PKCα retained more VE-cadherin at the junction, and more junctions remained intact, after thrombin stimulation than in MM control cells. Overall, our results support previous data suggesting PKCα regulates permeability by altering AJ stability, and is the first to show that PKCα is a critical regulator of lung permeability *in vivo*.

Furthermore, PKCα deletion reduces the permeability response elicited from LPS stimulation. PKCα has not been shown to be activated downstream of TLR-4, which is the receptor LPS binds on endothelial cells, however it is known to associate with My-D88 downstream of TLRs in other cell types (157). LPS increases intracellular Ca^{2+} in response to TLR-4 activation though TRPC-6 (63), which is

required for activation of PKCα. PKCα was recently shown to regulate permeability after LPS in brain microvascular cells (66), however we are the first to demonstrate that LPS-induced increased in permeability is dependent on PKCα signaling in the lung vasculature.

PKCα deletion did not fully abrogate the increase in permeability in response to PAR-1 activation or LPS stimulation. Increased permeability is due in part to dissociation of interendothelial junctions, as well as actin stress fiber formation and cell contraction. While PKCα can active RhoA, but there are PKCα-independent mechanisms of RhoA activation as well, which may explain the increase in permeability in the PKCα knockout mouse lungs.

PKCα has not been shown to directly bind VE-cadherin, but it is known to bind and phosphorylate p120 (150). As previously mentioned, p120 regulates cadherin membrane stability (32,33). Depletion of p120 causes decreased cadherin surface expression; likewise, increased p120 protein expression results in increased cadherin at the junction (32). We found PKCα and VE-cadherin inversely bound p120, and in the absence of PKCα, p120 remained bound to VE-cadherin after thrombin stimulation. This indicates PKCα is required to cause dissociation of p120 from VE-cadherin, and may be the elusive mechanism which regulates cadherin stability during inflammation.

The finding that PKCα activity is required for disassembly of the p120/VE-cadherin complex is consistent with the postulated role of post-translational modifications of p120 in promoting AJ disassembly during inflammation (114). Phosphorylation of tyrosine 658 on VE-cadherin by Src has been shown to decrease VE-cadherin binding to p120 (158), and cause p120 to preferentially bind N-cadherin and exclude VE-cadherin from AJs (159). However, Src activation is not sufficient to disrupt

endothelial barrier function, and the effects of tyrosine phosphorylation on permeability remain a controversial area (90). Potter *et. al* (2005) stated that tyrosine phosphorylation of 658 prevented binding of p120 altogether (160), lending the possibly that tyrosine phosphorylation of VE-cadherin does not cause p120 dissociation, but rather follows p120 dissociation after phosphorylation of S879. Re-association of p120 with VE-cadherin is not evident until 60 minutes after thrombin stimulation, and the delay in junctional reannealing may be in part due to tyrosine phosphorylation of VE-cadherin.

Much less research has focused on serine and threonine phosphorylation of p120. One study concluded that serine and threonine phosphorylation of p120 does not affect cadherin ligation, however S879 was not included in the study (148). Also, most serine/threonine phosphorylation on p120 is constitutive (161), except for S879, and there is speculation that phosphorylation of S879 leads to de-phosphorylation of other residues (95). S879 resides in a PKC consensus motif on the CTD domain on p120, and is phosphorylated downstream of PKCα in epithelial cells, fibroblasts and multiple carcinoma cell lines (149,150). We confirmed p120 is phosphorylated on S879 in endothelial cells in a PKCα-dependent manner in response to thrombin and LPS. p120 phosphorylated on S879 localized away from the junction, indicating that once p120 is phosphorylated on S879 it can no long bind VE-cadherin. Our results identified the essential role of PKCα phosphorylation at S879 in mediating the p120/VE-cadherin interaction and disruption of AJs.

We showed that PKCα increases VE-cadherin internalization by increasing binding of AP-2. As previously mentioned, VE-cadherin is primarily internalized by AP-2-dependent, clathrin-mediated endocytosis (80,81). It has also been shown that cadherin endocytosis is the primary mechanism

responsible for disassembly of AJs (162), and binding of p120 physically blocks the amino acids on VE-cadherin required for AP-2 binding (163). Mutation of these amino acids inhibits p120 binding, as well as prevents endocytosis by decreasing AP-2 association, confirming that p120 dissociation from VE-cadherin directly results in VE-cadherin endocytosis by allowing AP-2 binding (163). We showed that VE-cadherin in MM control cells increased binding to AP-2 after thrombin stimulation, but cells depleted of PKCα showed no increase in AP-2/VE-cadherin binding, since VE-cadherin was still bound to p120. Using cells expressing the phosphomimic p120 (S879D-p120), we demonstrated that S879 phosphorylation leads to increased association of VE-cadherin and AP-2. These results confirm that PKCα-mediated S879 phosphorylation induces p120 dissociation from VE-cadherin thus allowing AP-2 binding, and provides the mechanism in which PKCα increases VE-cadherin internalization in response to thrombin stimulation.

The strength of cadherin binding to p120 is weak compared to cadherin binding to β-catenin (86,164), suggesting the p120/cadherin interaction is more dynamic and easier to regulate through post-translational modifications. Our data gathered using SPR revealed that S879D-p120 has a lower binding affinity towards VE-cadherin than WT-p120. The VE-cadherin/p120 K_D value was less than values previously reported for epithelial (E)-cadherin and p120 (86), which may be due to intrinsic differences between the 2 cadherins and endothelial versus epithelial barrier restrictiveness. They also may reflect methodological differences (e.g., we used full-length construct while others have used fragments of p120) used to assess the interaction (86). Upon stimulation with thrombin, both the WT and S879D-p120 dissociated from VE-cadherin while the phosphodefective p120 (S879A-p120) increased association due to its greater VE-cadherin binding potential. Time-lapse imaging showed that

phosphodefective p120 remained at AJs, while S879D-p120 dissociated from AJs immediately following thrombin stimulation. This leads us to conclude that phosphorylation of S879 significantly weakens the interaction between p120 and VE-cadherin and causes translocation of p120 away from AJs. While our data does not negate the possibility that another protein may be involved, or that dissociation requires multiple post-translational modifications, it does show that PKCα-induced p120 phosphorylation functions to reduce p120 binding affinity to VE-cadherin, which appears to be a key factor regulating the plasticity of AJs.

The association between p120 and cadherins is often assumed to be the same among different cell types. The JMD, the domain which p120 binds, is the most highly conserved cadherin domain. However, VE-cadherin lacks the dileucine motif that has been shown to be important for AP-2 binding (86). Studies of VE-cadherin stability and internalization, including ours, consistently demonstrate AP-2 binds and induces endocytosis of VE-cadherin in a similar fashion as other cadherins, although how it binds without the dileucine motif is unknown (80,81). Due to the subtle differences in the amino acid sequence of cadherins, it remains to be seen if phosphorylation of S879 on p120 would induce dissociation from other cadherins. S879 phosphorylation occurs in many cell types, in response to inflammation and growth factor stimulation (149), suggesting it is a conserved mechanism. If that proves to be correct, it could have enormous implications not only for endothelial-specific prevention of edema, but also for invasive forms of cancer, where a common underlying pathology is decreased cadherin surface expression as well as decreased p120 stability (132,165,166).

We did not address the role of p120 once it dissociates from cadherins. Unbound p120 functions as a GDI, and binds and inhibits RhoA, decreasing stress fiber formation and cell contraction, possibly as a feedback mechanism to control increasing permeability (81,140). p120 may also directly contribute to AJ reformation through activation of Cdc42 and Rac1, monomeric GTPases that promote AJ re-annealing (67,72,159,167,168), in part through interaction with Group B p21-Activating Kinase (PAK) (142,169). Also, once p120 dissociates from cadherins it can translocate to the nucleus, bind Kaiso (102) and relieve Kaiso-mediated repression on canonical Wnt genes (98,170).

We also did not address how p120 interaction with VE-cadherin is re-established after PKCα-induced p120 phosphorylation. AJ disassembly is transient and the increase in permeability is restored within two hours of thrombin stimulation (72). One possibility is that internalized VE-cadherin recycles back to AJs after p120 is de-phosphorylated (undefined phosphatase) and returns to AJs. In support of this idea, we showed that p120 accumulation at junctions was restored by 60 min after thrombin stimulation. At the same time, the cytoplasmic expression of p120 was reduced to basal levels, indicating that p120 is most likely recycled, not degraded. The mechanism in which p120 is dephosphorylated and shuttled back to the membrane is unknown, however.

We presented data confirming that S879 phosphorylation affects VE-cadherin stability, endothelial monolayer permeability and lung permeability *in vivo.* Our data showed inhibition of S879 phosphorylation increased VE-cadherin retention at the junctions, and permeability to be maintained even after stimulation with thrombin. Furthermore, expression of the phosphodefective p120 (S879A-p120) in mouse lungs significantly abrogated the increase in vascular permeability induced by PAR-1

receptor activation. Based on this data, we believe S879 inhibition could potentially be used as a pharmaceutical target to combat increased permeability during inflammation. The PKCα blocking peptide we developed was successful in inhibiting S879 phosphorylation of p120 and reducing the permeability increase following thrombin stimulation, suggesting it may be effective in the pharmacological treatment of edema, and diseases with edema as the underlying pathophysiology such as Crohn's Disease, ARDS and diabetes-associated vascular disease (3,117,171).

Regulation of the cadherin/catenin complex has been a focus of research over the past 15 years. Our results show that PKCα-mediated phosphorylation of p120 on S879 decreases p120 association with VE-cadherin during inflammation, resulting in VE-cadherin internalization through increased binding to AP-2 and increased permeability. The model (Figure 33) describes the role of PKCα-mediated 879 phosphorylation of p120 in disrupting the p120/VE-cadherin complex, which in turn results in VE-cadherin internalization and AJ disassembly. These results raise the intriguing prospect that manipulation of S879 phosphorylation on p120 is a potentially important anti-inflammatory target.

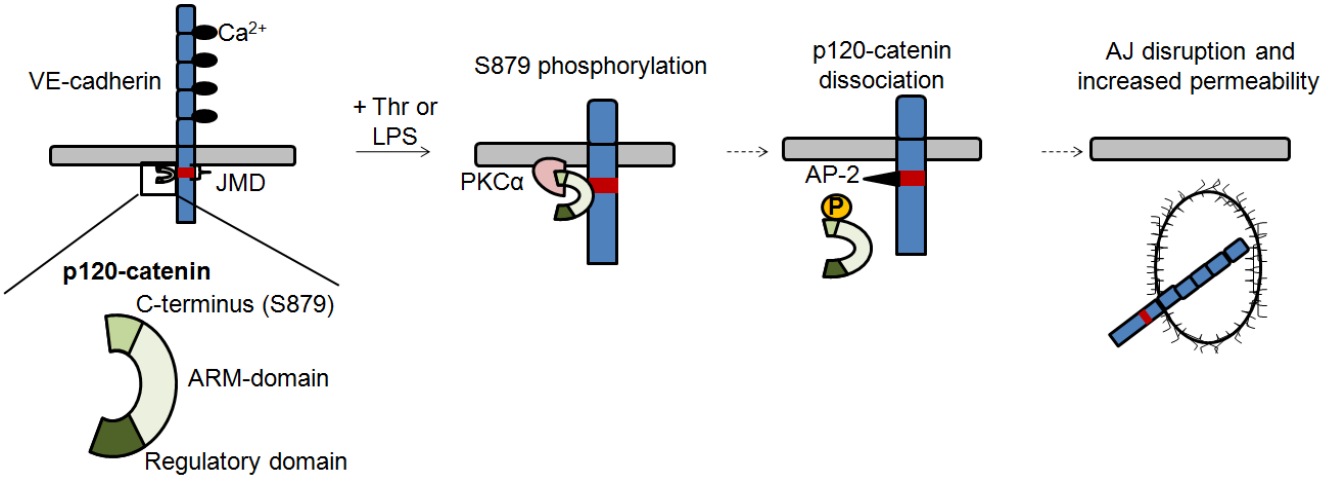

Figure 33: Model of effects of PKCα-dependent phosphorylation of S879 on p120 on AJ integrity. At AJs**,** p120 binds the JMD (aa 736-781) of VE-cadherin. Upon stimulation with thrombin or LPS, PKCα is activated and translocated to AJs where it phosphorylates S879 on p120. Phosphorylated p120 dissociates from VE-cadherin, leaving VE-cadherin susceptible to binding by AP-2. AP-2 recruits VE-cadherin into clathrin-coated pits, resulting in cadherin internalization and AJ disassembly. Reproduced with permission from Vandenbroucke St Amant, E. et al. *Circ Res* 2012;111:737-749 (155).

6. FUTURE DIRECTIONS

While many questions have been answered, this research has raised many questions as well. We uncovered the mechanism of p120/VE-cadherin regulation; however, the fate of p120 once dissociated from VE-cadherin is a mystery. Studies have shown that p120 does reside in the cytoplasm, where it regulates RhoA activity (140), and in the nucleus, where it functions as a transcriptional regulator (102). It is unclear how the different cytosolic pools of p120 are regulated, and what causes p120 to return to AJs to reform the junction. De-phosphorylation of p120 would be required to return to p120 to AJs, but no serine/threonine phosphatase has been shown to interact with p120 in endothelial cells. An important question to answer would involve how p120 is de-phosphorylated and what signals p120 return to AJs, to restore endothelial permeability.

Another intriguing arose as to how S879 phosphorylation affects binding to other cadherins. Since the JMD of cadherins is conserved (86), we hypothesize that S879 phosphorylation causes decreased binding affinity from other cadherins, such as E-cadherin, which may have implications in cancer progression and EMT. If it causes dissociation from N-cadherin, S879 phosphorylation may be a critical regulator during development and tissue remodeling. Studies have shown that S879 phosphorylation occurs in epithelial cells and fibroblasts as well, and it is important to understand its function in p120/cadherin regulation in other cell types as well as other cellular processes.

7. CITED LITERATURE

1. Mehta, D. and Malik, A.B. (2006) Signaling mechanisms regulating endothelial permeability. *Physiol Rev*, **86**, 279-367.

2. Ochoa, C. and Stevens, T. (2012) Studies on the cell biology of interendothelial cell gaps. *Am J of Physiol - Lung Cell Mol Physiol*, **302**, L275-L286.

3. Zimmerman, G.A., Albertine, K.H., Carveth, H.J., Gill, E.A., Grissom, C.K., Hoidal, J.R., Imaizumi, T.-a., Maloney, C.G., McIntyre, T.M., Michael, J.R. *et al.* (1999) Endothelial activation in ARDS. *Chest*, **116**, 18S-24.

4. Joyce, J.A. and Pollard, J.W. (2009) Microenvironmental regulation of metastasis. *Nat Rev Cancer*, **9**, 239-252.

5. Rabiet, M., Plantier, J., Rival, Y., Genoux, Y., Lampugnani, M. and Dejana, E. (1996) Thrombin-induced increase in endothelial permeability is associated with changes in cell-to-cell junction organization. *Arterioscler Thromb Vasc Biol*, **16**, 488-496.

6. Liu, A., Gong, P., Hyun, S.W., Wang, K.Z.Q., Cates, E.A., Perkins, D., Bannerman, D.D., Puche, A.C., Toshchakov, V.Y., Fang, S. *et al.* (2012) TRAF6 couples TLR4 signaling to Src family kinase activation and opening of the paracellular pathway in human lung microvascular endothelia. *J Biol Chem*, **287**, 16132-16145.

7. Andriopoulou, P., Navarro, P., Zanetti, A., Lampugnani, M.G. and Dejana, E. (1999) Histamine induces tyrosine phosphorylation of endothelial cell-to-cell adherens junctions. *Arterioscler Thromb Vasc Biol*, **19**, 2286-2297.

8. Bazzoni, G. (2006) Endothelial tight junctions: permeable barriers of the vessel wall. *J Cell Physiol*, **209**, 122-130.

9. Vandenbroucke, E., Mehta, D., Minshall, R. and Malik, A.B. (2008) Regulation of endothelial junctional permeability. *Ann N Y Acad Sci*, **1123**, 134-145.

10. Taylor, A.E. (1981) Capillary fluid filtration, starling forces and lymph flow. *Circ Res*, **49**, 557-575.

11. Yuan, S.Y. and Rigor, R.R. (2011) Regulation of endothelial barrier function. *Colloquium Series on Integrated Systems Physiology: From Molecule to Function*, **3**, 1-146.

12. Levick, J.R. (2004) Revision of the Starling principle: new views of tissue fluid balance. *J Physiol*, **557**, 704.

13. Becker, B.F., Chappell, D., Bruegger, D., Annecke, T. and Jacob, M. (2010) Therapeutic strategies targeting the endothelial glycocalyx: acute deficits, but great potential. *Cardiovasc Res*, **87**, 300-310.

14. Michel, C. and Curry, F. (1999) Microvascular permeability. *Physiol Rev*, **73**, 703-761.

15. Feng, D., Nagy, J.A., Hipp, J., Pyne, K., Dvorak, H.F. and Dvorak, A.M. (1997) Reinterpretation of endothelial cell gaps induced by vasoactive mediators in guinea-pig, mouse and rat: many are transcellular pores. *J Physiol*, **504**, 747-761.

16. Baluk, P., Hirata, A., Thurston, G., Fujiwara, T., Neal, C.R., Michel, C.C. and McDonald, D.M. (1997) Endothelial gaps: time course of formation and closure in inflamed venules of rats. *Am J Physiol Lung Cell Mol Physiol*, **272**, L155-L170.

17. Dejana, E., Orsenigo, F. and Lampugnani, M.G. (2008) The role of adherens junctions and VE-cadherin in the control of vascular permeability. *J Cell Sci*, **121**, 2115-2122.

18. Schulzke, J., Günzel, D., John, L. and Fromm, M. (2012) Perspectives on tight junction research. *Ann N Y Acad Sci*, **1257**, 1-19.

19. Morita, K., Sasaki, H., Furuse, M. and Tsukita, S. (1999) Endothelial claudin. *J Cell Biol*, **147**, 185-194.

20. Taddei, A., Giampietro, C., Conti, A., Orsenigo, F., Breviario, F., Pirazzoli, V., Potente, M., Daly, C., Dimmeler, S. and Dejana, E. (2008) Endothelial adherens junctions control tight junctions by VE-cadherin-mediated upregulation of claudin-5. *Nat Cell Biol*, **10**, 923-934.

21. Schrade, A., Sade, H., Couraud, P.-O., Romero, I., Weksler, B. and Niewoehner, J. (2012) Expression and localization of claudins-3 and -12 in transformed human brain endothelium. *Fluids Barriers CNS*, **9**, 6.

22. Kiuchi-Saishin, Y., Gotoh, S., Furuse, M., Takasuga, A., Tano, Y. and Tsukita, S. (2002) Differential expression patterns of claudins, tight junction membrane proteins, in mouse nephron segments. *J Am Soc Nephrol*, **13**, 875-886.

23. Dorfel, M. and Huber, O. (2012) Modulation of tight junction structure and function by kinases and phosphatases targeting occludin. *J Biomed Biotechnol*, Epub ahead of print.

24. Hirase, T., Staddon, J.M., Saitou, M., Ando-Akatsuka, Y., Itoh, M., Furuse, M., Fujimoto, K., Tsukita, S. and Rubin, L.L. (1997) Occludin as a possible determinant of tight junction permeability in endothelial cells. *J Cell Sci*, **110**, 1603-1613.

25. Lampugnani, M.G. (2012) Endothelial cell-to-cell junctions: adhesion and signaling in physiology and rathology. *Cold Spring Harbor Perspectives in Medicine*, Epub ahead of print.

26. Gory-Faure, S., Prandini, M.H., Pointu, H., Roullot, V., Pignot-Paintrand, I., Vernet, M. and Huber, P. (1999) Role of vascular endothelial-cadherin in vascular morphogenesis. *Development*, **126**, 2093-2102.

27. Shapiro, L., Fannon, A.M., Kwong, P.D., Thompson, A., Lehmann, M.S., Grubel, G., Legrand, J.-F., Als-Nielsen, J., Colman, D.R. and Hendrickson, W.A. (1995) Structural basis of cell-cell adhesion by cadherins. *Nature*, **374**, 327-337.

28. Nawroth, R., Poell, G., Ranft, A., Kloep, S., Samulowitz, U., Fachinger, G., Golding, M., Shima, D., Deutsch, U. and Vestweber, D. (2001) VE-PTP and VE-cadherin ectodomains interact to facilitate regulation of phosphorylation and cell contacts. *EMBO J*, **21**, 4885-4895.

29. Takeichi, M. (1977) Functional correlation between cell adhesive properties and some cell surface proteins. *J Cell Biol*, **75**, 464-474.

30. Gumbiner, B.M. (2005) Regulation of cadherin-mediated adhesion in morphogenesis. *Nat Rev Mol Cell Biol*, **6**, 622-634.

31. Reynolds, A., Herbert, L., Cleveland, J., Berg, S. and Gaut, J. (1992) p120, a novel substrate of protein tyrosine kinase receptors and of p60v-src, is related to cadherin-binding factors beta-catenin, plakoglobin and armadillo. *Oncogene*, **7**, 2439-2445.

32. Xiao, K., Allison, D.F., Buckley, K.M., Kottke, M.D., Vincent, P.A., Faundez, V. and Kowalczyk, A.P. (2003) Cellular levels of p120 catenin function as a set point for cadherin expression levels in microvascular endothelial cells. *J Cell Biol*, **163**, 535-545.

33. Iyer, S., Ferreri, D.M., DeCocco, N.C., Minnear, F.L. and Vincent, P.A. (2004) VE-cadherin-p120 interaction is required for maintenance of endothelial barrier function. *Am J Physiol Lung Cell Mol Physiol*, **286**, L1143-1153.

34. Pokutta, S., Drees, F., Takai, Y., Nelson, W.J. and Weis, W.I. (2002) Biochemical and structural definition of the l-afadin- and actin-binding sites of alpha-catenin. *J Biol Chem*, **277**, 18868-18874.

35. Lampugnani, M.G., Corada, M., Caveda, L., Breviario, F., Ayalon, O., Geiger, B. and Dejana, E. (1995) The molecular organization of endothelial cell to cell junctions: differential association of plakoglobin, beta-catenin, and alpha- catenin with vascular endothelial cadherin (VE-cadherin). *J Cell Biol*, **129**, 203-217.

36. Drees, F., Pokutta, S., Yamada, S., Nelson, W.J. and Weis, W.I. (2005) alpha-catenin is a molecular switch that binds E-cadherin-beta-catenin and regulates actin-filament assembly. *Cell*, **123**, 903-915.

37. Komarova, Y.A., Mehta, D. and Malik, A.B. (2007) Dual regulation of endothelial junctional permeability. *Sci STKE*, **2007**, re8.

38. Troyanovsky, R.B., Klingelhofer, J. and Troyanovsky, S.M. (2011) alpha-Catenin contributes to the strength of E-cadherin-p120 interactions. *Mol Biol Cell*, **22**, 4247-4255.

39. Liaw, C., Cannon, C., Power, M., Kiboneka, P. and Rubin, L. (1990) Identification and cloning of two species of cadherins in bovine endothelial cells. *EMBO J.*, **9**, 2701-2708.

40. Navarro, P., Ruco, L. and Dejana, E. (1998) Differential localization of VE- and N-cadherins in human endothelial cells: VE-cadherin competes with N-cadherin for junctional localization. *J Cell Biol*, **140**, 1475-1484.

41. Luo, Y. and Radice, G.L. (2005) N-cadherin acts upstream of VE-cadherin in controlling vascular morphogenesis. *J Cell Biol*, **169**, 29-34.

42. Sabatini, P.J.B., Zhang, M., Silverman-Gavrila, R., Bendeck, M.P. and Langille, B.L. (2008) Homotypic and endothelial cell adhesions via N-cadherin determine polarity and regulate migration of vascular smooth muscle cells. *Circ Res*, **103**, 405-412.

43. Gerhardt, H., Wolburg, H. and Redies, C. (2000) N-cadherin mediates pericytic-endothelial interaction during brain angiogenesis in the chicken. *Dev Dyn*, **218**, 472-479.

44. Breviario, F., Caveda, L., Corada, M., Martin-Padura, I., Navarro, P., Golay, J., Introna, M., Gulino, D., Lampugnani, M.G. and Dejana, E. (1995) Functional properties of human vascular endothelial cadherin (7B4/Cadherin-5), an endothelium-specific cadherin. *Arterioscler Thromb Vasc Biol*, **15**, 1229-1239.

45. Vestweber, D. (2008) VE-cadherin: The major endothelial adhesion molecule controlling cellular junctions and blood vessel formation. *Arterioscler Thromb Vasc Biol*, **28**, 223-232.

46. Crosby, C.V., Fleming, P.A., Argraves, W.S., Corada, M., Zanetta, L., Dejana, E. and Drake, C.J. (2005) VE-cadherin is not required for the formation of nascent blood vessels but acts to prevent their disassembly. *Blood*, **105**, 2771-2776.

47. Luo, Y., Ferreira-Cornwell, M., Baldwin, H., Kostetskii, I., Lenox, J., Lieberman, M. and Radice, G. (2001) Rescuing the N-cadherin knockout by cardiac-specific expression of N- or E-cadherin. *Development*, **128**, 459-469.

48. Ferreri, D.M., Minnear, F.L., Yin, T., Kowalczyk, A.P. and Vincent, P.A. (2008) N-Cadherin levels in endothelial cells are regulated by monolayer maturity and p120 availability. *Cell Commun Adhes*, **15**, 333-349.

49. Taulet, N., Comunale, F., Favard, C., Charrasse, S., Bodin, S. and Gauthier-Rouviere, C. (2009) N-cadherin/p120 catenin association at cell-cell contacts occurs in cholesterol-rich membrane domains and is required for RhoA activation and myogenesis. *J Biol Chem*, **284**, 23137-23145.

50. Vogel, S.M., Gao, X., Mehta, D., Ye, R.D., John, T.A., Andrade-Gordon, P., Tiruppathi, C. and Malik, A.B. (2000) Abrogation of thrombin-induced increase in pulmonary microvascular permeability in PAR-1 knockout mice. *Physiol Genomics*, **4**, 137-145.

51. Pober, J.S. and Sessa, W.C. (2007) Evolving functions of endothelial cells in inflammation. *Nat Rev Immunol*, **7**, 803-815.

52. Vouret-Craviari, V., Boquet, P., Pouyssegur, J. and Van Obberghen-Schilling, E. (1998) Regulation of the actin cytoskeleton by thrombin in human endothelial cells: role of Rho proteins in endothelial barrier function. *Mol Biol Cell*, **9**, 2639-2653.

53. Carbajal, J. and Jr., M.S. (1999) RhoA inactivation enhances endothelial barrier function. *Am J Physiol*, **277**, C955-C964.

54. Tinsley, J.H., De Lanerolle, P., Wilson, E., Ma, W. and Yuan, S.Y. (2000) Myosin light chain kinase transference induces myosin light chain activation and endothelial hyperpermeability. *Am J Physiol Cell Physiol*, **279**, C1285-1289.

55. McKenzie, J.A. and Ridley, A.J. (2007) Roles of Rho/ROCK and MLCK in TNF-alpha-induced changes in endothelial morphology and permeability. *J Cell Physiol*, **213**, 221-228.

56. Amerongen, G.P.v.N., Delft, S.v., Vermeer, M.A., Collard, J.G. and van Hinsbergh, V.W.M. (2000) Activation of RhoA by thrombin in endothelial hyperpermeability. *Circ Res*, **87**, 335-340.

57. Moy, A.B., Van Engelenhoven, J., Bodmer, J., Kamath, J., Keese, C., Giaever, I., Shasby, S. and Shasby, D.M. (1996) Histamine and thrombin modulate endothelial focal adhesion through centripetal and centrifugal forces. *J Clin Invest*, **97**, 1020-1027.

58. Medzhitov, R. (2001) Toll-like receptors and innate immunity. *Nat Rev Immunol*, **1**, 135-145.

59. Dauphinee, S.M. and Karsan, A. (2005) Lipopolysaccharide signaling in endothelial cells. *Lab Invest*, **86**, 9-22.

60. Martin, G., Mannino, D. and Moss, M. (2006) The effect of age on the development and outcome of adult sepsis. *Crit Care Med*, **34**, 15-21.

61. Zeuke, S., Ulmer, A.J., Kusumoto, S., Katus, H.A. and Heine, H. (2002) TLR4-mediated inflammatory activation of human coronary artery endothelial cells by LPS. *Cardiovasc Res*, **56**, 126-134.

62. Gong, P., Angelini, D.J., Yang, S., Xia, G., Cross, A.S., Mann, D., Bannerman, D.D., Vogel, S.N. and Goldblum, S.E. (2008) TLR4 signaling is coupled to Src family kinase activation, tyrosine phosphorylation of zonula adherens proteins, and opening of the paracellular pathway in human lung microvascular endothelia. *J Biol Chem*, **283**, 13437-13449.

63. Tauseef, M., Knezevic, N., Chava, K.R., Smith, M., Sukriti, S., Gianaris, N., Obukhov, A.G., Vogel, S.M., Schraufnagel, D.E., Dietrich, A. *et al.* (2012) TLR4 activation of TRPC6-dependent calcium signaling mediates endotoxin-induced lung vascular permeability and inflammation. *J Exp Med*, **209**, 1953-1968.

64. Wang, Y., Malik, A., Sun, Y., Hu, S., Reynolds, A., Minshall, R. and Hu, G. (2011) Innate immune function of the adherens junction protein p120-catenin in endothelial response to endotoxin. *J Immunol*, **186**, 3180-3187.

65. Asehnoune, K., Strassheim, D., Mitra, S., Yeol Kim, J. and Abraham, E. (2005) Involvement of PKCalpha/beta in TLR4 and TLR2 dependent activation of NF-KappaB. *Cell Signal*, **17**, 385-394.

66. He, F., Yin, F., Omran, A., Yang, L.-f., Xiang, Q.-l. and Peng, J. (2012) PKC and RhoA signals cross-talk in Escherichia coli endotoxin induced alterations in brain endothelial permeability. *Biochem Biophys Res Commun*, **425**, 182-188.

67. Kouklis, P., Konstantoulaki, M., Vogel, S., Broman, M. and Malik, A.B. (2004) Cdc42 regulates the restoration of endothelial barrier function. *Circ Res*, **94**, 159-166.

68. Tauseef, M., Kini, V., Knezevic, N., Brannan, M., Ramchandaran, R., Fyrst, H., Saba, J., Vogel, S.M., Malik, A.B. and Mehta, D. (2008) Activation of sphingosine kinase-1 reverses the increase in lung vascular permeability through sphingosine-1-phosphate receptor signaling in endothelial cells. *Circ Res*, **103**, 1164-1172.

69. Johnson, K.R., Becker, K.P., Facchinetti, M.M., Hannun, Y.A. and Obeid, L.M. (2002) PKC-dependent activation of sphingosine kinase 1 and translocation to the plasma membrane. . *J Biol Chem*, **277**, 35257-35262.

70. Tiruppathi, C., Minshall, R.D., Paria, B.C., Vogel, S.M. and Malik, A.B. (2002) Role of Ca2+ signaling in the regulation of endothelial permeability. *Vascul Pharmacol*, **39**, 173-185.

71. Birukova, A.A., Smurova, K., Birukov, K.G., Kaibuchi, K., Garcia, J.G.N. and Verin, A.D. (2004) Role of Rho GTPases in thrombin-induced lung vascular endothelial cells barrier dysfunction. *Microvasc Res*, **67**, 64-77.

72. Broman, M.T., Kouklis, P., Gao, X., Ramchandran, R., Neamu, R.F., Minshall, R.D. and Malik, A.B. (2006) Cdc42 regulates adherens junction stability and endothelial permeability by inducing alpha-catenin interaction with the vascular endothelial cadherin complex. *Circ Res*, **98**, 73-80.

73. Adamson, R.H., Sarai, R.K., Altangerel, A., Thirkill, T.L., Clark, J.F. and Curry, F.-R.E. (2010) Sphingosine-1-phosphate modulation of basal permeability and acute inflammatory responses in rat venular microvessels. *Cardiovasc Res*, **88**, 344-351.

74. Birukova, A.A., Tian, Y., Dubrovskyi, O., Zebda, N., Sarich, N., Tian, X., Wang, Y. and Birukov, K.G. (2012) VE-cadherin trans-interactions modulate Rac activation and enhancement of lung endothelial barrier by iloprost. *J Cell Physiol*, **227**, 3405-3416.

75. Singleton, P.A., Dudek, S.M., Chiang, E.T. and Garcia, J.G.N. (2005) Regulation of sphingosine 1-phosphate-induced endothelial cytoskeletal rearrangement and barrier enhancement by S1P1 receptor, PI3 kinase, Tiam1/Rac1, and alpha-actinin. *The FASEB Journal*, **19**, 1646-1656.

76. Timmerman, I., Hoogenboezem, M., Bennett, A.M., Geerts, D., Hordijk, P.L. and van Buul, J.D. (2012) The tyrosine phosphatase SHP2 regulates recovery of endothelial adherens junctions through control of beta-catenin phosphorylation. *Mol Biol Cell*.

77. Knezevic, N., Tauseef, M., Thennes, T. and Mehta, D. (2009) The G protein {beta}{gamma} subunit mediates reannealing of adherens junctions to reverse endothelial permeability increase by thrombin. *J Exp Med*, **206**, 2761-2777.

78. Miyashita, Y. and Ozawa, M. (2007) A dileucine motif in its cytoplasmic domain directs Î²-catenin-uncoupled E-cadherin to the lysosome. *J Cell Sci*, **120**, 4395-4406.

79. Lampugnani, M.G., Zanetti, A., Breviario, F., Balconi, G., Orsenigo, F., Corada, M., Spagnuolo, R., Betson, M., Braga, V. and Dejana, E. (2002) VE-Cadherin regulates endothelial actin activating Rac and increasing membrane association of tiam. *Mol Biol Cell*, **13**, 1175-1189.

80. Xiao, K., Garner, J., Buckley, K.M., Vincent, P.A., Chiasson, C.M., Dejana, E., Faundez, V. and Kowalczyk, A.P. (2005) p120-catenin regulates clathrin-dependent endocytosis of VE-cadherin. *Mol Biol Cell*, **16**, 5141-5151.

81. Chiasson, C.M., Wittich, K.B., Vincent, P.A., Faundez, V. and Kowalczyk, A.P. (2009) p120-catenin inhibits VE-cadherin internalization through a Rho-independent mechanism. *Mol Biol Cell*, **20**, 1970-1980.

82. Paing, M.M., Johnston, C.A., Siderovski, D.P. and Trejo, J. (2006) Clathrin adaptor AP2 regulates thrombin receptor constitutive internalization and endothelial cell resensitization. *Mol Cell Biol*, **26**, 3231-3242.

83. Davis, M.A., Ireton, R.C. and Reynolds, A.B. (2003) A core function for p120-catenin in cadherin turnover. *J Cell Biol*, **163**, 525-534.

84. Ireton, R.C., Davis, M.A., van Hengel, J., Mariner, D.J., Barnes, K., Thoreson, M.A., Anastasiadis, P.Z., Matrisian, L., Bundy, L.M., Sealy, L. *et al.* (2002) A novel role for p120 catenin in E-cadherin function. *J Cell Biol*, **159**, 465-476.

85. Gentil-dit-Maurin, A., Oun, S., Almagro, S., Bouillot, S., Courcon, M., Linnepe, R., Vestweber, D., Huber, P. and Tillet, E. (2010) Unraveling the distinct distributions of VE- and N-cadherins in endothelial cells: A key role for p120-catenin. *Exp Cell Res*, **316**, 2587-2599.

86. Ishiyama, N., Lee, S.-H., Liu, S., Li, G.-Y., Smith, M.J., Reichardt, L.F. and Ikura, M. (2010) Dynamic and static interactions between p120 catenin and E-cadherin regulate the stability of cell-cell adhesion. *Cell*, **141**, 117-128.

87. Nollet, F., Kools, P. and van Roy, F. (2000) Phylogenetic analysis of the cadherin superfamily allows identification of six major subfamilies besides several solitary members. *J Mol Biol*, **299**, 551-572.

88. Esser, S., Lampugnani, M.G., Corada, M., Dejana, E. and Risau, W. (1998) Vascular endothelial growth factor induces VE-cadherin tyrosine phosphorylation in endothelial cells. *J Cell Sci*, **111**, 1853-1865.

89. Lampugnani, M.G., Corada, M., Andriopoulou, P., Esser, S., Risau, W. and Dejana, E. (1997) Cell confluence regulates tyrosine phosphorylation of adherens junction components in endothelial cells. *J Cell Sci*, **110**, 2065-2077.

90. Adam, A.P., Sharenko, A.L., Pumiglia, K. and Vincent, P.A. (2010) Src-induced tyrosine phosphorylation of VE-cadherin is not sufficient to decrease barrier function of endothelial monolayers. *J Biol Chem*, **285**, 7045-7055.

91. Alcaide, P., Martinelli, R., Newton, G., Williams, M.R., Adam, A., Vincent, P.A. and Luscinskas, F.W. (2012) p120-Catenin prevents neutrophil transmigration independently of RhoA inhibition by impairing Src dependent VE-cadherin phosphorylation. *Am J Physiol Cell Physiol*, **303**, C385-C395.

92. Reynolds, A.B. (2010) Exposing p120 catenin's most intimate affair. *Oncogene*, **141**, 20-22.

93. Marrin, N., Zamorano, P., Carrasco, R., Mujica, P., Gonzalez, F.G., Quezada, C., Meininger, C.J., Boric, M.P., Duran, W.N. and Sanchez, F. (2012) S-nitrosation of beta-catenin and p120 catenin: a novel regulatory mechanism in endothelial hyperpermeability. *Circ Res*, epub ahead of print.

94. Watanabe, T., Sato, K. and Kaibuchi, K. (2009) Cadherin-mediated intercellular adhesion and signaling cascades involving small GTPases. *Cold Spring Harbor Perspectives in Biology*, **1**.

95. Petrova, Y.I., Spano, M.M. and Gumbiner, B.M. (2012) Conformational epitopes at cadherin calcium-binding sites and p120-catenin phosphorylation regulate cell adhesion. *Mol Biol Cell*, **23**, 2092-2108.

96. Giampietro, C., Taddei, A., Corada, M., Sarra-Ferraris, G.M., Alcalay, M., Cavallaro, U., Orsenigo, F., Lampugnani, M.G. and Dejana, E. (2012) Overlapping and divergent signaling pathways of N-cadherin and VE-cadherin in endothelial cells. *Blood*, **119**, 2159-2170.

97. Dejana, E. (2010) The role of Wnt signaling in physiological and pathological angiogenesis. *Circ Res*, **107**, 943-952.

98. Corada, M., Nyqvist, D., Orsenigo, F., Caprini, A., Giampietro, C., Taketo, M.M., Iruela-Arispe, M.L., Adams, R.H. and Dejana, E. (2010) The Wnt/beta-catenin pathway modulates vascular remodeling and specification by upregulating Dll4/Notch signaling. *Dev Cell*, **18**, 938-949.

99. Kim, T.H., Xiong, H., Zhang, Z. and Ren, B. (2004) [beta]-Catenin activates the growth factor endothelin-1 in colon cancer cells. *Oncogene*, **24**, 597-604.

100. Masckauchán, T.N.H., Shawber, C.J., Funahashi, Y., Li, C.-M. and Kitajewski, J. (2005) Wnt/β-catenin signaling induces proliferation, survival and interleukin-8 in human endothelial cells. *Angiogenesis*, **8**, 43-51.

101. Kelly, K.F., Spring, C.M., Otchere, A.A. and Daniel, J.M. (2004) NLS-dependent nuclear localization of p120ctn is necessary to relieve Kaiso-mediated transcriptional repression. *J Cell Sci*, **117**, 2675-2686.

102. Daniel, J.M. and Reynolds, A.B. (1999) The catenin p120 ctn interacts with Kaiso, a novel BTB/POZ domain zinc finger transcription factor. *Mol Cell Biol*, **19**, 3614-3623.

103. Park, J., Ji, H., Jun, S., Gu, D., Hikasa, H., Li, L., Sokol, S.Y. and McCrea, Pierre D. (2006) Frodo links dishevelled to the p120-catenin/Kaiso pathway: distinct catenin subfamilies promote Wnt signals. *Dev Cell*, **11**, 683-695.

104. Beckers, C.M.L., Garcia-Vallejo, J.J., van Hinsbergh, V.W.M. and van Nieuw Amerongen, G.P. (2008) Nuclear targeting of Beta-catenin and p120ctn during thrombin-induced endothelial barrier dysfunction. *Cardiovasc Res*, **79**, 679-688.

105. Lum, H. and Malik, A.B. (1994) Regulation of vascular endothelial barrier function. *Am J Physiol*, **267**, L223-241.

106. Webb, B.L.J., Hirst, S.J. and Giembycz, M.A. (2000) Protein kinase C isoenzymes: a review of their structure, regulation and role in regulating airways smooth muscle tone and mitogenesis. *Br J Pharmacol*, **130**, 1433-1452.

107. Alvi, F., Idkowiak-Baldys, J., Baldys, A., Raymond, J. and Hannun, Y. (2007) Regulation of membrane trafficking and endocytosis by protein kinase C: emerging role of the pericentrion, a novel protein kinase C-dependent subset of recycling endosomes. *Cell Mol Life Sci*, **64**, 263-270.

108. Steinberg, S.F. (2008) Structural basis of protein kinase C isoform function. *Physiol Rev*, **88**, 1341-1378.

109. Asaoka, Y., Nakamura, S.-i., Yoshida, K. and Nishizuka, Y. (1992) Protein kinase C, calcium and phospholipid degradation. *Trends Biochem Sci*, **17**, 414-417.

110. Mochly-Rosen, D., Khaner, H. and Lopez, J. (1991) Identification of intracellular receptor proteins for activated protein kinase C. *Proc Natl Acad Sci*, **88**, 3997-4000.

111. Yuan, S.Y., Ustinova, E.E., Wu, M.H., Tinsley, J.H., Xu, W., Korompai, F.L. and Taulman, A.C. (2000) Protein kinase C activation contributes to microvascular barrier dysfunction in the heart at early stages of diabetes. *Circ Res*, **87**, 412-417.

112. Lynch, J.J., Ferro, T.J., Blumenstock, F.A., Brockenauer, A.M. and Malik, A.B. (1990) Increased endothelial albumin permeability mediated by protein kinase C activation. *J Clin Invest*, **85**, 1991-1998.

113. Sandoval, R., Malik, A.B., Minshall, R.D., Kouklis, P., Ellis, C.A. and Tiruppathi, C. (2001) Ca(2+) signalling and PKCalpha activate increased endothelial permeability by disassembly of VE-cadherin junctions. *J Physiol*, **533**, 433-445.

114. Konstantoulaki, M., Kouklis, P. and Malik, A.B. (2003) Protein kinase C modifications of VE-cadherin, p120, and {beta}-catenin contribute to endothelial barrier dysregulation induced by thrombin. *Am J Physiol Lung Cell Mol Physiol*, **285**, L434-442.

115. Mehta, D., Rahman, A. and Malik, A.B. (2001) Protein kinase C-alpha signals Rho-guanine nucleotide dissociation inhibitor phosphorylation and Rho activation and regulates the endothelial cell barrier function. *J Biol Chem*, **276**, 22614-22620.

116. Holinstat, M., Mehta, D., Kozasa, T., Minshall, R.D. and Malik, A.B. (2003) Protein kinase C{alpha}-induced p115RhoGEF phosphorylation signals endothelial cytoskeletal rearrangement. *J Biol Chem*, **278**, 28793-28798.

117. Clarke, M. and Dodson, P.M. (2007) PKC inhibition and diabetic microvascular complications. *Best Pract Res Clin Endocrinol Metab*, **21**, 573-586.

118. Das Evcimen, N. and King, G.L. (2007) The role of protein kinase C activation and the vascular complications of diabetes. *Pharmacol Res*, **55**, 498-510.

119. Lorenzo, P.S. and Dennis, P.A. (2003) Modulating protein kinase C (PKC) to increase the efficacy of chemotherapy: stepping into darkness. *Drug Resist Updat*, **6**, 329-339.

120. Ferro, T., Neumann, P., Gertzberg, N., Clements, R. and Johnson, A. (2000) Protein kinase C-alpha mediates endothelial barrier dysfunction induced by TNF-alpha. *Am J Physiol Lung Cell Mol Physiol*, **278**, L1107-L1117.

121. Reynolds, A., Roesel, D., Kanner, S. and Parsons, J. (1989) Transformation-specific tyrosine phosphorylation of a novel cellular protein in chicken cells expressing oncogenic variants of the avian cellular src gene. *Mol Cell Biol.*, **9**, 629.

122. Keirsebilck, A., Bonne, S., Staes, K., van Hengel, J., Nollet, F., Reynolds, A. and van Roy, F. (1998) Molecular cloning of the human p120ctn catenin gene (CTNND1): expression of multiple alternatively spliced isoforms. *Genomics*, **50**, 129-146.

123. Montonen, O., Aho, M., Uitto, J. and Aho, S. (2001) Tissue distribution and cell type-specific expression of p120ctn isoforms. *J Histochem Cytochem*, **49**, 1487-1495.

124. Yu, J., Miao, Y., Xu, H., Liu, Y., Jiang, G., Stoecker, M., Wang, E. and Wang, E. (2012) N-terminal 1-54 amino acid sequence and armadillo repeat domain are indispensable for p120-catenin isoform 1A in regulating E-cadherin. *PLoS ONE*, **7**, e37008.

125. Markham, N., Cooper, T., Goff, M., Gribben, E.M., Carnahan, R.H. and Reynolds, A.B. (2012) Monoclonal antibodies to DIPA: A novel binding partner of p120-catenin isoform 1. *Hybridoma*, **31**, 246-254.

126. Xiao, K., Oas, R.G., Chiasson, C.M. and Kowalczyk, A.P. (2007) Role of p120-catenin in cadherin trafficking. *Biochim Biophys Acta*, **1773**, 8-16.

127. Ho, C., Zhou, J., Medina, M., Goto, T., Jacobson, M., Bhide, P.G. and Kosik, K.S. (2000) δ-catenin is a nervous system-specific adherens junction protein which undergoes dynamic relocalization during development. *J Comp Neurol*, **420**, 261-276.

128. Sirotkin, H., O'Donnell, H., DasGupta, R., Halford, S., Jore, B.S., Puech, A., Parimoo, S., Morrow, B., Skoultchi, A., Weissman, S.M. *et al.* (1997) Identification of a new human catenin gene family member (ARVCF) from the region deleted in Velo-Cardio-Facial syndrome. *Genomics*, **41**, 75-83.

129. Hatzfeld, M. and Nachtsheim, C. (1996) Cloning and characterization of a new armadillo family member, p0071, associated with the junctional plaque: evidence for a subfamily of closely related proteins. *J Cell Sci*, **109**, 2767-2778.

130. Schmidt, A., Langbein, L., Rode, M., Prätzel, S., Zimbelmann, R. and Franke, W.W. (1997) Plakophilins 1a and 1b: widespread nuclear proteins recruited in specific epithelial cells as desmosomal plaque components. *Cell Tissue Res*, **290**, 481-499.

131. Carnahan, R.H., Rokas, A., Gaucher, E.A. and Reynolds, A.B. (2010) The molecular evolution of the p120-catenin subfamily and its functional associations. *PLoS ONE*, **5**, e15747.

132. Reynolds, A.B. and Roczniak-Ferguson, A. (2004) Emerging roles for p120-catenin in cell adhesion and cancer. *Oncogene*, **23**, 7947-7956.

133. Macpherson, I.R., Hooper, S., Serrels, A., McGarry, L., Ozanne, B.W., Harrington, K., Frame, M.C., Sahai, E. and Brunton, V.G. (2007) p120-catenin is required for the collective invasion of

squamous cell carcinoma cells via a phosphorylation-independent mechanism. *Oncogene*, **26**, 5214-5228.

134. Perez-Moreno, M., Davis, M.A., Wong, E., Pasolli, H.A., Reynolds, A.B. and Fuchs, E. (2006) p120-catenin mediates inflammatory responses in the skin. *Cell*, **124**, 631-644.

135. Oas, R.G., Xiao, K., Summers, S., Wittich, K.B., Chiasson, C.M., Martin, W.D., Grossniklaus, H.E., Vincent, P.A., Reynolds, A.B. and Kowalczyk, A.P. (2010) p120-catenin is required for mouse vascular development. *Circ Res*, **106**, 941-951.

136. Smalley-Freed, W.G., Efimov, A., Burnett, P.E., Short, S.P., Davis, M.A., Gumucio, D.L., Washington, M.K., Coffey, R.J. and Reynolds, A.B. (2010) p120-catenin is essential for maintenance of barrier function and intestinal homeostasis in mice. *J Clin Invest*, **120**, 1824-1835.

137. Stairs, Douglas B., Bayne, Lauren J., Rhoades, B., Vega, Maria E., Waldron, Todd J., Kalabis, J., Klein-Szanto, A., Lee, J.-S., Katz, Jonathan P., Diehl, J.A. *et al.* (2011) Deletion of p120-catenin results in a tumor microenvironment with inflammation and cancer that establishes it as a tumor suppressor gene. *Cancer cell*, **19**, 470-483.

138. Zhang, J., O'Donnell Iii, J.J., Holian, O., Vincent, P.A., Kim, K.S. and Lum, H. (2010) P120 catenin represses transcriptional activity through Kaiso in endothelial cells. *Microvasc Res*, **80**, 233-239.

139. O'Donnell, J.J., Zhuge, Y., Holian, O., Cheng, F., Thomas, L.L., Forsyth, C.B. and Lum, H. (2011) Loss of p120 catenin upregulates transcription of pro-inflammatory adhesion molecules in human endothelial cells. *Microvasc Res*, **82**, 105-112.

140. Anastasiadis, P.Z., Moon, S.Y., Thoreson, M.A., Mariner, D.J., Crawford, H.C., Zheng, Y. and Reynolds, A.B. (2000) Inhibition of RhoA by p120 catenin. *Nat Cell Biol*, **2**, 637-644.

141. Chen, X., Kojima, S.-i., Borisy, G.G. and Green, K.J. (2003) p120 catenin associates with kinesin and facilitates the transport of cadherin/catenin complexes to intercellular junctions. *J Cell Biol*, **163**, 547-557.

142. Wildenberg, G.A., Dohn, M.R., Carnahan, R.H., Davis, M.A., Lobdell, N.A., Settleman, J. and Reynolds, A.B. (2006) p120-Catenin and p190RhoGAP regulate cell-cell adhesion by coordinating antagonism between Rac and Rho. *Cell*, **127**, 1027-1039.

143. Jiang, G., Wang, Y., Dai, S., Liu, Y., Stoecker, M., Wang, E. and Wang, E. (2012) p120-catenin isoforms 1 and 3 regulate proliferation and cell cycle of lung cancer cells via beta-catenin and Kaiso respectively. *PLoS ONE*, **7**, e30303.

144. Mariner, D.J., Anastasiadis, P., Keilhack, H., Bohmer, F.-D., Wang, J. and Reynolds, A.B. (2001) Identification of Src phosphorylation sites in the catenin p120ctn. *J Biol Chem*, **276**, 28006-28013.

145. Castano, J., Solanas, G., Casagolda, D., Raurell, I., Villagrasa, P., Bustelo, X.R., Garcia de Herreros, A. and Dunach, M. (2007) Specific phosphorylation of p120-catenin regulatory domain differently modulates its binding to RhoA. *Mol Cell Biol*, **27**, 1745-1757.

146. Herron, C.R., Lowery, A.M., Hollister, P.R., Reynolds, A.B. and Vincent, P.A. (2011) p120 regulates endothelial permeability independently of its NH2 terminus and Rho binding. *Am J Physiol Heart Circ Physiol*, **300**, H36-H48.

147. Xia, X., Mariner, D.J. and Reynolds, A.B. (2003) Adhesion-associated and PKC-modulated changes in serine/threonine phosphorylation of p120-catenin. *Biochemistry*, **42**, 9195-9204.

148. Xia, X., Carnahan, R.H., Vaughan, M.H., Wildenberg, G.A. and Reynolds, A.B. (2006) p120 serine and threonine phosphorylation is controlled by multiple ligand-receptor pathways but not cadherin ligation. *Exp Cell Res*, **312**, 3336-3348.

149. Vaughan, M., Xia, X., Wang, X., Chronopoulou, E., Gao, G., Campos-Gonzalez, R. and Reynolds, A. (2007) Generation and characterization of a novel phospho-specific monoclonal antibody to p120-catenin serine 879 *Hybridoma*, **26(6)**, 407-416.

150. Brown, M.V., Burnett, P.E., Denning, M.F. and Reynolds, A.B. (2009) PDGF receptor activation induces p120-catenin phosphorylation at serine 879 via a PKC[alpha]-dependent pathway. *Exp Cell Res*, **315**, 39-49.

151. Damiano, B.P., Cheung, W.-M., Santulli, R.J., Fung-Leung, W.-P., Ngo, K., Ye, R.D., Darrow, A.L., Derian, C.K., de Garavilla, L. and Andrade-Gordon, P. (1999) Cardiovascular responses mediated by protease-activated ceceptor-2 (PAR-2) and thrombin receptor (PAR-1) are distinguished in mice deficient in PAR-2 or PAR-1. *J Pharmacol Exp Ther* **288**, 671-678.

152. Braz, J.C., Gregory, K., Pathak, A., Zhao, W., Sahin, B., Klevitsky, R., Kimball, T.F., Lorenz, J.N., Nairn, A.C., Liggett, S.B. *et al.* (2004) PKC-[alpha] regulates cardiac contractility and propensity toward heart failure. *Nat Med*, **10**, 248-254.

153. Kawabuchi, M., Satomi, Y., Takao, T., Shimonishi, Y., Nada, S., Nagai, K., Tarakhovsky, A. and Okada, M. (2000) Transmembrane phosphoprotein Cbp regulates the activities of Src-family tyrosine kinases. *Nature*, **404**, 999-1003.

154. Martelli, A.M., Bortul, R., Tabellini, G., Faenza, I., Cappellini, A., Bareggi, R., Manzoli, L. and Cocco, L. (2002) Molecular characterization of protein kinase C-α binding to lamin A. *J Cell Biochem*, **86**, 320-330.

155. Vandenbroucke St Amant, E., Tauseef, M., Vogel, S.M., Gao, X., Mehta, D., Komarova, Y. and Malik, A.B. (2012) PKCalpha activation of p120-catenin serine 879 phospho-switch disassembles VE-cadherin junctions and disrupts vascular integrity. *Circ Res*, **111**, 739-749.

156. Harrington, E.O., Brunelle, J.L., Shannon, C.J., Kim, E.S., Mennella, K. and Rounds, S. (2003) Role of protein kinase C isoforms in rat epididymal microvascular endothelial barrier function. *Amer J Respir Cell Mol Biol*, **28**, 626-636.

157. Langlet, C., Springael, C., Johnson, J., Thomas, S., Flamand, V., Leitges, M., Goldman, M., Aksoy, E. and Willems, F. (2009) PKC-α controls MYD88-dependent TLR/IL-1R signaling and cytokine production in mouse and human dendritic cells. *Eur J Immunol*, **40**, 505-515.

158. Potter, M.D., Barbero, S. and Cheresh, D.A. (2005) Tyrosine phosphorylation of VE-cadherin prevents binding of p120- and beta-catenin and maintains the cellular mesenchymal state. *J Biol Chem*, **280**, 31906-31912.

159. Hatanaka, K., Simons, M. and Murakami, M. (2011) Phosphorylation of VE-cadherin controls endothelial phenotypes via p120-catenin coupling and Rac1 activation. *Am J Physiol Heart Circ Physiol*, **300**, H162-H172.

160. Potter, M.D., Barbero, S. and Cheresh, D.A. (2005) Tyrosine phosphorylation of VE-cadherin prevents binding of p120- and beta-catenins and maintains the cellular mesenchymal state. *J Biol Chem*, **280**, 31906-31912.

161. Ratcliffe, M.J., Rubin, L.L. and Staddon, J.M. (1997) Dephosphorylation of the cadherin-associated p100/p120 proteins in response to activation of protein kinase C in epithelial cells. *J Biol Chem*, **272**, 31894-31901.

162. Troyanovsky, R.B., Sokolov, E.P. and Troyanovsky, S.M. (2006) Endocytosis of cadherin from intracellular junctions is the driving force for cadherin adhesive dimer disassembly. *Mol Biol Cell*, **17**, 3484-3493.

163. Nanes, B.A., Chiasson-MacKenzie, C., Lowery, A.M., Ishiyama, N., Faundez, V., Ikura, M., Vincent, P.A. and Kowalczyk, A.P. (2012) p120-catenin binding masks an endocytic signal conserved in classical cadherins. *J Cell Biol*, **199**, 365-380.

164. Choi, H.-J., Huber, A.H. and Weis, W.I. (2006) Thermodynamics of beta-catenin-ligand interactions. *J Biol Chem*, **281**, 1027-1038.

165. Wendt, M.K., Taylor, M.A., Schiemann, B.J. and Schiemann, W.P. (2011) Down-regulation of epithelial cadherin is required to initiate metastatic outgrowth of breast cancer. *Mol Biol Cell*, **22**, 2423-2435.

166. Xiong, H., Hong, J., Du, W., Lin, Y., Ren, L., Wang, Y., Su, W., Wang, J., Cui, Y., Wang, Z. *et al.* (2012) Roles of STAT3 and ZEB1 proteins in E-cadherin down-regulation and human colorectal cancer epithelial-mesenchymal transition. *J Biol Chem*, **287**, 5819-5832.

167. Hatanaka, K., Simons, M. and Murakami, M. (2011) Phosphorylation of VE-cadherin controls endothelial phenotypes via p120-catenin coupling and Rac1 activation. *American Journal of Physiology - Heart and Circulatory Physiology*, **300**, H162-H172.

168. Tzima, E. (2006) Role of small GTPases in endothelial cytoskeletal dynamics and the shear stress response. *Circ Res*, **98**, 176-185.

169. Wong, L.E., Reynolds, A.B., Dissanayaka, N.T. and Minden, A. (2010) p120-catenin is a binding partner and substrate for Group B Pak kinases. *J Cell Biochem*, **110**, 1244-1254.

170. Park, J., Kim, S.W., Lyons, J.P., Ji, H., Nguyen, T.T., Cho, K., Barton, M.C., Deroo, T., Vleminckx, K. and McCrea, P.D. (2005) Kaiso/p120-catenin and TCF/beta-catenin complexes coordinately regulate canonical Wnt gene targets. *Dev Cell*, **8**, 843-854.

171. Roifman, I., Sun, Y.C., Fedwick, J.P., Panaccione, R., Buret, A.G., Liu, H., Rostom, A., Anderson, T.J. and Beck, P.L. (2009) Evidence of endothelial dysfunction in patients with inflammatory bowel disease. *Clin Gastroenterol Hepatol*, **7**, 175-182.

8. VITA

NAME	Emily Elizabeth Vandenbroucke St Amant
EDUCATION	Ph.D. Pharmacology, University of Illinois, Chicago, Illinois, 2012 (Expected) B.A. Zoology and Psychology, Miami University, Oxford, Ohio, 2005.
HONORS	Klaus Unna Award, Department of Pharmacology, University of Illinois at Chicago, September 2012. ASBMB Hill Day, September 2012. Doris Woeltjen Poster Award, Department of Pharmacology, University of Illinois at Chicago, October 2010. American Heart Association Midwest Affiliate Pre-Doctoral Fellowship, 2010-2012. Graduate Student Council Travel Award, University of Illinois at Chicago, May 2009. ASPET Best Abstract Award, Division of Molecular Pharmacology, April 2009. AAAS Excellence in Science Program, February 2009. NIH Lung Biology and Pathobiology Training Grant, University of Illinois at Chicago, 2008- 2010. OARS Undergraduate Research Grant, Miami University, April 2005.
PUBLICATIONS	Vandenbroucke St Amant E, Tauseef M, Vogel S, Gao X, Mehta D, Komarova Y and AB Malik. (2012) PKCα activation of p120-catenin at serine 879 phosphoswitch disassembles VE-cadherin junctions and disrupts vascular integrity. *Circulation Research.* 111:739-749. Minshall RD, Vandenbroucke EE, Holinstat M, Place AT, Tiruppathi C, Vogel SM, van Nieuw Amerongen GP, Mehta D and AB Malik. (2010) Role of protein kinase Cζ in thrombin-induced RhoA activation and interendothelial gap formation of human dermal microvessel endothelial cell monolayers. *Microvascular Research.* 80(2):240-9.

VITA (continued)

Vandenbroucke E, Mehta D, Minshall R and Asrar B Malik. (2008) Regulation of Endothelial Junctional Permeability. *Annals of the New York Academy of Sciences.* 1123:134-145.

ABSTRACTS

Vandenbroucke EE, Tauseef M, Gao, X, Mehta D, Komarova Y, Malik AB: Phosphorylation of p120-catenin on S879 induces dissociation from VE-cadherin and disassembly of adherens junctions. Gordon conference: Cell contact and adhesion. Mount Snow, VT, 2011.

Vandenbroucke EE, Tauseef M, Gao, X, Mehta D, Komarova Y, Malik AB: Phosphorylation of p120-catenin on S879 regulates increased permeability of the endothelial barrier. Arteriosclerosis, Thrombosis and Vascular Biology 2011 Scientific Sessions. Chicago, IL, 2011.

Vandenbroucke, EE, Vogel S, Gao X, Komarova Y, Malik AB:, PKCalpha-mediated signaling in regulating adherens junction integrity. Experimental Biology. New Orleans, LA, 2009.

Vandenbroucke, EE, Vogel S, Gao X, Komarova Y, Malik AB: Deletion of PKCalpha in mice attenuates the thrombin-induced increase in lung vascular permeability. Experimental Biology. San Diego, CA, 2008.